NUREG/IA–0025

International Agreement Report

RELAP5/MOD3 Subcooled Boiling Model Assessment

Prepared by
A. S. Devkin and A. S. Podosenov

Nuclear Safety Institute
Russian Research Centre
"Kurchatov Institute"
Kurchatov Square, 1
123182, Moscow
Russia

Office of Nuclear Regulatory Research
U.S. Nuclear Regulatory Commission
Washington, DC 20555–0001

May 1998

Prepared as part of
The Agreement on Research Participation and Technical Exchange
under the International Code Application and Maintenance Program (CAMP)

Published by
U.S. Nuclear Regulatory Commission

NUREG/IA–0025

International Agreement Report

RELAP5/MOD3 Subcooled Boiling Model Assessment

Prepared by
A. S. Devkin and A. S. Podosenov

Nuclear Safety Institute
Russian Research Centre
"Kurchatov Institute"
Kurchatov Square, 1
123182, Moscow
Russia

Office of Nuclear Regulatory Research
U.S. Nuclear Regulatory Commission
Washington, DC 20555–0001

May 1998

Prepared as part of
The Agreement on Research Participation and Technical Exchange
under the International Code Application and Maintenance Program (CAMP)

Published by
U.S. Nuclear Regulatory Commission

DISCLAIMER

ABSTRACT

This report presents the assessment of the RELAP5/Mod3 (5m5 version) code subcooled boiling process model, which is based on a variety of experiments. The accuracy of the model is confirmed for a wide range of regime parameters for the case of uniform heating along the channel. The condensation rate is rather underpredicted, which may lead to considerable errors in void fraction behavior prediction in subcooled boiling regimes for nonuniformly or unheated channels.

Contents

1. INTRODUCTION

The flow in the core for some reactors such as RBMK or BWR is in two - phase conditions in nominal regimes. Nonboiling reactors such conditions may exist in the hottest channels, as for WWER-1000. For accidental regimes fluid boiling in the core appears practically for any of transients scenarios. Calculational analysis of these processes are fulfilling by using the codes having the capability for accurate description the appearing and behavior of vapor phase in reactor channels . The description of such processes in the "best estimate codes" is based on two-fluid models, which gives the possibility to describe the process of boiling in the core accurate enough for arbitrary distribution of power along the channels and for any transients. It being known that the description of saturated boiling process don't give rise to difficulties. But as for subcooled boiling and vapor condensation processes the situation is more complicated because it needs to describe such processes as vapor appearance and it's generation at the heated walls , vapor condensation in the subcooled water, interface heat and mass transfer and so on.

This work purpose is the evaluation of the accuracy of the models used in RELAP5/MOD3 (version 5m5) code [1] for subcooled boiling process by comparison of the calculational and experimental date in wide range of regime parameters.

2. MODEL DESCRIPTION

Governing equations system used in RELAP5/MOD3 code are as following.

Mass equations:

$$\frac{\partial}{\partial t}(\alpha_g \rho_g) + \frac{1}{A}\frac{\partial}{\partial x}(\alpha_g \rho_g V_g A) = \Gamma_g \,, \tag{1}$$

$$\frac{\partial}{\partial t}(\alpha_f \rho_f) + \frac{1}{A}\frac{\partial}{\partial x}(\alpha_f \rho_f V_f A) = -\Gamma_g, \tag{2}$$

where $\alpha_g = 1 - \alpha_f$ - vapor void fraction ; ρ_g, ρ_f - specific densities of vapor and liquid phases; V_g, V_f - phase velocities , A - cross section area; Γg-vapor generating rate which consists of two parts - volume generation (interface) rate - Γ_{ig} and wall generation rate - Γ_w , such as

$$\Gamma_g = \Gamma_{ig} + \Gamma_w \tag{3}$$

Energy equations :

$$\frac{\partial}{\partial t}(\alpha_g \rho_g U_g) + \frac{1}{A}(\alpha_g \rho_g U_g V_g) = -P\frac{\partial}{\partial t}\alpha_g - \frac{P}{A}\frac{\partial}{\partial x}(\alpha_g V_g A) + Q_{wg} + Q_{ig} + \\ + \Gamma_{ig} h_g^* + \Gamma_w h_g^* + DISS_g \tag{4}$$

$$\frac{\partial}{\partial t}(\alpha_f \rho_f U_f) + \frac{1}{A}(\alpha_f \rho_f U_f V_f) = -P\frac{\partial}{\partial t}\alpha_f - \frac{P}{A}\frac{\partial}{\partial x}(\alpha_f V_f A) + Q_{wf} + Q_{if} - \\ - \Gamma_{if} h_f^* - \Gamma_w h_f^* + DISS_f \tag{5}$$

where $U_{k=g,f}$ - specific internal energy of k-phase , P - pressure , $Q_{wk(\,k=g,f)}$ - specific heat flux from wall to "k"-phase; $Q_{ik\ (k=g,f\ )}$ - interface heat flux , $\Gamma_{ig}\ h_k^*$ - interface latent heat , $\Gamma_w\ h_k^*$ - wall latent heat, $DISS_k$ - wall friction dissipation .

The momentum equations are not considered here , because the relative motion of phases are minor for subcooled boiling process . It should be noted that the phase velocities are determined by using the reliable enough

correlations, especially for upward flows in channels. Vapor generation rate in the two-phase volume is determined as:

$$\Gamma = \frac{H_{ig}(T_s - T_g) + H_{if}(T_s - T_f)}{h_g^* - h_f^*}, \tag{6}$$

where "s" - is related for saturated conditions ,T_k- "k" - phase temperature

$h_g^* = h_g^s$ - for condensation and $h_g^* = h_g$ - for vaporization,

$h_f^* = h_f^s$ - for condensation and $h_f^* = h_f$ - for vaporization .

Interface heat fluxes are determined as :

$$Q_{ig} = H_{ig}\,(Ts-Tg) + ((1-\varepsilon)/2)\;\Gamma_w\,(h_g^s - h_f^s), \tag{7}$$

$$Q_{if} = H_{if}\,(Ts-Tg) + ((1+\varepsilon)/2)\;\Gamma_w\,(h_g^s - h_f^s), \tag{8}$$

where $\varepsilon=1$, if $\Gamma_w > 0$ and $\varepsilon=-1$ if $\Gamma_w < 0$.
Wall generation rate is equal :

$$\Gamma_w = \frac{Q_{ig} + Q_{if} + \Gamma_{ig}\left(h_g^* - h_f^*\right)}{h_f^* - h_g^*} \tag{9}$$

Such way the net vapor generation rate is determined as

$$\Gamma_g = \frac{H_{ig}(T_s - T_g) + H_{if}(T_s - T_f)}{h_g^* - h_f^*} \tag{10}$$

H_{ig} and H_{if} in this expression are the products of interface area value A_i and heat transfer coefficient h_{ik} from interface to phase "k" $H_{ik} = A_i\ h_{ik}$, which are depending from the two-phase flow regime: bubble, slug, annular and so on. Here we not consider the whole spectrum of regimes but only specific for subcooled boiling process : bubbly and slug

2.1 BUBBLE REGIME

If the flow is in a bubble regime and the fluid temperature is below the saturation, the interface heat transfer coefficient is calculated using Unal formula [20]

$$h_{if} = (C\ F\ h_{fg} * d) / (2 * (1/\rho_g - 1/\rho_f)), \quad (11)$$

where $h_{fg} = h_g^{\ s} - h_f^{\ s}$, $\rho_{k=g,\,f}$ - specific densities of phases,

$$F = 1, \quad \text{for } V_f \leq 0.61 \text{ m/s}, \quad (12)$$

$$F = \left| \frac{V_f}{0.61} \right|^{0.47}, \quad \text{for } V_f > 0.61 \text{ m/s}, \quad (13)$$

$C = 65 - 5.69 * 10^{-5} (P - 10^5)$, for $10^5 \leq P \leq 10^6$ Pa,
$C = 0.25 * 10^{10} * P^{-1.418}$, for $10^6 < P \leq 17.7 * 10^6$ Pa,
d - bubble diameter , which is calculated using critical Weber number

$$We_{crit} = \rho_f (V_g - V_f)^2 * d_{max} / \sigma = 10, \quad (14)$$

where σ - surface tension coefficient.

This expression gives the maximal bubble diameter. Mean bubble diameter is determined as $d_0 = d_{max} / 2$, and interface area is

$$A_i = 3.6\ \alpha_g / d_0 \quad (15)$$

Using this expression and Unal's formula (11) one can obtain

$$H_{if} = h_{if}\ A_i = 1.8\ \alpha_g\ C\ F\ h_{fg}\ \rho_f\ \rho_g / (\rho_f - \rho_g) \quad (16)$$

This expression used in the code to calculate the heat transfer between interface surface and subcooled liquid. The field of parameter recommended to use Unal's

formula is : pressure P= 0.1 - 17.7 MPa , heat flux q= 0.47 - 10.64 MWt/ m^2 , liquid velocity V_f = 0.9 - 9.15 m/s , liquid subcooling ΔT= 3 - 86 K , maximal bubble diameter d= 0.08-1.24 mm .

The heat transfer with vapor phase in subcooled boiling regime does not introduce significant influence on the process. It should be noted only that large values of interface heat transfer coefficient on the vapor side ensure the vapor conditions closed to saturation.

2.2 SLUG REGIME

Interface heat flux (for volume unit) is determined as :

$$Q_i = \frac{h_s A_s \Delta T}{V} + \frac{h_b A_b \Delta T}{V}, \qquad (17)$$

where index "s" concerned to slugs, and "b"- to bubbles,
h - interface heat transfer coefficient,
A - interface surface area .

Interface surface area for slugs regime is determined from the expression D_s =0.88D, where D is the hydraulic diameter and A_s= 4/D_s = 4.5/D. Volume fraction for slugs is :

$$\alpha_{gs} = (\alpha_g - \alpha_{bub}) / (1 - \alpha_{bub}), \qquad (18)$$

where a_{bub}- void fraction of small bubbles in liquid bridges and near the wall which is determined as:

$$\alpha_{bub} = \alpha_{bs} \exp [-8 *(\alpha_g - \alpha_{bs})/(\alpha_{sa} - \alpha_{bs})], \qquad (19)$$

where α_{bs}- void fraction for the bubble-slug transition, α_{sa}- void fraction for slug-annular transition .

Liquid side interface heat flux equals to:

$$Q_{if}^{s} = 1.18942 * Re_f^{0.5} * Pr_f^{0.5} *(k_f / D) * A_s \alpha_{bub} * (T_s - T_f), \qquad (20)$$

where $Pr_f = Cp_f \mu_f / k_f$, $Re_f = \rho_f D * \min [V_f - V_g ; 0.8] / \mu_f$,

μ_f, k_f - coefficients of dynamic viscosity and heat conductivity of liquid.

Interface heat flux for bubbles is determined by the same way as for bubble regime taking into account that interface area is equal to

$$A_b = 3.6 \ \alpha_{bub} \ (1 - \alpha_s) / d_0 , \qquad (21)$$

2.3. WALL HEAT TRANSFER.

All heat flux from the wall for subcooled boiling process is consumed to vapor generation and liquid heating , so $Q_{wg} = 0$ and heat transfer coefficient is determined by modified Chen correlation.

2.4. VAPOR GENERATION RATE

Vapor generation rate on the wall is calculated as

$$\Gamma_w = q_{wf} \ A_w \ \chi / (V \ (h_{gs} - h_f)), \qquad (22)$$

where q_{wf} - heat flux from wall to liquid phase , A_w - heated surface of cell with volume V, χ - vapor generation fraction of the wall heat flux . This fraction is:

$$\chi = (h_f - h_b) / ((h_f^s - h_b) (1 + \varepsilon)), \qquad (23)$$

where

$$\varepsilon = \rho_f (h_f^s - h_b) / (\rho_g h_{fg}), \qquad (24)$$

h_b- the critical enthalpy , which is computed using Saha-Zuber formula:

$$h_b = h_f^s - St \ Cp_f / 0.0065, \text{ at } Pe > 70*10^4 , \qquad (25)$$

$$h_b = h_f^s - Nu \ Cp_f / 4.45, \quad \text{at } Pe \leq 70*10^4 , \qquad (26)$$

$$St = Nu / Pe, \quad Nu = q_{wf} D_e / k_f \ , \quad Pe = G \ D_e Cp_f / k_f \ ,$$

D_e - heated equivalent diameter, G - mass flux, Cp_f, k_f - specific heat capacity and heat conductivity of fluid.

3. ANALYSIS OF THE RELAP5/MOD3 SUBCOOLED BOILING MODEL

3.1 TESTS DESCRIPTION

All tests chosen for the comparison with calculational results were simple enough. They were carried out at steady state conditions and for simple geometry as a rule. The majority of this works were fulfilled with using the round tube as a test section [2,5-7,18]. One work was chosen to evaluate the code capability for some exotic case as [19] for very narrow flat test section. The main parameter in this tests to be compared with calculational data is the void fraction distribution along the channel or the dependence of void fraction via equilibrium quality. The accuracy of void measurement for all experiments is near equal, the method used for them is identical - γ -beam absorption method with some variations. In references 2, 4, 5 and 18 the wide beam was used that demands careful graduating. A narrow beam was used in reference 19, that allows to get a void distribution in the cross section of the channel and a more accurate mean value of void fraction. The absolute value of the void fraction error is less than 0.04 for all tests used. The other errors of this tests concerned to accuracy of the measurements of the regime parameters: pressure, inlet temperature, heat and mass fluxes. For example maximal values of regime parameters errors have been estimated in [5] as following:

$\Delta T = 2K,$
$\delta G = 0.02,$
$\delta P = 0.03,$
$\delta q = 0.01$

3.2 Comparison of calculational and experimental data

Subcooled boiling process could take place in the reactors of various type in wide enough range of regime parameters, especially in transient conditions. Therefore the assessment of the model have to be checked in wide range of parameters too and by using the large amount of the experimental data.

The results of the investigations of this process could be found in many works. A careful study of subcooled boiling was made in Russia , for example see reference [5] , where the experimental data about void fraction distribution along the round uniformly heated tube inlet diameter of 12 mm were presented.

The nodalization scheme for base case calculations for the tests described in [7] is presented at fig. 51. It consists of one element "pipe" devided in 14 subvolumes 0.1 m length each, two elements "tmdpvol" - to set the conditions at the inlet - liquid temperature and outlet of the pipe - pressure. Inlet flowrate was set at the element "tmdpjun" connecting the inlet "tmdpvol" and "pipe". Upper "tmdpvol" is connected with "pipe " through the element "sngljun". Heat structure is connected with element "pipe" and it is devided in 14 parts. First 10 parts have the internal heat sources and last 4 parts are without heating.

The calculation have been performed at "transient" mode until all parameters were not changed in time.

The experimental (from [5]) and calculational results for high pressures and mass fluxes are adduced on figures 1-6. The accordance between calculational and experimental data is good enough, but it must be noted that some underprediction of the void fraction on fig. 5-6 and some wrong account of heat flux influence in the model (fig.1 and fig.5). This test series have been fulfilled with G and P near equal but with different levels of heat flux, the latest being higher the discrepancies were higher too.

Similar data for P=11 MPa are submitted on figures 7-10. Coordination of calculational and experimental data is very good even for low flow rates (G =500 kg/m^2s, fig.7).

The results for P=7MPa and G=960-998kg/m^2s at various heat fluxes q=440-1980 KWt/m^2 are presented at fig. 11-15 and the fig. 16 is the summary schedule for this series of the experiments. Obviously that for these parameters the RELAP's model is enough truthfully reflects the parameters influence on the void fraction behavior.

Data presented on fig. 17-21 illustrate the mass flux influence on void distribution along the channel (that is equivalent to the void fraction dependence from equilibrium quality in the case of uniform heat flux distribution along the channel). Obviously that the sharp discrepancy between calculational and experimental data are presented at low flow rates G=405kg/m^2s (fig.18).

Fig. 22-24 illustrate the influence of pressure on void distribution with fixed values of mass flux G = 990 kg/m^2s [5]. Here should be paid attention on that at small voids the calculational data are little below than experimental ones and that the calculational curve has an a break at quality equals to 0.05 , which is caused by increasing of vapor drift at transition from slug to annular flow.

The analogous behavior of the void fraction have been received by using the experimental results from [4] at P= 6.8 MPa, G=419kg/m^{2}s and q = 443 KWt/m^2.

Figures 25 and 26 illustrate the void fraction behavior as Voidg(quality) and Voidg(z), where z is axial coordinate of the channel. Note here that the break of the curve was not fixed in the experimental data. At more higher mass fluxes (G = 962kg/m^{2}s) the transition between slug and annular regimes could be identified at quality equals to 0.0 as in calculations, as in experiments , though it was expressed very weak (fig.27).

The comparison of calculational and experimental data for very low flow rates is showed on fig.36- 39. Obviously that the calculational results for all considered experiments from [2] are some higher than the experimental ones the discrepancy being more depending on the inadequate description of relative motion of phases.

On fig.38 are adduced (dashed line) the calculational results with using the homogenous equilibrium model . The area of equilibrium boiling takes the large area and significant distinction between calculational (homogeneous model) and experimental data in it is stipulated only by the relative motion of phases. And , as it is visible from fig. 36-36, calculational values of vapor drift is some less, than experimental.

The region of subcooled boiling takes very insignificant area in this tests and the distinction between calculational and experimental data is caused only by the reliability of interface friction model. Obviously that vapor drift according to RELAP5/MOD3 model is considerably underestimated and more real values for void fraction one could get only with using the dependencies for annular-mist regime. It testifies in our opinion about the necessity of some updating of flow regimes map, in particular, for transition between slug and annular-mist regimes at low pressures.

As it is known the velocity difference between vapor and liquid phases increased at low pressures. Therefore it is rather interesting to evaluate the reliability of code models at a very low pressures. The comparison of calculational and experimental data for P= 1 MPa are adduced on fig.40-42. Obviously that the RELAP5/mod3 technique gives strongly overestimated results for these parameters. Especially it is visible on fig.42.

The results of calculations and experimental data from [18] for very low pressures are presented on fig.43-45 . Also the conditions of this experiments were the following: geometry of the test section - 0.5 m length annular pipe

with heated inner rod 7mm diameter and outer diameter 13 mm, pressure near the atmospheric P = 1.128 bar, mass flux - G= 1416 kg/m^2/s, heat flux - q=885KWt/m^2. The results are presented as the void fraction dependence from the fluid subcooling (fig.43). One can see that there is a very large discrepancy between the Relap and experimental data for this conditions.

The analysis of the experimental data showed that in such conditions it is very important to set the boundary conditions for pressure. In spite of the little length of the test section the outlet - inlet pressure difference is the same order as the pressure. Therefore the value of pressure given in [18] may be set at the inlet of the channel or at its outlet. The results of this calculations are shown on figure 44 .The void distribution along the channel is rather differed from each other , but for the dependence of the void fraction from equilibrium quality we have the same curves for both cases (fig. 45). That is why one must be careful when using the low pressure data and choosing of their presentation method.

It is interesting to evaluate the trustworthy of the model in some exotic geometry as used in the [19] . It was used there a very narrow flat channel 50 * 2 mm. The method enabled the distribution of the local void fraction in a cross section to be measured at about 100 locations (along 2 mm) and from these local values it was possible to determine accurate mean void fraction values. Fig. 46 demonstrates the calculational and experimental results for one of the tests with conditions : pressure P= 141.85 bar , mass flux G =750 kg/m^2/s, heat flux q=0.4 MWt/m^2. The different curves on this figure demonstrate the dependence of the calculational results for different number of cells along the channel (total length is 1.5 m) and the size of the circles around the experimental points corresponds to the experimental error of determining of mean value of void fraction. One can see that the accordance between the experimental and calculational data is good enough for such geometry too, but the Relap's data are some lower then experimental ones.

Returning to the results of [4] one can use them to evaluate also the ability of model to take into account the influence of fluid subcooling at the channel inlet at other fixed parameters and the influence of non - uniformity of heat flux distribution along the channel also.

The calculational and experimental results for three tests at inlet temperatures T=221,240 and 255 C and for increased along the channel heat flux under the low q(z)=0.397+0.801*z, P=4.4 MPa, G =1000 kg/m2/s (average heat flux equal to q=436 KWt/m2) are presented on fig.28. The RELAP model takes into account the influence of inlet temperature enough well, however as in

previous cases gives sharp change of vapor drift at transition to annular-mist flow.

The results for test with decreasing along the channel heat flux q=430 KWt/m2 and q=796.5KWt/m2 are presented on figures 29 and 30. One can see that for the test with more intensive decreasing of heat flux the calculational data being higher than experimental ones. It is obviously that the reason of this discrepancy is the nonadequate description of vapor phase condensation process in the subcooled boiling region with low heat fluxes.

As described in chapter 1 the rate of vapor generation according to RELAP5/MOD3 model is determined in main by two processes: the rate of vapor generation on the channel walls and vapor condensation in the subcooled liquid. Good enough tuning of this two values can give good results, that however does not mean that each of this processes is described enough precisely. The analysis of results , adduced on fig. 29 -30 permits to assume , that the RELAP5/mod3 model gives the underestimated rates of condensation Therefore it is rather interesting to evaluate the reliability of model at absence of vapor generation on the wall.

On fig.31-32 are presented the calculational and experimental results [7], received at research of void fraction behavior in the pipe by general length 1.5 m at step change of heat flux q=1200 kWt/m2 on length from 0 up to 1.0 m and q= 0.0 at last 0.5m. Tests were performed with different values of subcooling at the channel outlet, so for test presented on fig.32 the conditions of flow at the outlet of the channel were such that the condensation of vapor does not occur.

One can see from these figures that the discrepancy between experimental and calculational data is especially for nonheated part of the channel, and in all considered experiments the calculational rate of void fraction decreasing is less than experimental one.

It testifies that the calculational rate of condensation which is determined by interface heat flux on liquid side is essentially underestimated (the interface heat flux from vapor side in considered mode is rather small as the temperature of vapor phase is close to saturation).

During the calculation execution the increasing of values interface heat transfer coefficient H_{if} in a number of cases (especially for large subcooling) was not caused any changes of the calculational results. The conducted analysis of the algorithm has shown that it contains some limitations on interface heat flux and wall vapor generation values, which introduced into the model to make stable the numerical scheme.

One of such limitations is the "umbrella" one, which decreased the heat transfer coefficient values when void fraction is near the zero or one.

$$Hif = \min [Hif , 17539 * \max (4.724, 472.4\ \alpha_g (1- \alpha_g))] * \\ * \max [0, \min (1 , (\alpha_g - 1.0 * 10^{-10})/ (0.1 - 1.0*10^{-10}))] \quad (27)$$

This limitation realizes only by using the semi-explicit numerical scheme. The nearly-implicit scheme does not consist such limitation, therefore the results of calculations with using this two schemes differed from each other as it showed on fig. 31. Besides that the interface heat flux is limited by the condition:

$$A1= [\ \Gamma_w - H_{if} *(T_s - T_f) /h_{fg}] * \Delta t , \quad (28)$$

$$A2 = 0.5\ \alpha_g\ \rho_g\ (1- x), \quad (29)$$

$$-A1 > A2 , \quad (30)$$

that is the amount of appearing (disappearing) vapor in the volume at one time step must be less than a half of amount of vapor in this volume. The presence of such hard limitation leads to considerable lowering of interface heat transfer coefficient (for high subcoolings and large values of H_{if}) and dependence of the results from time step. The degree of H_{if} decreasing depends on ratio between the amount of disappearing vapor and its amount in volume and it is equal to

$$H_{if}^{new} = H_{if}^{old}\ A2/A1 \quad (31)$$

It must be noted that value of H_{if}^{old} is not calculated from (16-20) but is also the corrected value and it is computed from the time relaxation procedure

$$H_{if}^{old} = H_{if}^{m+1} (H_{if}^{m}/H_{if}^{m+1})^{\gamma} \quad (32)$$

$$\gamma = \exp (- 10 *\Delta t)*(1+ 0.25 (T_s - T_f)), \quad (33)$$

where H_{if}^{m+1} is calculated from (16) (20) and H_{if}^{m} is the H_{if} from previous time step. Therefore large values of interface heat transfer coefficients are reduced in

some orders and the results of calculations become independent of type of correlations used.

For regimes with low subcooling or for condensation case in the unheated part of the channel the limitations described do not play the essential role and the interface heat transfer coefficient is calculated with using Unal's formula which in our opinion doesn't describe truthfully physics of condensation process in the unheated channels, because this correlation was originally obtained for the conditions rather differed from the under consideration ones.

Field of applicability of the Unal's formula apparently must be restricted by the conditions, when the vapor bubbles are attached to the channel wall, i.e. from the location of their appearance until the departure location. The appearance location may be determined as following

$$T_w = T_s \text{ or } T_f = T_s - q_w / h_{conv},$$

and the location of vapor bubbles departure as it was shown in [17] is the same point as the point of intensive growth of vapor void fraction. This point can be determined by the Zuber- Saha formula [13]. This region is large enough and as it was estimated in [17] as

$$|x_a| = 3|x_b| ,$$

where x_a - relative enthalpy of fluid (quality) at the point of bubbles appearance and x_b - relative fluid enthalpy at the point of intensive growth of vapor fraction and calculated by Zuber-Saha formula. More reasonable in our opinion is using of correlation from [8] obtained for subcooled boiling and condensation processes and having an experimental confirmation [12].

$$St = 0.228 * Re_f^{-0.3} * Pr_f^{-0.5} * (\rho_f / \rho / (1 - \alpha_g))^{0.25} , \qquad (33)$$

where

$$St = Nu / Pe, \quad Nu = q_{wf} * D_e / k_f , \quad Pe = G \; D_e \; Cp_f / k_f ,$$

This formula was used in our calculations only for nonheated part of the pipe when the subcooling is not too high, that is for those conditions when the restrictions (31)-(32) do not deform the calculational results. The latest ones were considerably better for bubble mode. Data from [6] are presented on fig.33 for the following parameters : pressure P=7.0 MPa , mass flux G=2960 kg/s*m2 ,

heat flux q=1200kWt/m2 , inlet flow temperature T=526.5 K . The geometry of the channel : internal diameter of a channel d=12.1mm, heated length l=1.235m, unheated length l=1.235m. There are three curves on the figure: with using semi-explicit scheme, nearly implicit, and with using (16) and (33) for nonheated part of the channel (nearly-implicit scheme).

It is obviously , that the presence of "umbrella" restriction reduces the rate of condensation , other limitations on H_{if} value do not deform the results of calculations for unheated zone. We note also that in this made of flow on all length of the channel was identified on accepted the code model as a bubble one, top border of existence of which i.e. the transition from bubble to slug regime is calculated in the code according to:

$$\alpha_{bs} = \alpha_{bs}^{*} \quad , \text{ if } G < 2000 \text{ kg/m}^2\text{/s},$$

$$\alpha_{bs} = \alpha_{bs}^{*} \; [(0.5 - \alpha_{bs}^{*})/1000] \; (G-2000), \text{ if } 2000 < G < 3000 \text{ kg/m}^2\text{/s},$$

$$\alpha_{bs} = 0.5, \text{ if } G > 3000 \text{ kg/m}^2\text{/s},$$

where $\alpha_{bs}^{*} = \max[\, 0.25 \min (1.0, (0.045\, D^{*})^{8}), 0.001]$,

$D^{*} = D \, [\, g \, (\rho_f - \rho_g)/\sigma]^{0.5}$, D - hydraulic diameter, σ – surface tension coefficient. The most reasonable results , well agreed with experimental data were obtained by use of the formula (33).

For low mass fluxes (G < 2000) and regime parameters and geometry under consideration the (34) gives the α_{bs}=0.001 that contradicts in our opinion to experimental data. So for example according to a map used in the code RETRAN [9] ,for a given mass fluxes this value is α_{bs}=0.2-0.4 in code TRAC α_{bs}=0.3-0.5 that will be agreed with experimental data [11], [15-16] and theoretical prediction [14].

Share of bubbles in slug regime is defined as

$$\alpha_{bub} = \exp [\, - 8 * (\alpha_g - \alpha_{bs}) / (\alpha_{sa} - \alpha_{bs})] * \alpha_{bs} \qquad (35)$$

As follows from α_{bub} in slug mode aims to zero very quickly and at α_{bs}=0.001 this value are actually away, at that the interface heat flux from bubbles has the main contribution on total heat flux from interface to liquid (due to considerably greater area of interface surface).

The validation of influence of change of α_{bs} on the condensation rate was conducted. The void fraction profiles along the channel are presented on fig.34 for the parameters P=7.0 MPa, G = 730 kg/s m^2, q= 618 kWt/m^2, T_{inlet}= 492 K and geometry as for fig. 33. The calculations were carried out with using the "nearly-implicit" numerical scheme and with α_{bs}=0.2, respectively increased values of H_{if} for non-heated part.

Curve 1 on this figure shows the results of original model , curve 2 - the results with α_{bs}=0.2. More better accordance for latest case testifies about the presence of bubble flow regime in the nonheated part of the channel and that the corrected value of α_{bs}=0.2 is more reasonable. As was marked earlier the correlation (33) in the regime with presence of bubbles may give some better results. Curve 3 shows the behavior of void fraction by use (33) instead of (16) in the unheated part of the channel and at α_{bs}=0.2. In both latest cases the interface heat transfer coefficient are higher and the calculated data are more close to experimental ones.

The results of experiments of [7] has been obtained with test section of 1m long unheated and 0.4m heated parts and inner diameter 12.03mm. The experimental and calculational results of test with following parameters: P=6.95 MPa , G=980 kg/s m^2, q=824 kWt/m2, Tinlet=504 K are presented on fig.35. The marks on this figure are the same as on previous one. One can see that the change of the transition from bubbles to slug regimes causes the more good accordance between the experimental and calculational data and the rate of condensation is increased by using (33).

It seems logical to make the system of closer equations for vapor generation and condensation terms for both parts of the channel including the heated zone. But such attempts were unsuccessful , because it is impossible to receive the reasonable values of the parameters because of excess of 50% limit on condensation and vaporization rates. The attempts of soften this conditions resulted in catastrophic growth of parameters oscillations.

4. SENSITIVITY ANALYSIS

The conducted calculations showed that the heaviest inlet parameters influence on the results were the regimes with vapor condensation in the unheated zone of channel. Therefore the sensitivity analysis results are presented for such conditions in main.

The data of void distribution for the experiments from [7] are presented at fig. 47, where the results for different number of subvolumes are presented. Obviously that for number of subvolumes greater then N=14 , (that corresponds to the subvolumes length $\Delta z = 0.1$ m) the calculational results do not practically change. Therefore all the calculations had been conducted with approximately such sizes of subvolumes.

The results of calculations, showed the influence of inlet temperature error are presented at fig. 48. As a rule this value was approximately 1 K. Obviously that the calculational results depend strongly on this value.

The influence of heat flux error on void distribution along the channel is presented in fig. 49. For the experiments from [7] the maximum value of relative error of heat flux measurements makes $\delta q = 3\%$. Obviously that this error gives the maximal contribution on the void fraction distribution along the channel.

Other errors - mass flow and pressure ones have much smaller influence in the α_g behavior at given parameters. However, as was indicated earlier, the influence of pressure error increases for low pressures. Moreover as was found out, the influence of time step on the results increases at low pressures also.

We note that practically all made calculations which were conducted by use the RELAP 5 /mod 3 version 5m5 were repeated by use of RELAP5/mod 3 version 7j and RELAP5 / mod3.1 codes. The calculational results of this two codes, as has appeared, coincide by the RELAP5 /mod 3 version 5m5 code results, but it was found out that at low pressures 9 for [18] tests at the same time step the latest two codes may give nonphysical void distribution (fig. 50) along the channel which one can remove by reducing of time step value.

5. RUN STATISTICS

All the calculations were carried out with computer IBM PC-386 and only small part of them with IBM RISK 6000 computer to evaluate the possible difference between the results. The most part of calculations have been performed with time step Δt =0.05s, which guarantees the absence of parameters oscillation and dependense of calculational results from time step. Further decreasing of time step have no influence on the results. Therefore the plot of time steps as a function of real transient time is simple constant function Δt =0.05s and it is not provided in this report.

Typical grind time for IBM PC-386 computer was

(CPU time)*10^3 /((Number of volumes) (Number of time steps)) =

= 35*10^3 /(14*150) = 8.3

For IBM RISK 6000 grind time was 1.08.

6. CONCLUSIONS

Trustworthiness of RELAP5/mod3 version 5m5 models for subcooled boiling process was verified using a lot of experimental data. It was found out that the code models give good enough results for uniformly heated channels except of very low pressure case. For more complicated lows of power distribution along the channel the rates of vapor generation and condensation are not compatible and the discrepancies between calculational and experimental data become too large. The main causes of this are the limitations of heat transfer rate terms implemented into the code due to imperfections of code numerical scheme.

REFERENCES

1. Carlson K.E . et al . RELAP5/Mod3 Code Manual, vol. 1, - NUREG/CR-5535, 1990., Idaho.
2. Rouhani S.Z., Axelsson E. Calculation of Void Volume Fraction in Subcooled and Quality Boiling Regions, - International Journal of Heat and Mass Transfer, V.13, pp. 383-393.
3. Marchaterre J.F. Natural and Forced Circulation Boiling Studies, - ANL-5735, May, 1960.
4. Bartolomey G.G., Sabotinov L. S. Void fraction at subcooled boiling at different heat distribution lows along the channel. Nuclear Energy, 1976, N3, Sofia, (in Bulgarian).
5. Bartolomey G.G. et al. Experimental investigation of void fraction at subcooled boiling mode in tubes. Teploenergetika, 1982, N3, pp. 20-22. (in Russian).
6. Labuntsov D.A. et al. Void fraction investigation of nonequilibrium two-phase flows. ENIN transactions, Heat transfer and hydrodynamics, v. 35. pp. 88-98. (in Russian).
7. Bartolomey G.G. Void fraction of diabatic flows in tubes at different heat distribution lows. Heat and mass transfer - VI, International Conference, Minsk, 1980, v.5, pp. 38-43.
8. Avdeev A.A., Pehterev V.P. Subcooled boiling of liquid at forced convection conditions, High Temperature Thermal Engineering, 1986, v.24, N5, pp. 912-920.(in Russian).
9. RETRAN -02 - A Program for Transient Thermal-Hydraulic Analysis of Complex Fluid Flow Systems, EPRI NP-1850-CCMA, V.1, 1984.
10. TRAC-PF1 - An Advanced Best Estimate Computer Program for Pressurized Water Reactor Analysis. NUREG/CR - 3567, LA-9944-MS, Los Alamos, 1984.
11. Bennet A.W. Hewitt G.F. , - Flow Visualization Studies of Boiling Water at High Pressure, AERE-R 4874, 1965.
12. Avdeev A.A Reynolds analogy application for subcooled boiling process at forced convection conditions. High Temperature Thermal Engineering, 1986,v.24,N1, pp. 111-119. (in Russian).
13. Saha P., Zuber N., Point of Net Vapor Generation and Vapor Void Fraction in Subcooled Boiling, - Proc. 5-th Intern. Heat Transfer Conf., Tokyo, 1974, v.4, pp. 175-179.

14. Mishima K., Ishii M., Flow Regime Transition Criteria for Upward Two-phase Flow in Vertical Tubes. International Journal of Heat and Mass Transfer, V.27, N5, pp.723-737, 1984.
15. Hosler E.R., Flow Patterns in High Pressure Two-phase Flow with Heat Addition., Chem. Eng. Symp. Ser., V.64, N82, p.54, 1968.
16. Doroschuc V.E., Borevsky L.Ja., Levitan L.L., Holographic Investigation of Steam-water Flows in Heated and Unheated Channels. Heat Transfer. 1982. Proc. VII Intern. Heat Transfer Conference, Munich, 1982, V.5, pp. 277-281.
17. Bartolomey G.G. Mihailov V.N. Intensive vapor production beginning enthalpy. -Teploenergetica, 1987, N2, pp. 17-20. (in Russian).
18. Evangelisti R., Lupoli P. The void fraction in an annular channel at atmospheric pressure. - International Journal of Heat and Mass Transfer, 1969, v.12, №6, pp. 699-711.
19. Martin R. Measurement of the Local Void Fraction at High Pressure in a Heated Channel, - Nuclear Science and Engineering, 1972, v.48, №2, pp.125-138.
20. Unal H.S. Maximum Bubble Diameter, Maximum Bubble-Growth Time and Bubble-Growth Rate During the Subcooled Boiling of Water up to 17 Mn/m^2 , - International Journal of Heat and Mass Transfer, v.19,1976, pp. 643-649.

Appendix 1

Input Deck for BARTOLOMEY Experiment

APPENDIX 1
INPUT DECK FOR BARTOLOMEY EXPERIMENT

```
= pipe BARTOLOMEY TEST WITH CONDENSATION
0000100   new   transnt
*-------------------------------------------------
*       end  dtmin dtmax
0000201 30.0 1.0-7  0.025   00011   5  100000  100000
*-------------------------------------------------
0000301  p   004010000
0000302  p   004140000
0000303 quals 004010000
0000304 quals 004140000
0000305 velfj 004010000
0000307 velg  004140000
0000308 velf  004140000
0000309 voidg 004140000
0000310 quale 004140000
0000312   ug 004140000
0000313   uf 004140000
0000314 tempf 004140000
0000315 tempg 004140000
*=================================================
*           component 002
*
*-------------------------------------------------
0020000   inlet   tmdpvol
*
*         vol area   vol length   vol vol  ahor  aver  elev   rough  dhy
0020101   1.13606-4  0.075          0     0     90.0  0.075  1.0-4   0     0
*
*          ebt
0020200    003
*
*        time  pres      temp
0020201  0.0  6.9600+6  504.0
*
*=================================================
*           component 003
*
*-------------------------------------------------
0030000  inlet  tmdpjun
*
*        from             to        area
0030101 002000000   004000000  1.13606-4
*
0030200  1
*
*        time    flowf    flowg
0030201  0.0     0.1113    0.0  0.0 **
*=================================================
```

```
*          component 004
*          work pipe
*-------------------------------------------------------------
0040000  tube   pipe
0040001   14   * nvol
*
*          vol  area   vol no
0040101   1.13606-4      14
*
*        vol length  vol no
0040301   0.1000       14
*
*         aver       vol no
0040601   90.0         14
*
*        rough      dhy       vol no
0040801   1.0-4      0.0       14
*
*        floss        rloss   jun no
0040901   0.0          0.0     13
*
*          pvbfe                vol no
0041001   00000                  14
*
*          fvcahs               jun no
0041101   001000                 13
*
*          ebt     press     temp
0041201   103     6.9600+6    504.0   0   0   0    14
*
*         flowf    flowg    win   jun no
0041301   0.1113    0.00     0.0   13
*
*=============================================================
*          component 005
*
*-------------------------------------------------------------
0050000  outlet   sngljun
*
*          from          to             area    floss   rloss   fvcahs
0050101   004010000   006000000    1.13606-4   0       0      001000
*
*              flowf      flowg       win
0050201    1   0.1113      0.00        0.0
*=============================================================
*          component 006
*
*-------------------------------------------------------------
0060000  outlet   tmdpvol
*
*          vol  area    vol length   vol vol  ahor   aver   elev  rough   dhy
0060101    1.13606-4    0.2            0      0     90.0    0.2   1.0-4     0   0
*
*      ebt
```

```
0060200  102
*
*          time    pres      x
0060201  0.0   6.9600+6  0.000
*
*
*=============================================================================
*            component 008
*            work pipe
*-----------------------------------------
*
*           nh  np  geom st-st   left
10080000    14  11  2       1     6.015-3
*
10080100    0   1
*
10080101    10      7.015-3
*
10080201    1       10
*
10080301    1.0     10
*
10080400    0
*
10080401    500.0       11
*
10080501    004010000  010000    1       1   0.1     14
*
10080601    0               0     2701    1   0.1     14
*
10080701      025   0.1   0   0    10
10080702      025   0.0   0   0    14
*
* left        chf    lhf   lhb    gslf gslr glcf  gcr bf   no
10080801      1.2-2   20.  20.     0.  0.   0.   0.  1.   14
*
10080901      1.60-2  20.  20.     0.  0.   0.   0.  1.   14
*-----------------------------------------------------------------------------
*-----------------------------------------------------------------------------
20270100       htmrate
*
20270101        0.0       0.0    * without heat losses
20270102       1.0e6      0.0
*-----------------------------------------------------------------------------
20100100      s-steel
*-----------------------------------------------------
20202500    power
*
*
20202501    0.0       3.112594+4
20202502    2.0       3.112594+4
20202503    11.0      3.112594+4
20202504    1.0+6     3.112594+4
     end  of  input  deck
```

Appendix 2

Figures

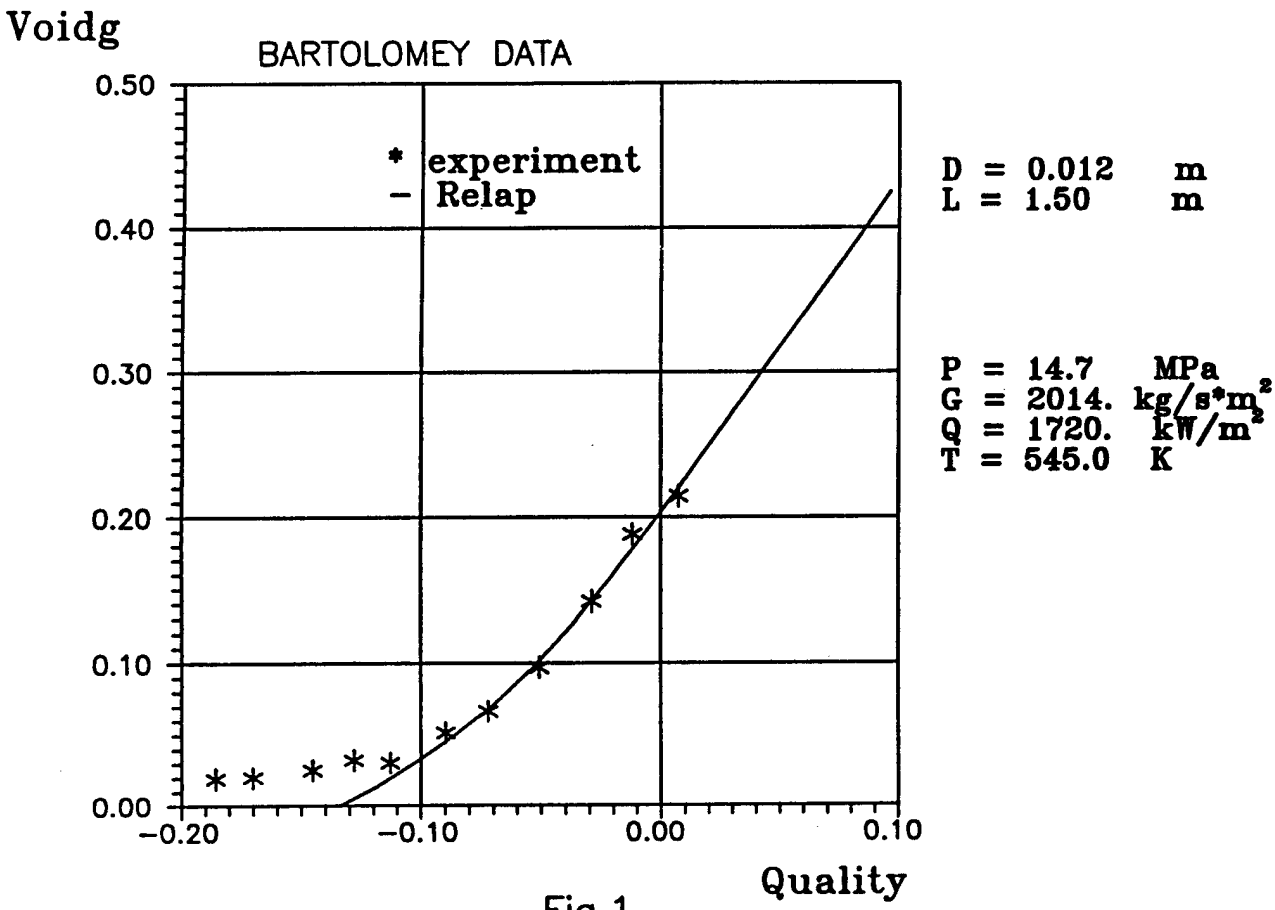
Voidg
BARTOLOMEY DATA
0.50
0.40
0.30
0.20
0.10
0.00
* experiment
– Relap
D = 0.012 m
L = 1.50 m
P = 14.7 MPa
G = 2014. kg/s*m²
Q = 1720. kW/m²
T = 545.0 K
−0.20
−0.10
0.00
0.10
Quality

Fig.1

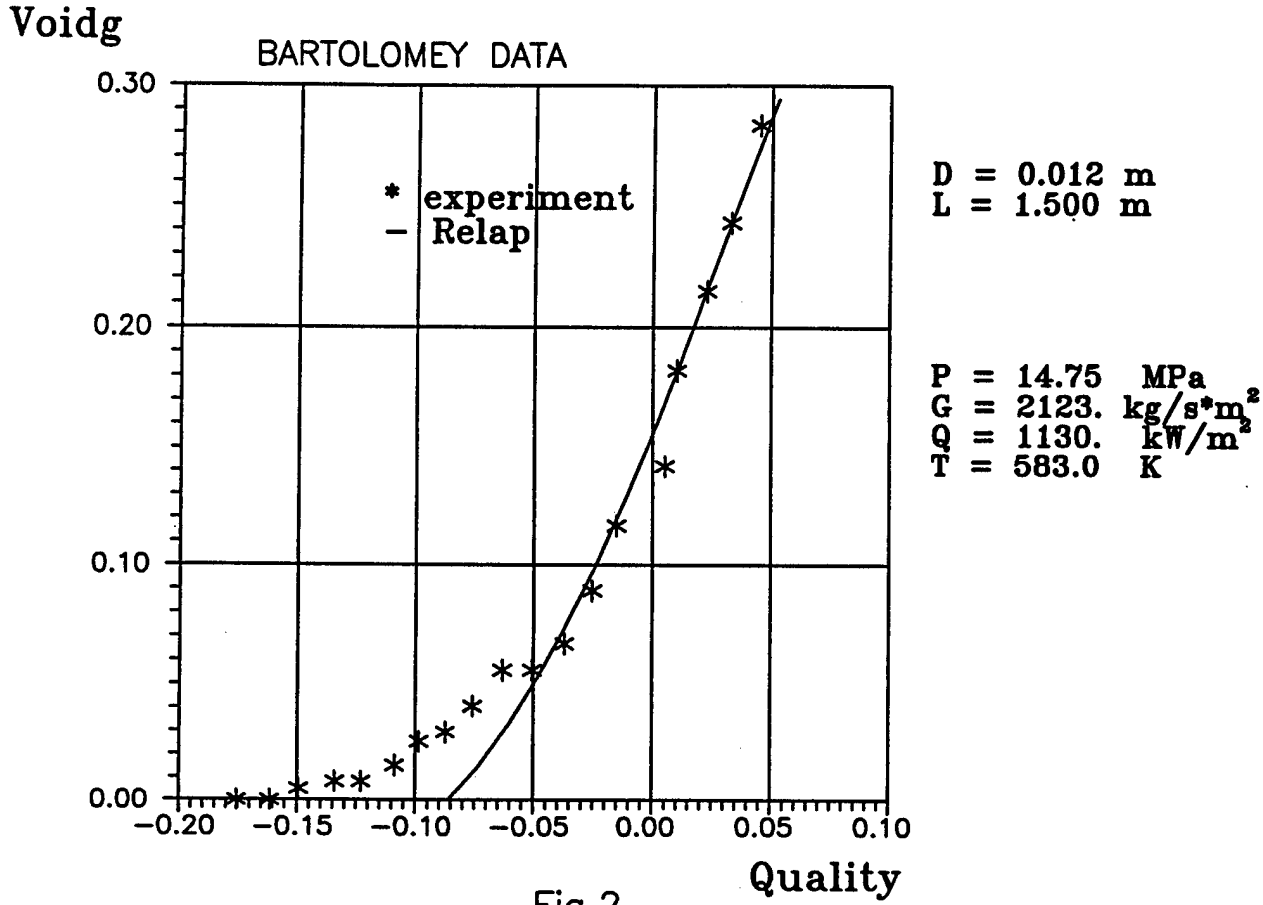
Voidg
BARTOLOMEY DATA
0.30
0.20
0.10
0.00
* experiment
– Relap
D = 0.012 m
L = 1.500 m
P = 14.75 MPa
G = 2123. kg/s*m²
Q = 1130. kW/m²
T = 583.0 K
−0.20
−0.15
−0.10
−0.05
0.00
0.05
0.10
Quality

Fig.2

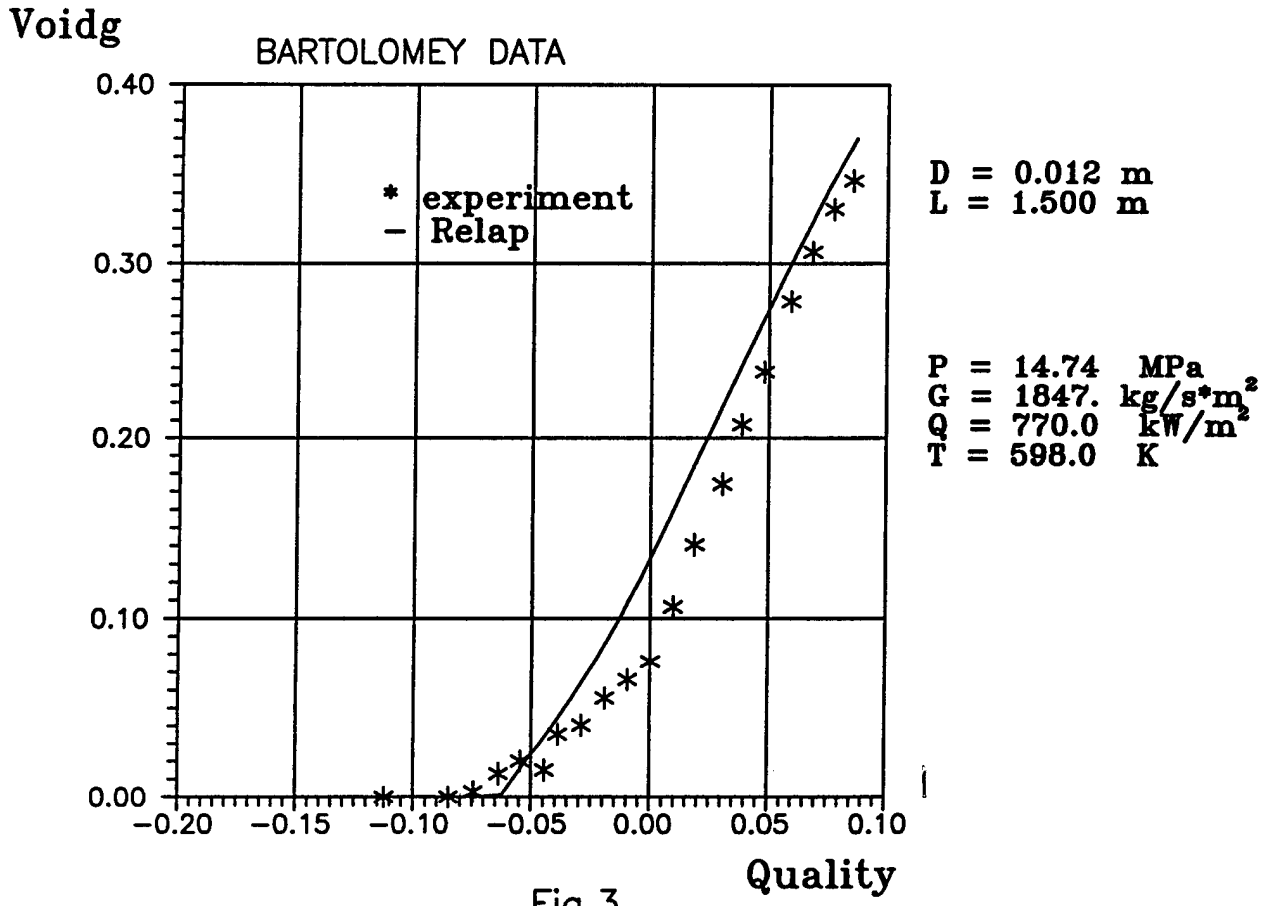
Voidg
BARTOLOMEY DATA
0.40
0.30
0.20
0.10
0.00
* experiment
– Relap
−0.20
−0.15
−0.10
−0.05
0.00
0.05
0.10
Quality
D = 0.012 m
L = 1.500 m
P = 14.74 MPa
G = 1847. kg/s*m²
Q = 770.0 kW/m²
T = 598.0 K

Fig.3

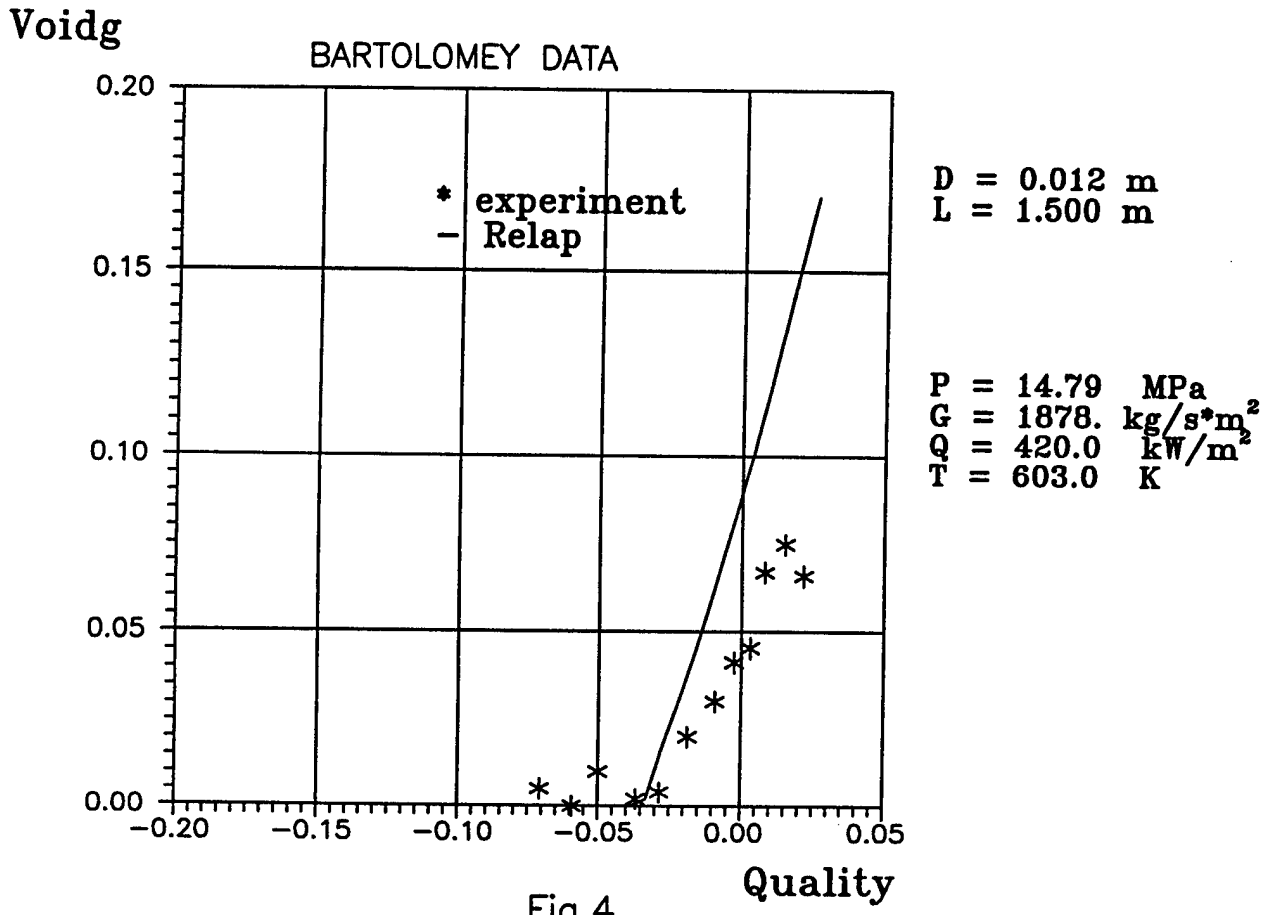
Voidg
BARTOLOMEY DATA
0.20
0.15
0.10
0.05
0.00
−0.20
−0.15
−0.10
−0.05
0.00
0.05
Quality
* experiment
– Relap
D = 0.012 m
L = 1.500 m
P = 14.79 MPa
G = 1878. kg/s*m²
Q = 420.0 kW/m²
T = 603.0 K

Fig.4

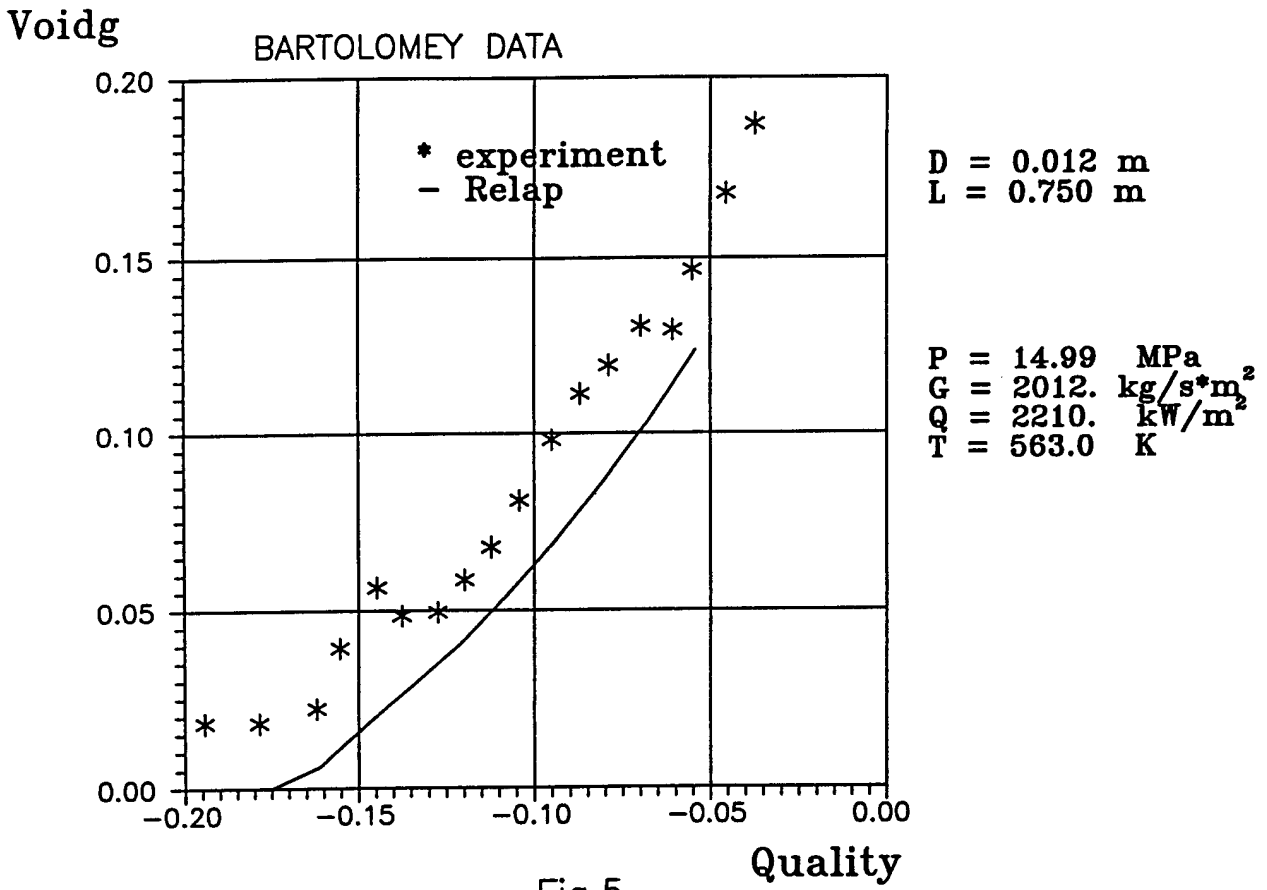
Voidg
BARTOLOMEY DATA
0.20
0.15
0.10
0.05
0.00
* experiment
– Relap
D = 0.012 m
L = 0.750 m
P = 14.99 MPa
G = 2012. kg/s*m2
Q = 2210. kW/m2
T = 563.0 K
−0.20
−0.15
−0.10
−0.05
0.00
Quality

Fig.5

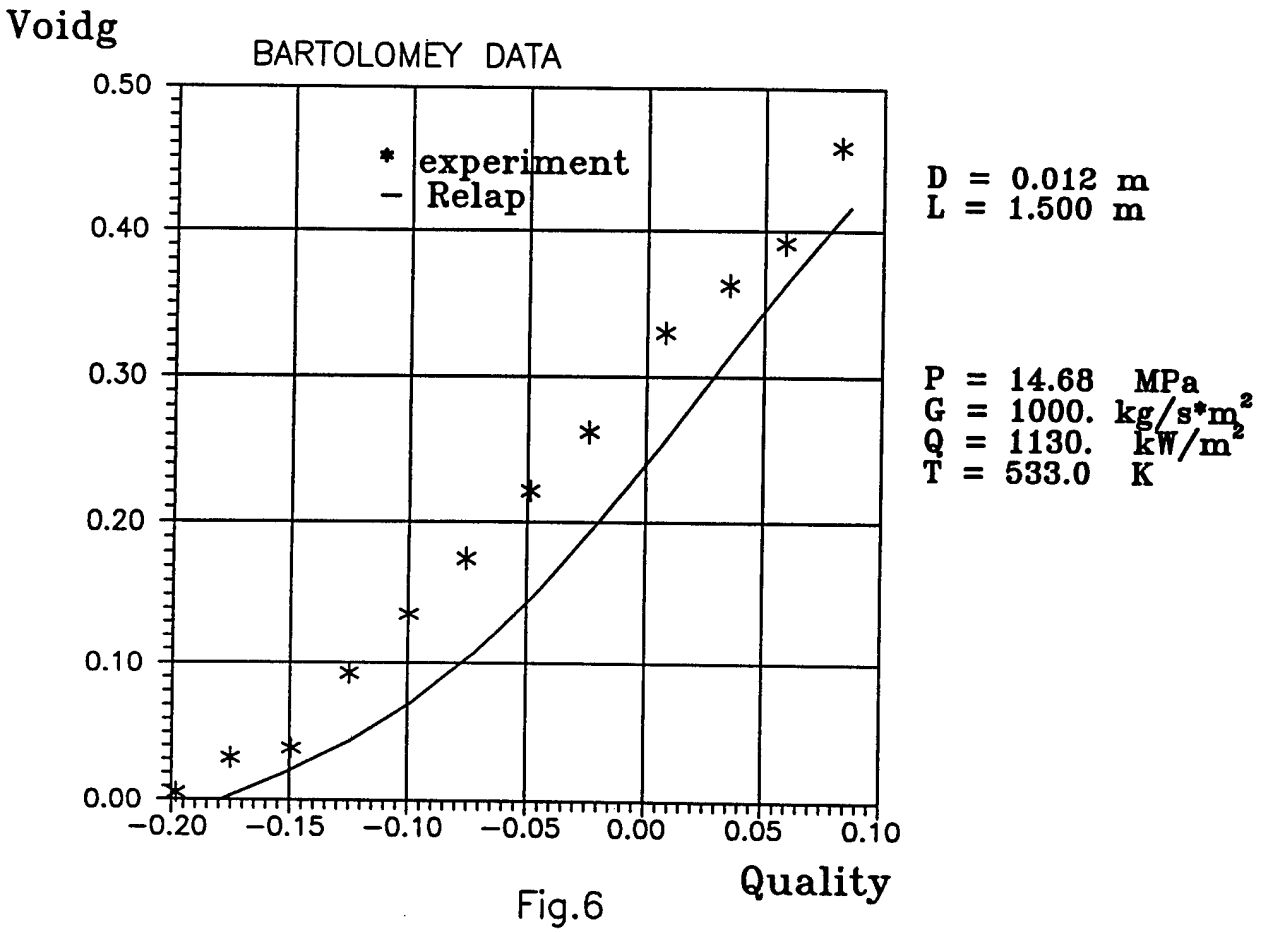
Voidg
BARTOLOMEY DATA
0.50
0.40
0.30
0.20
0.10
0.00
* experiment
– Relap
−0.20
−0.15
−0.10
−0.05
0.00
0.05
0.10
Quality
D = 0.012 m
L = 1.500 m
P = 14.68 MPa
G = 1000. kg/s*m²
Q = 1130. kW/m²
T = 533.0 K

Fig.6

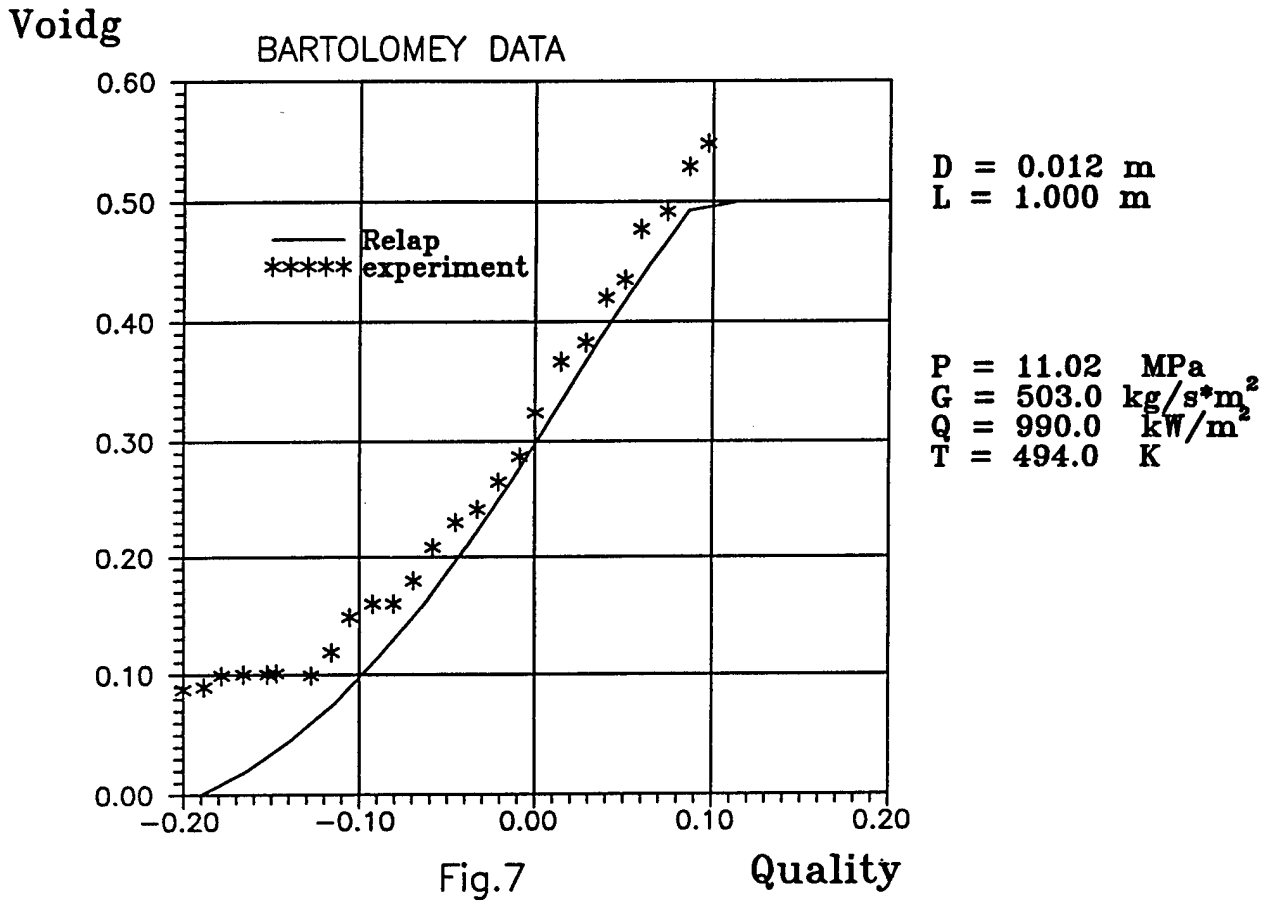
Voidg
BARTOLOMEY DATA
0.60
0.50
0.40
0.30
0.20
0.10
0.00
Relap
experiment
−0.20
−0.10
0.00
0.10
0.20
Quality
D = 0.012 m
L = 1.000 m
P = 11.02 MPa
G = 503.0 kg/s*m²
Q = 990.0 kW/m²
T = 494.0 K

Fig.7

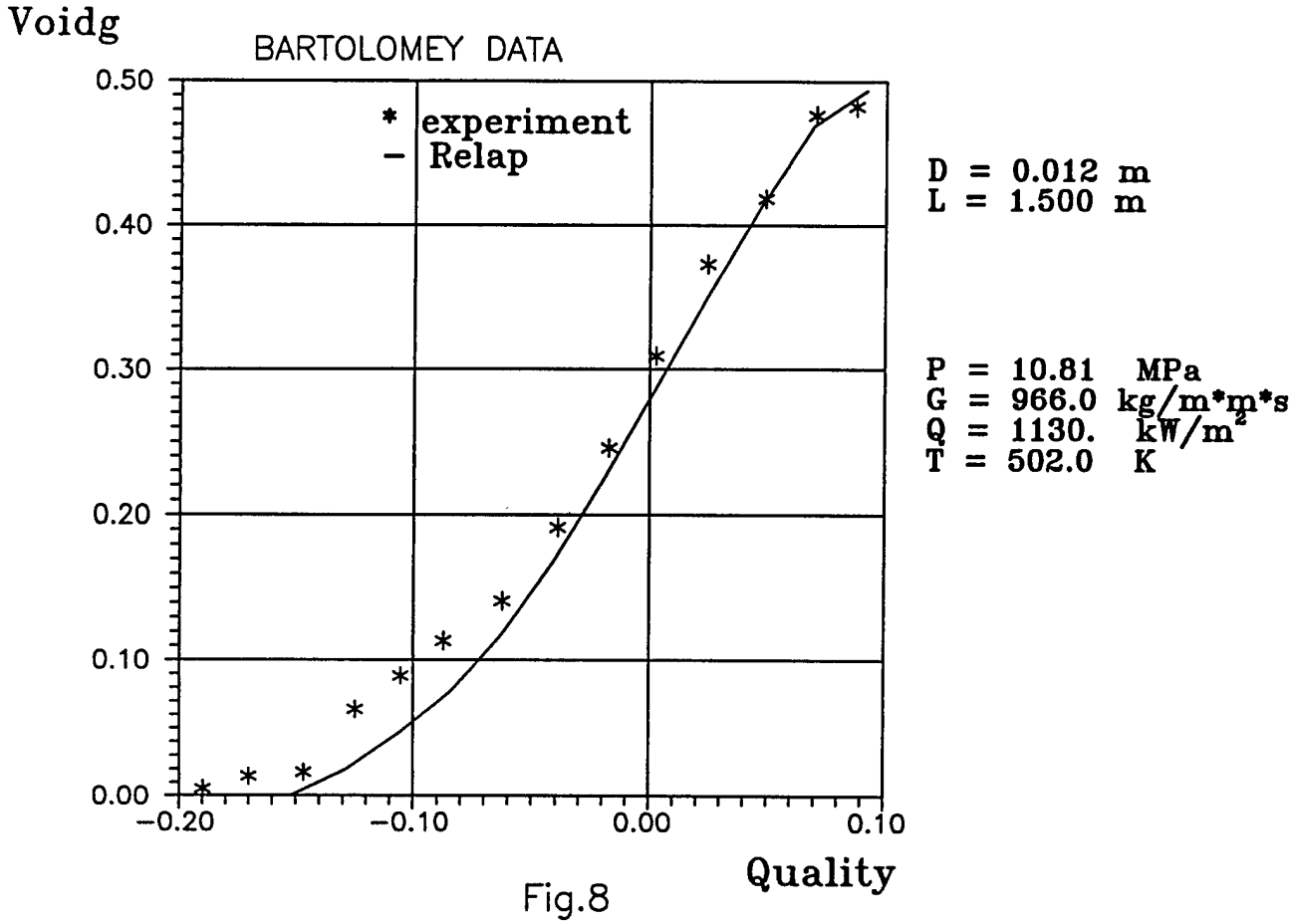
Voidg
BARTOLOMEY DATA
* experiment
– Relap
0.50
0.40
0.30
0.20
0.10
0.00
−0.20
−0.10
0.00
0.10
Quality
D = 0.012 m
L = 1.500 m
P = 10.81 MPa
G = 966.0 kg/m*m*s
Q = 1130. kW/m²
T = 502.0 K

Fig.8

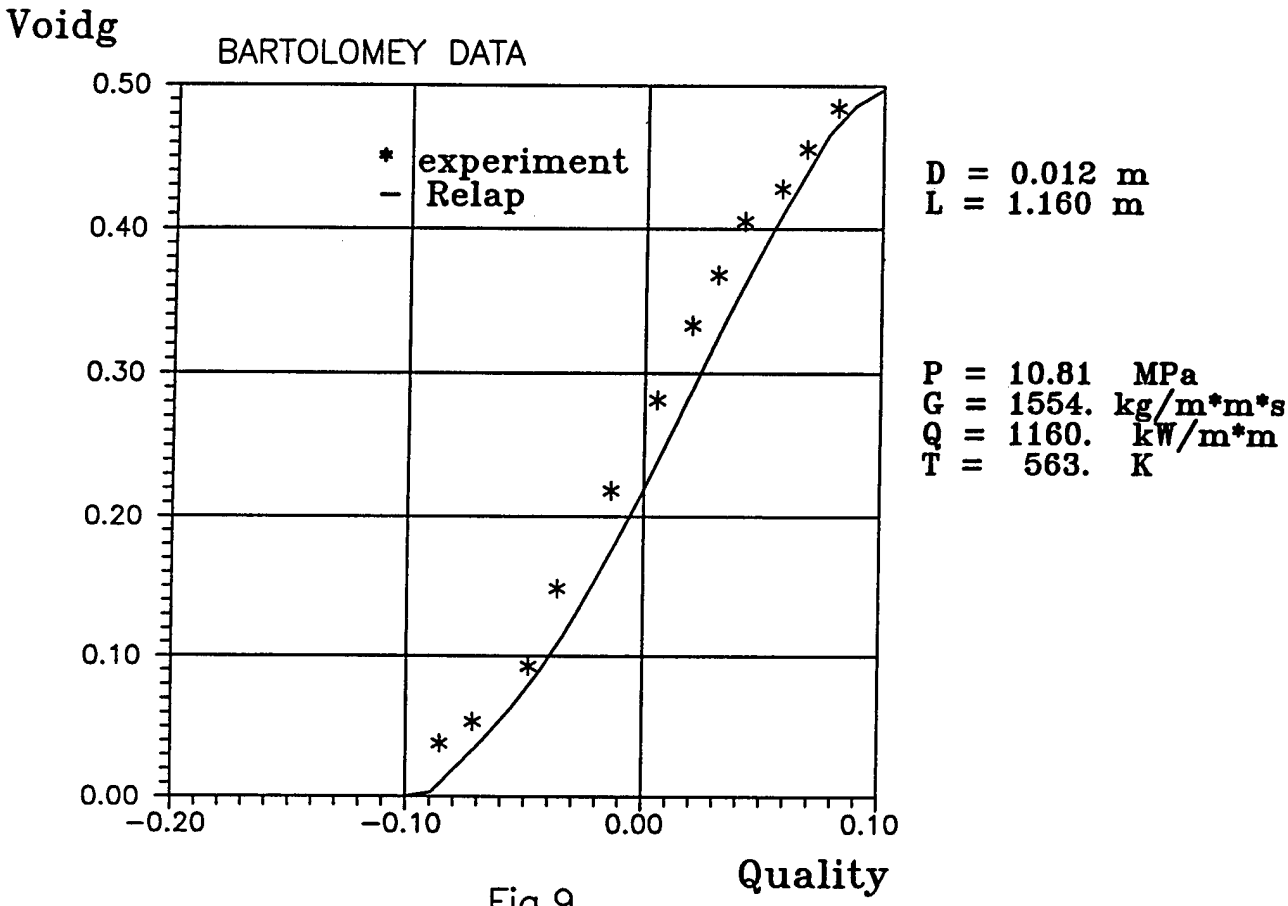
Voidg
BARTOLOMEY DATA
0.50
0.40
0.30
0.20
0.10
0.00
* experiment
– Relap
−0.20
−0.10
0.00
0.10
Quality
D = 0.012 m
L = 1.160 m
P = 10.81 MPa
G = 1554. kg/m*m*s
Q = 1160. kW/m*m
T = 563. K

Fig.9

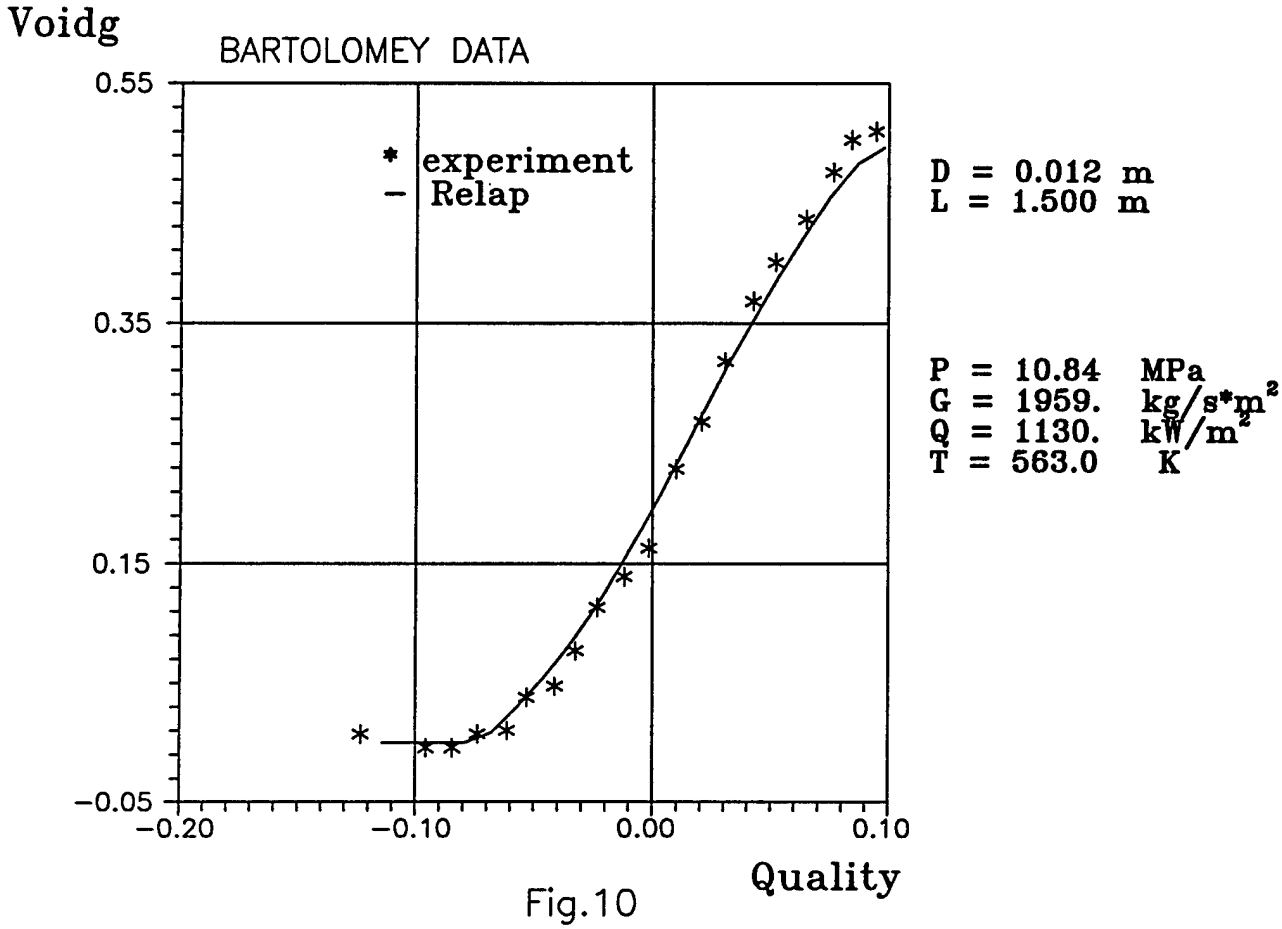
Voidg
BARTOLOMEY DATA
0.55
0.35
0.15
−0.05
−0.20
−0.10
0.00
0.10
Quality
* experiment
– Relap
D = 0.012 m
L = 1.500 m
P = 10.84 MPa
G = 1959. kg/s*m²
Q = 1130. kW/m²
T = 563.0 K

Fig.10

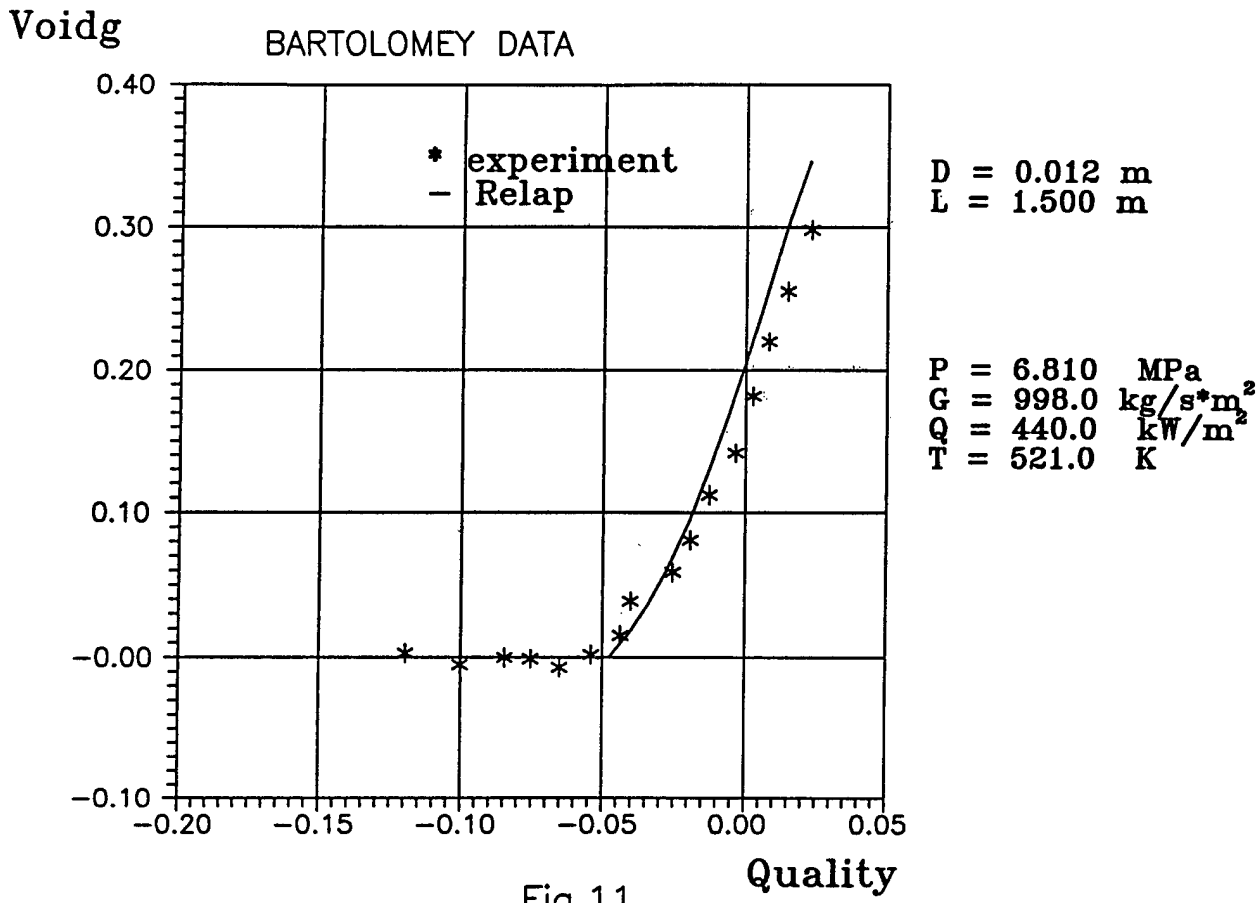
Voidg
BARTOLOMEY DATA
0.40
0.30
0.20
0.10
−0.00
−0.10
* experiment
– Relap
D = 0.012 m
L = 1.500 m
P = 6.810 MPa
G = 998.0 kg/s*m²
Q = 440.0 kW/m²
T = 521.0 K
−0.20
−0.15
−0.10
−0.05
0.00
0.05
Quality

Fig.11

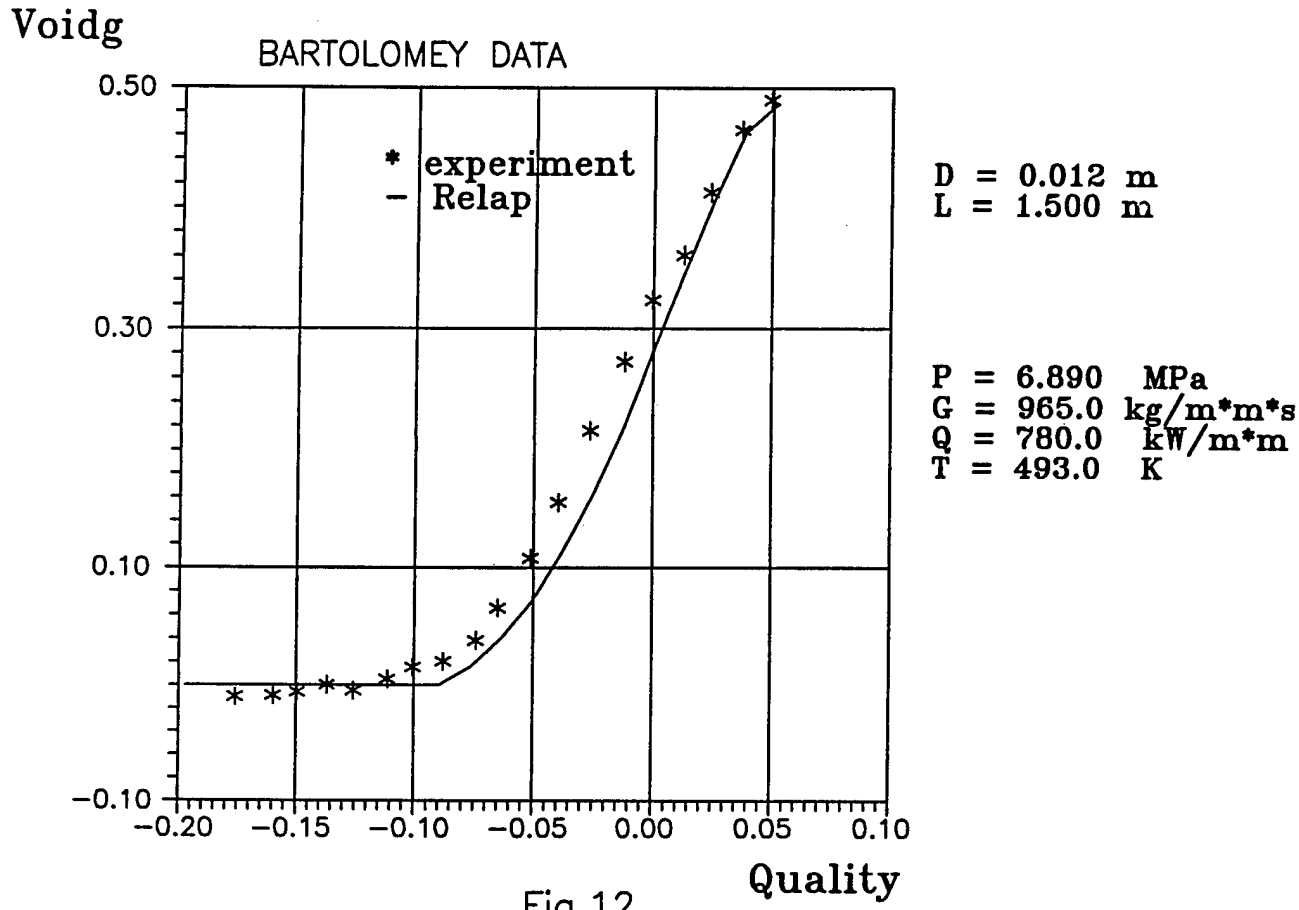
Voidg
BARTOLOMEY DATA
0.50
0.30
0.10
−0.10
* experiment
– Relap
D = 0.012 m
L = 1.500 m
P = 6.890 MPa
G = 965.0 kg/m*m*s
Q = 780.0 kW/m*m
T = 493.0 K
−0.20
−0.15
−0.10
−0.05
0.00
0.05
0.10
Quality

Fig.12

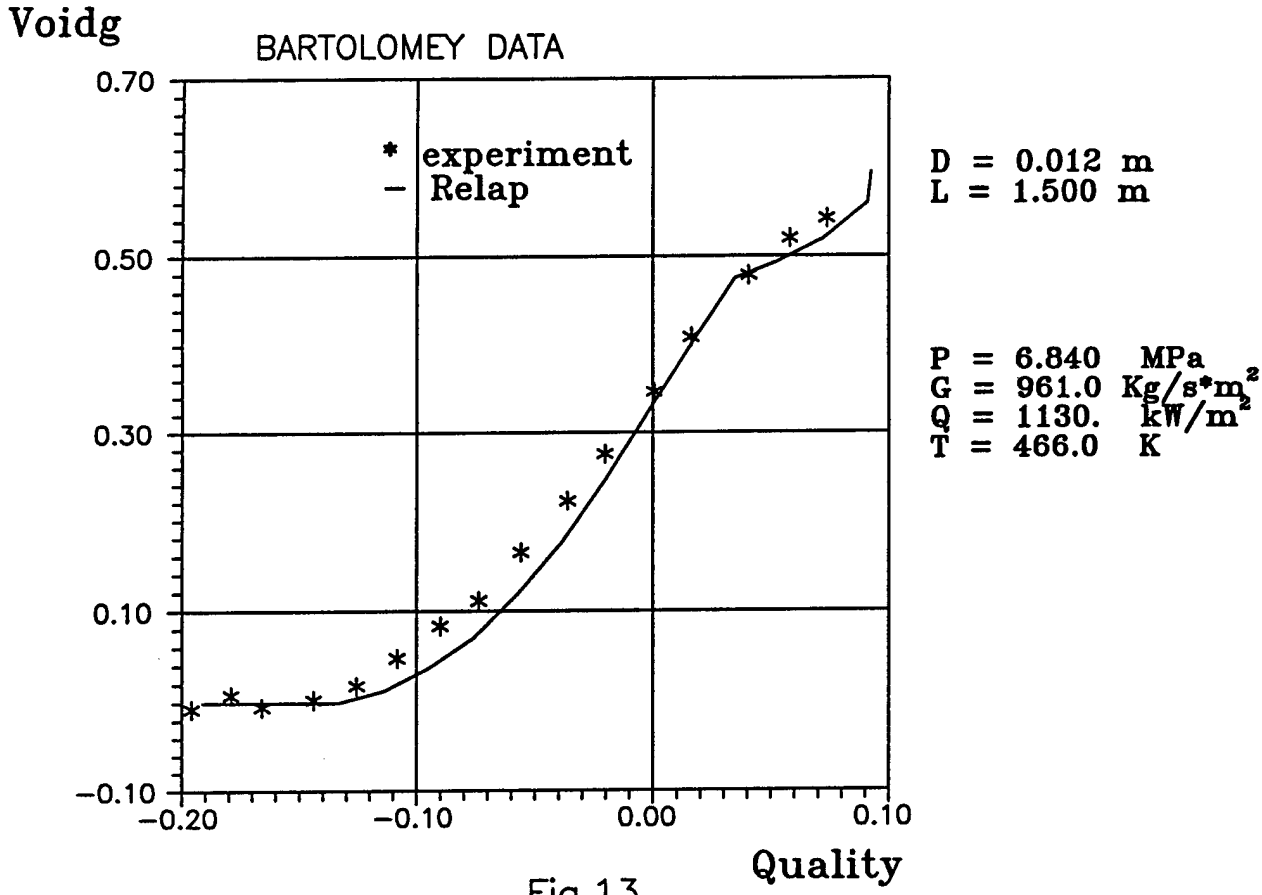
Voidg
BARTOLOMEY DATA
0.70
0.50
0.30
0.10
−0.10
−0.20
−0.10
0.00
0.10
Quality
* experiment
– Relap
D = 0.012 m
L = 1.500 m
P = 6.840 MPa
G = 961.0 Kg/s*m²
Q = 1130. kW/m²
T = 466.0 K

Fig.13

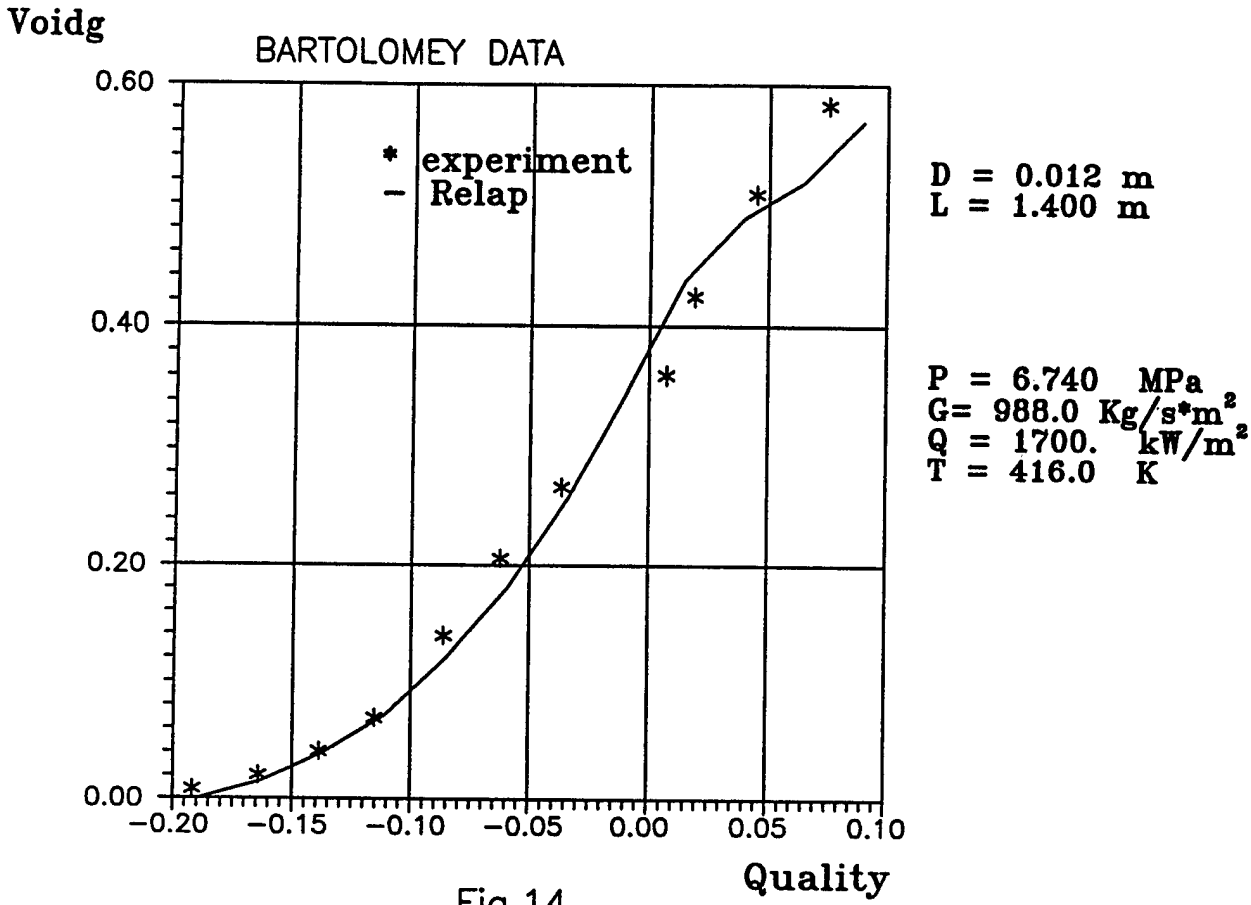
Voidg
BARTOLOMEY DATA
0.60
0.40
0.20
0.00
* experiment
– Relap
D = 0.012 m
L = 1.400 m
P = 6.740 MPa
G= 988.0 Kg/s*m²
Q = 1700. kW/m²
T = 416.0 K
−0.20
−0.15
−0.10
−0.05
0.00
0.05
0.10
Quality

Fig.14

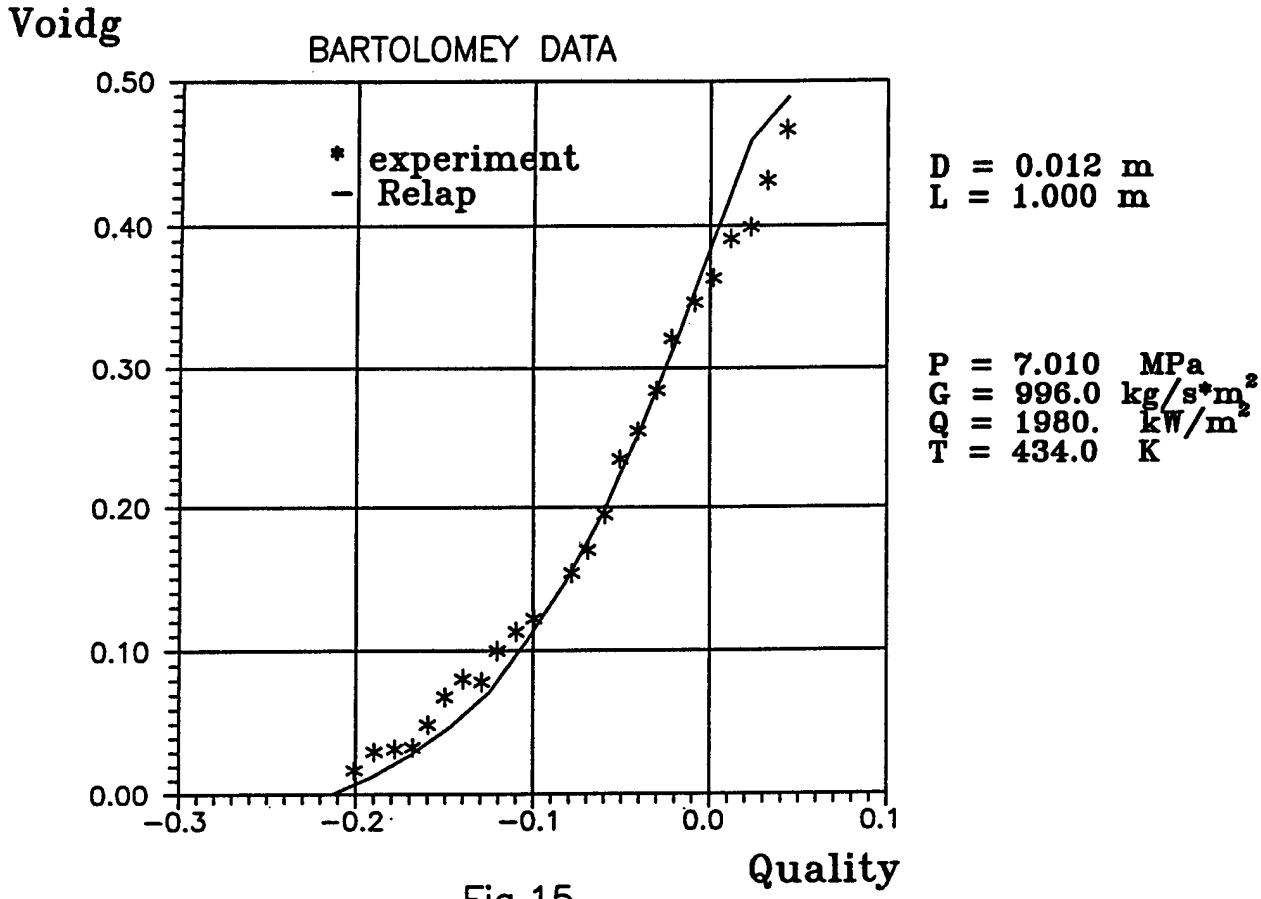
Voidg
BARTOLOMEY DATA
0.50
0.40
0.30
0.20
0.10
0.00
* experiment
– Relap
D = 0.012 m
L = 1.000 m
P = 7.010 MPa
G = 996.0 kg/s*m²
Q = 1980. kW/m²
T = 434.0 K
−0.3
−0.2
−0.1
0.0
0.1
Quality

Fig.15

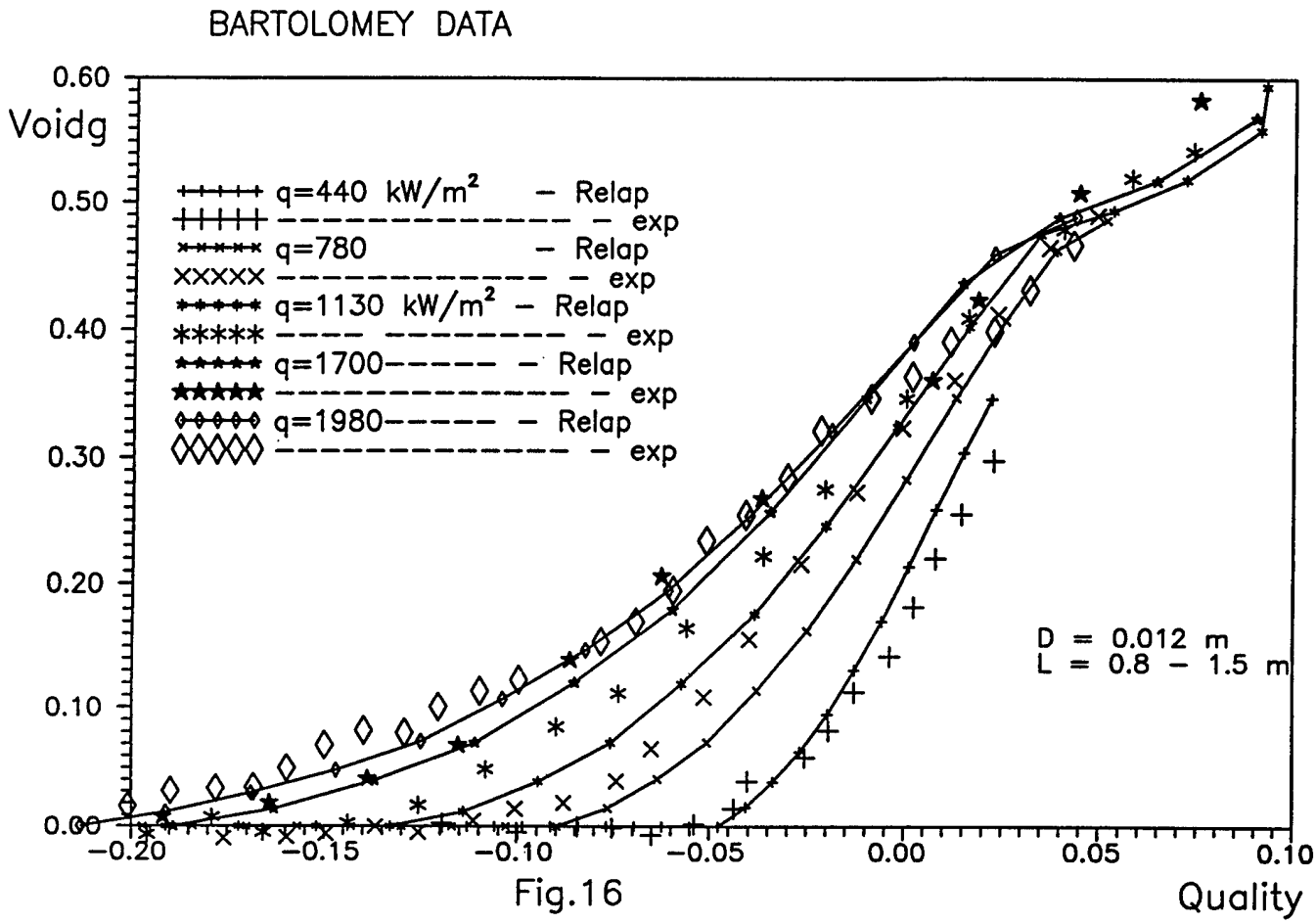
BARTOLOMEY DATA
Voidg
0.60
0.50
0.40
0.30
0.20
0.10
0.00
q=440 kW/m² – Relap
– exp
q=780 – Relap
– exp
q=1130 kW/m² – Relap
– exp
q=1700 – Relap
– exp
q=1980 – Relap
– exp
D = 0.012 m
L = 0.8 – 1.5 m
−0.20
−0.15
−0.10
−0.05
0.00
0.05
0.10
Quality

Fig.16

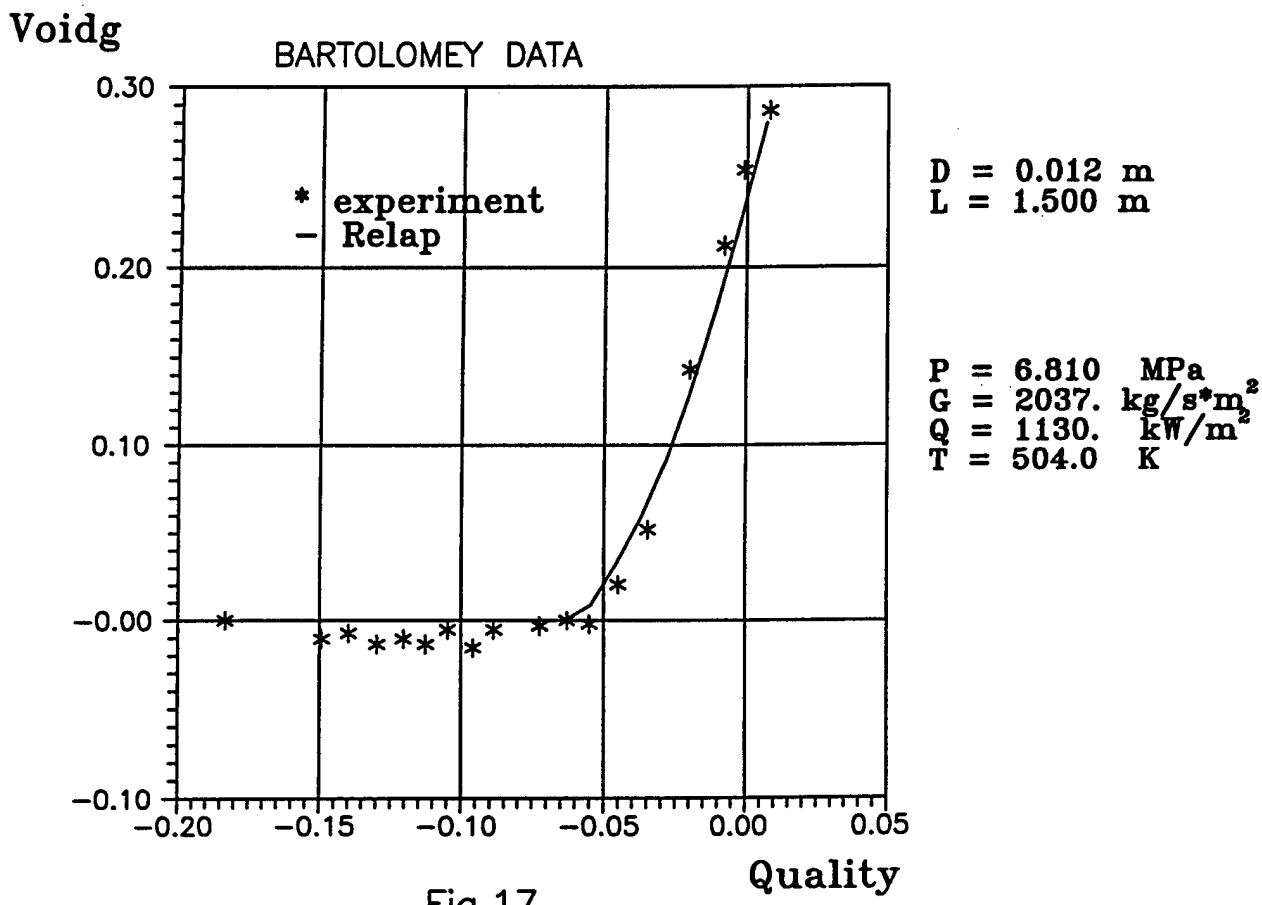
Voidg
BARTOLOMEY DATA
0.30
0.20
0.10
−0.00
−0.10
−0.20
−0.15
−0.10
−0.05
0.00
0.05
Quality
* experiment
– Relap
D = 0.012 m
L = 1.500 m
P = 6.810 MPa
G = 2037. kg/s*m²
Q = 1130. kW/m²
T = 504.0 K

Fig.17

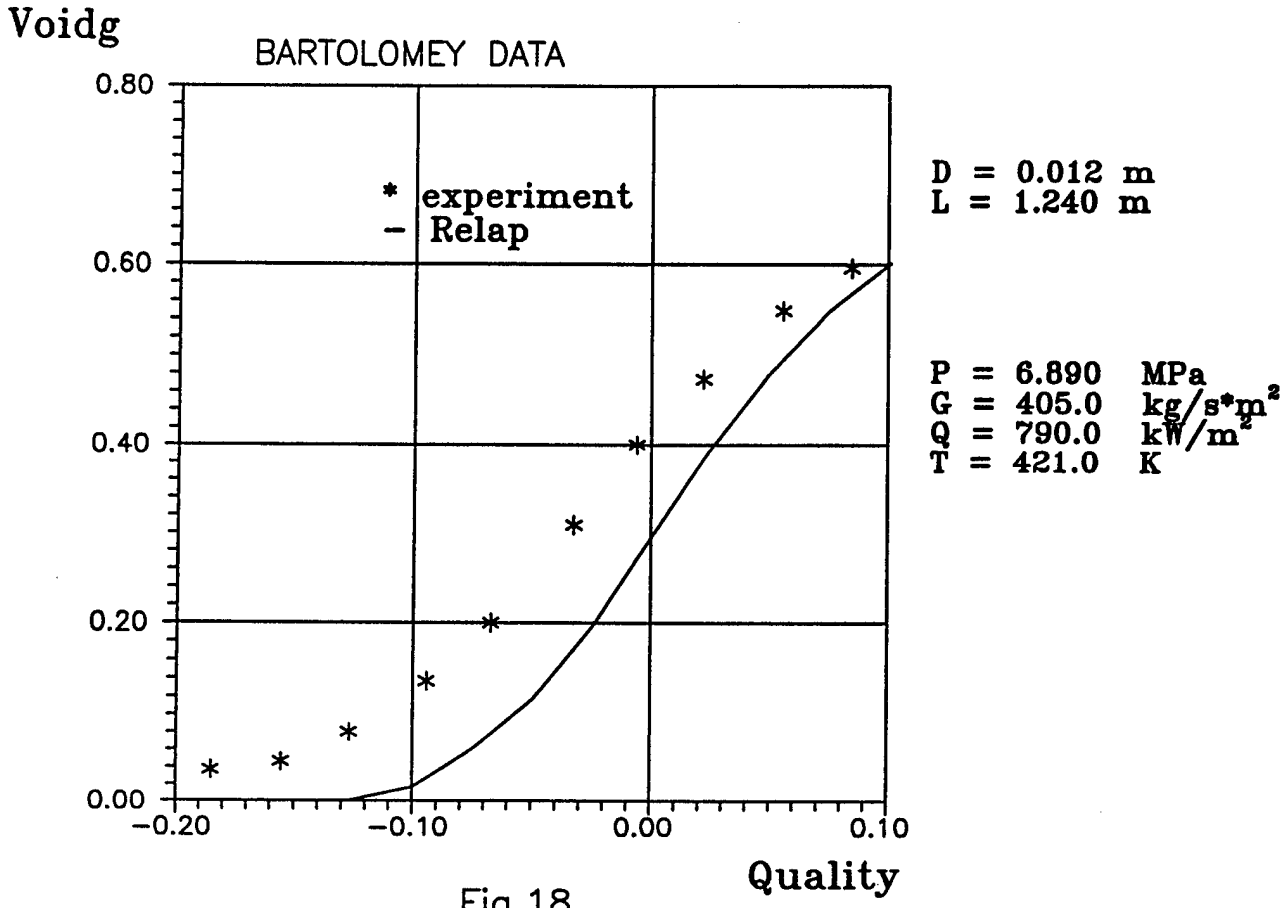
Voidg
BARTOLOMEY DATA
0.80
0.60
0.40
0.20
0.00
−0.20
−0.10
0.00
0.10
Quality
* experiment
– Relap
D = 0.012 m
L = 1.240 m
P = 6.890 MPa
G = 405.0 kg/s*m²
Q = 790.0 kW/m²
T = 421.0 K

Fig.18

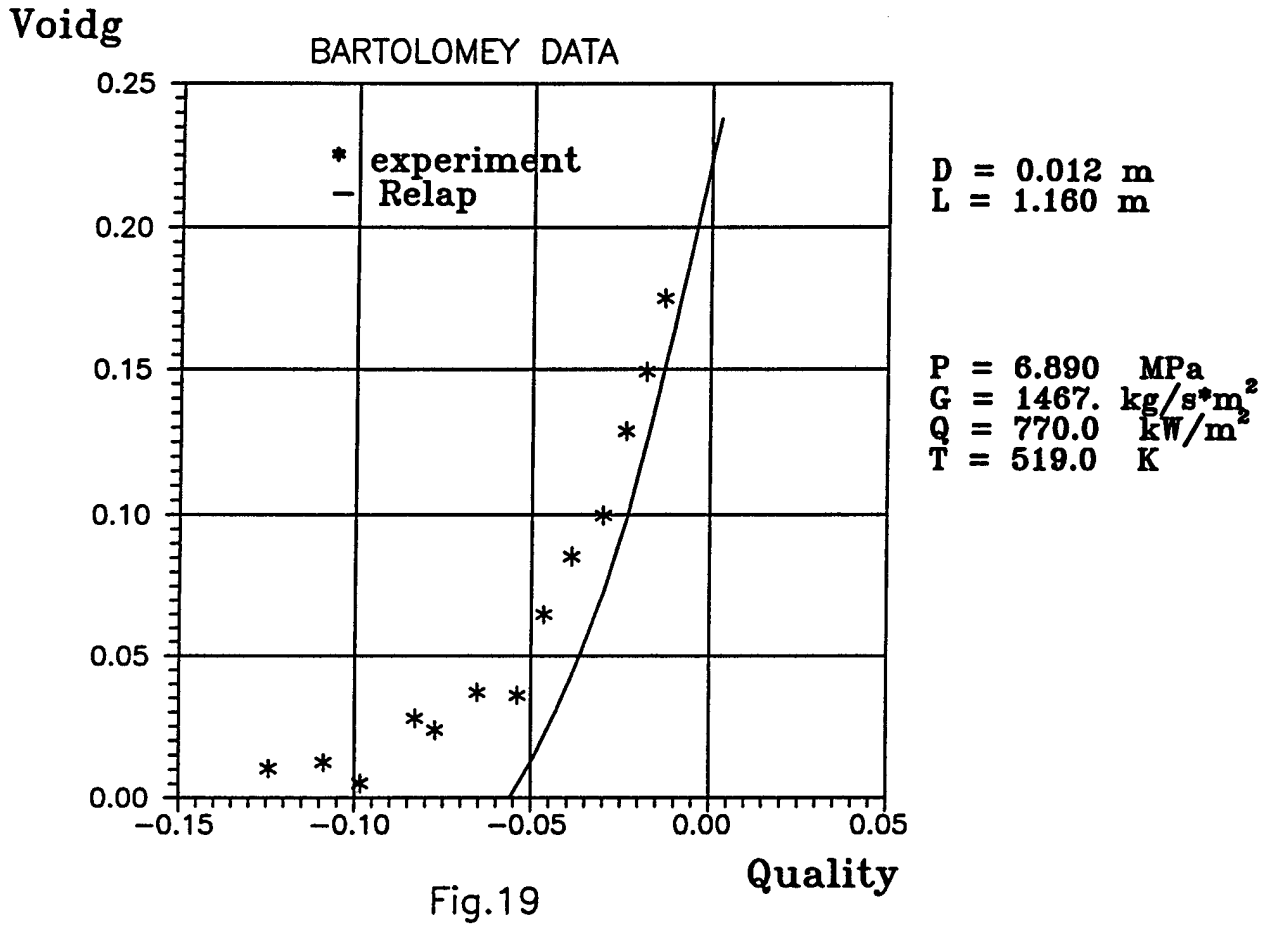
Voidg
BARTOLOMEY DATA
0.25
0.20
0.15
0.10
0.05
0.00
* experiment
– Relap
D = 0.012 m
L = 1.160 m
P = 6.890 MPa
G = 1467. kg/s*m²
Q = 770.0 kW/m²
T = 519.0 K
−0.15
−0.10
−0.05
0.00
0.05
Quality

Fig.19

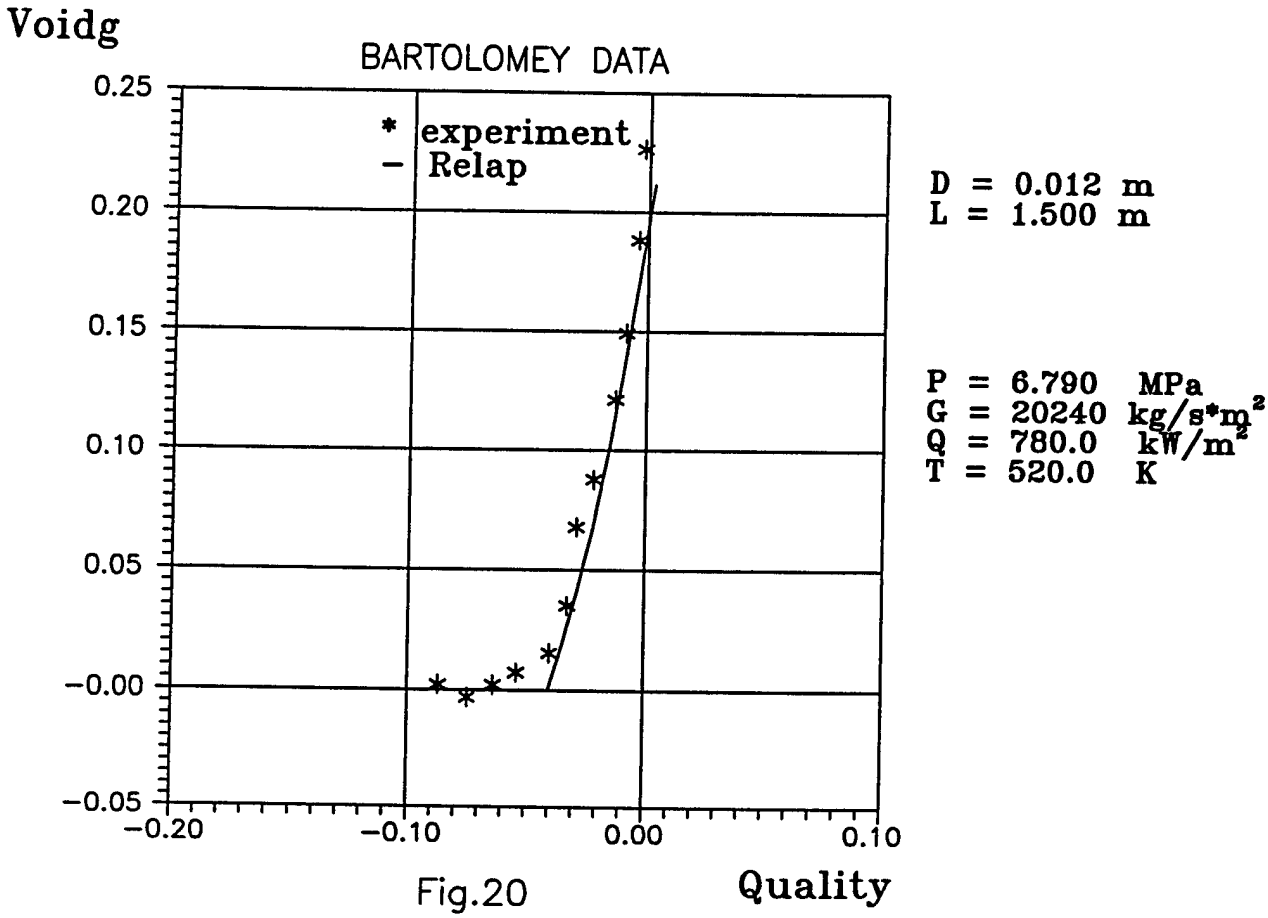
Voidg
BARTOLOMEY DATA
* experiment
– Relap
0.25
0.20
0.15
0.10
0.05
−0.00
−0.05
−0.20
−0.10
0.00
0.10
Quality
D = 0.012 m
L = 1.500 m
P = 6.790 MPa
G = 20240 kg/s*m²
Q = 780.0 kW/m²
T = 520.0 K

Fig.20

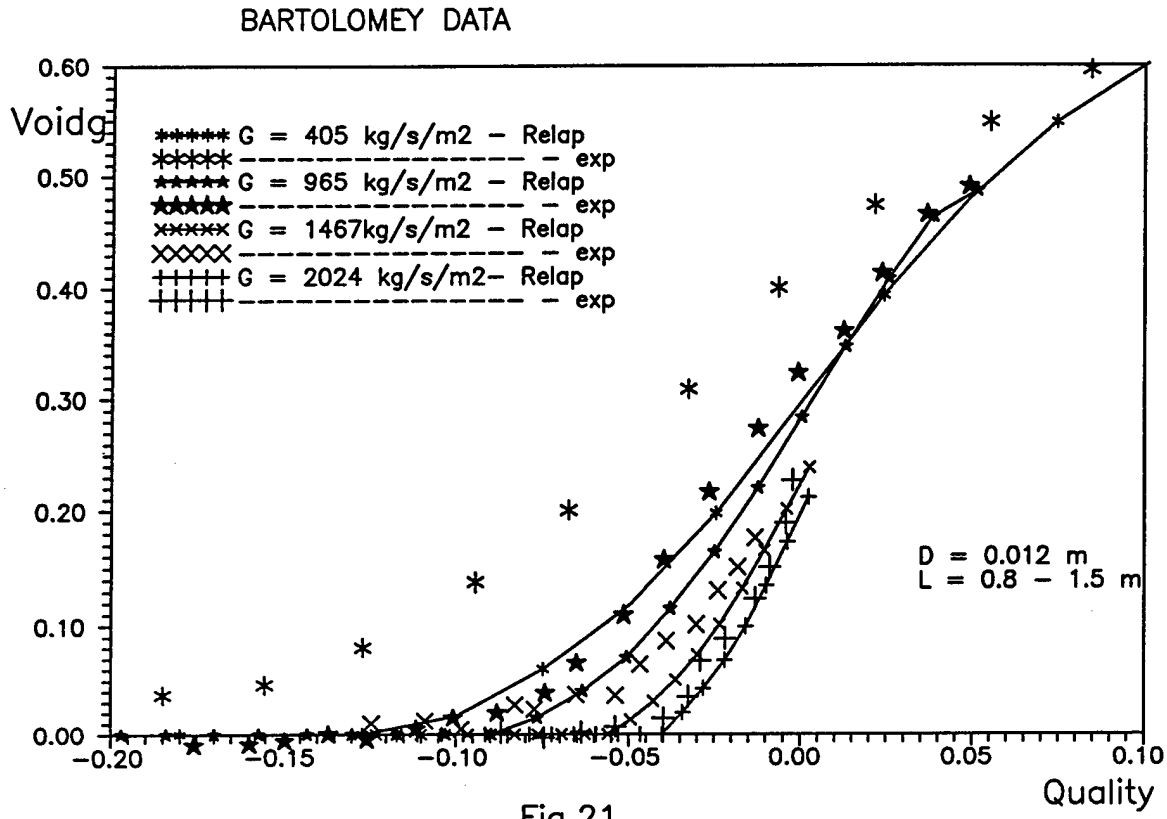
BARTOLOMEY DATA
Voidg
0.60
0.50
0.40
0.30
0.20
0.10
0.00
G = 405 kg/s/m2 – Relap
– exp
G = 965 kg/s/m2 – Relap
– exp
G = 1467kg/s/m2 – Relap
– exp
G = 2024 kg/s/m2– Relap
– exp
D = 0.012 m
L = 0.8 – 1.5 m
−0.20
−0.15
−0.10
−0.05
0.00
0.05
0.10
Quality

Fig.21

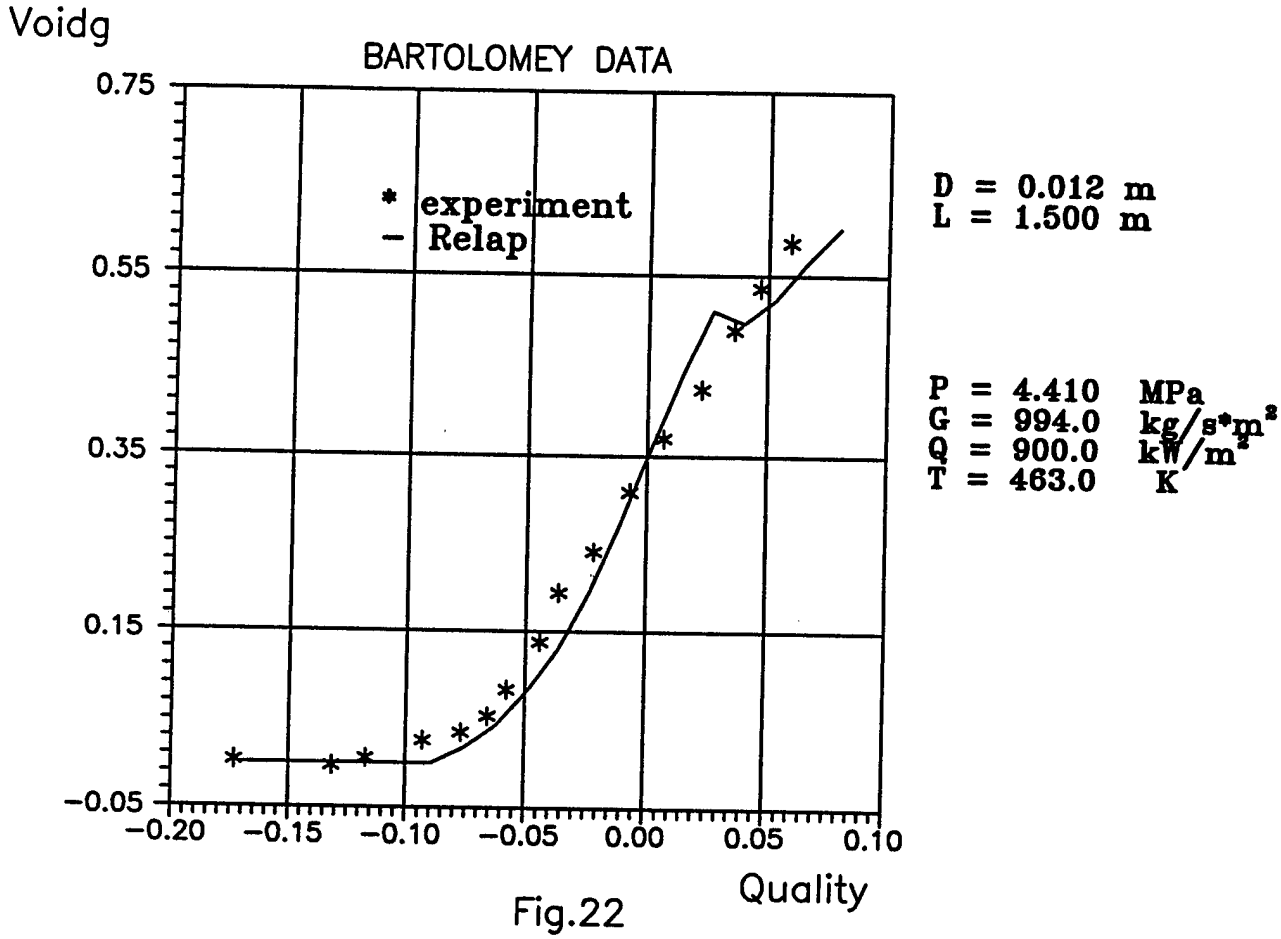
Voidg
BARTOLOMEY DATA
0.75
0.55
0.35
0.15
−0.05
−0.20
−0.15
−0.10
−0.05
0.00
0.05
0.10
Quality
* experiment
– Relap
D = 0.012 m
L = 1.500 m
P = 4.410 MPa
G = 994.0 kg/s*m²
Q = 900.0 kW/m²
T = 463.0 K

Fig.22

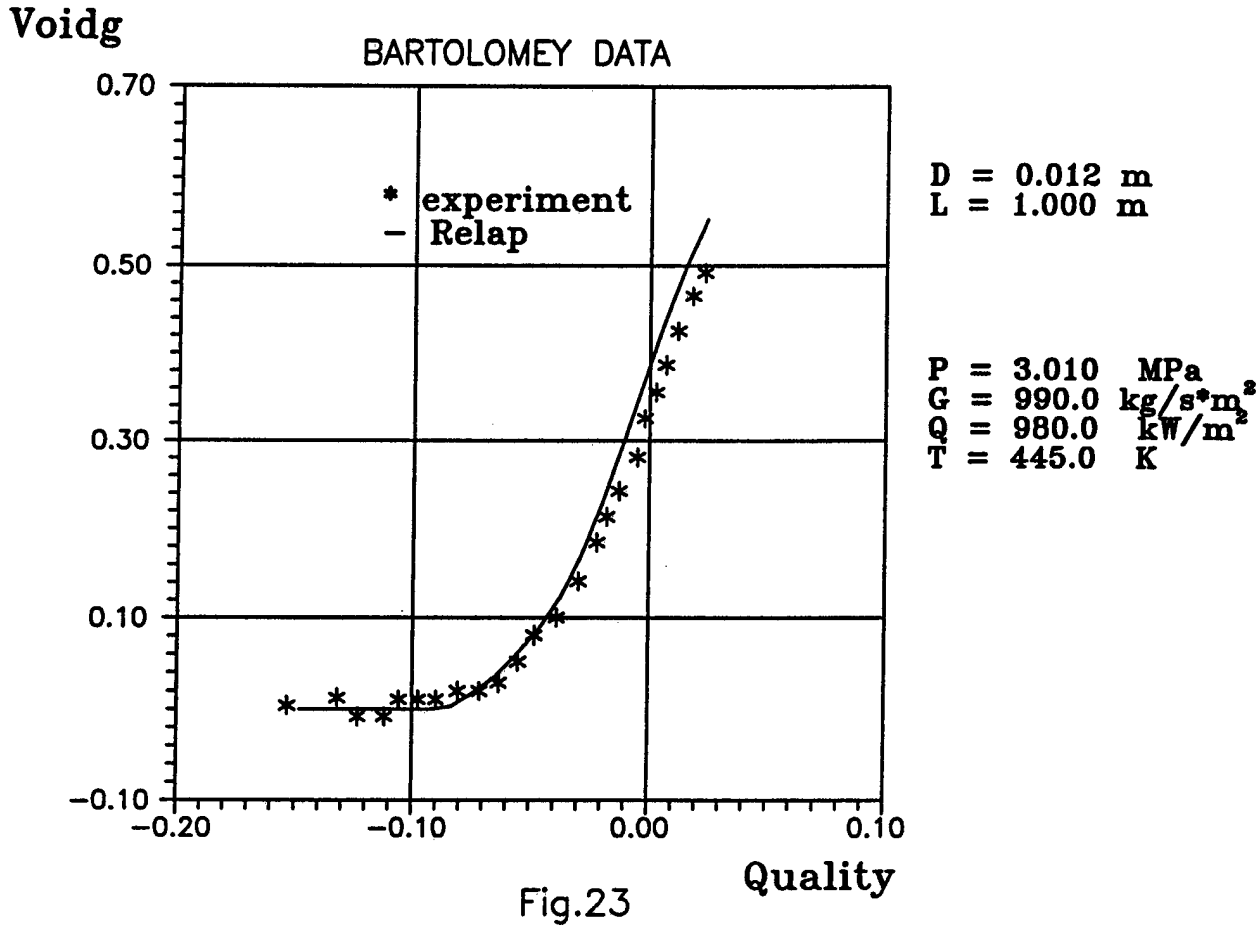
Voidg
BARTOLOMEY DATA
0.70
0.50
0.30
0.10
-0.10
-0.20
-0.10
0.00
0.10
Quality
* experiment
– Relap
D = 0.012 m
L = 1.000 m
P = 3.010 MPa
G = 990.0 kg/s*m²
Q = 980.0 kW/m²
T = 445.0 K

Fig.23

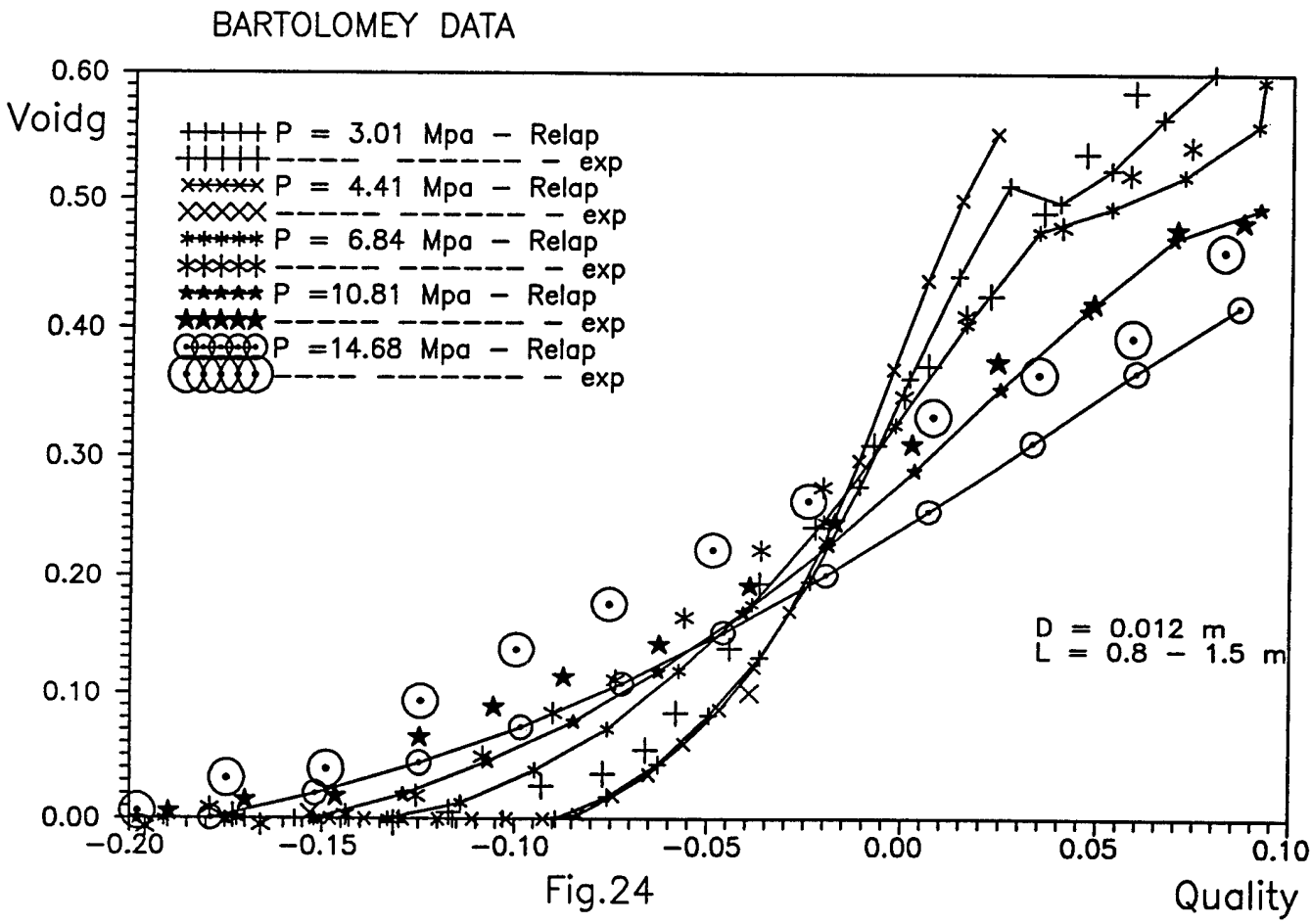
BARTOLOMEY DATA
Voidg
0.60
0.50
0.40
0.30
0.20
0.10
0.00
P = 3.01 Mpa – Relap
– exp
P = 4.41 Mpa – Relap
– exp
P = 6.84 Mpa – Relap
– exp
P =10.81 Mpa – Relap
– exp
P =14.68 Mpa – Relap
– exp
D = 0.012 m
L = 0.8 – 1.5 m
−0.20
−0.15
−0.10
−0.05
0.00
0.05
0.10
Quality

Fig.24

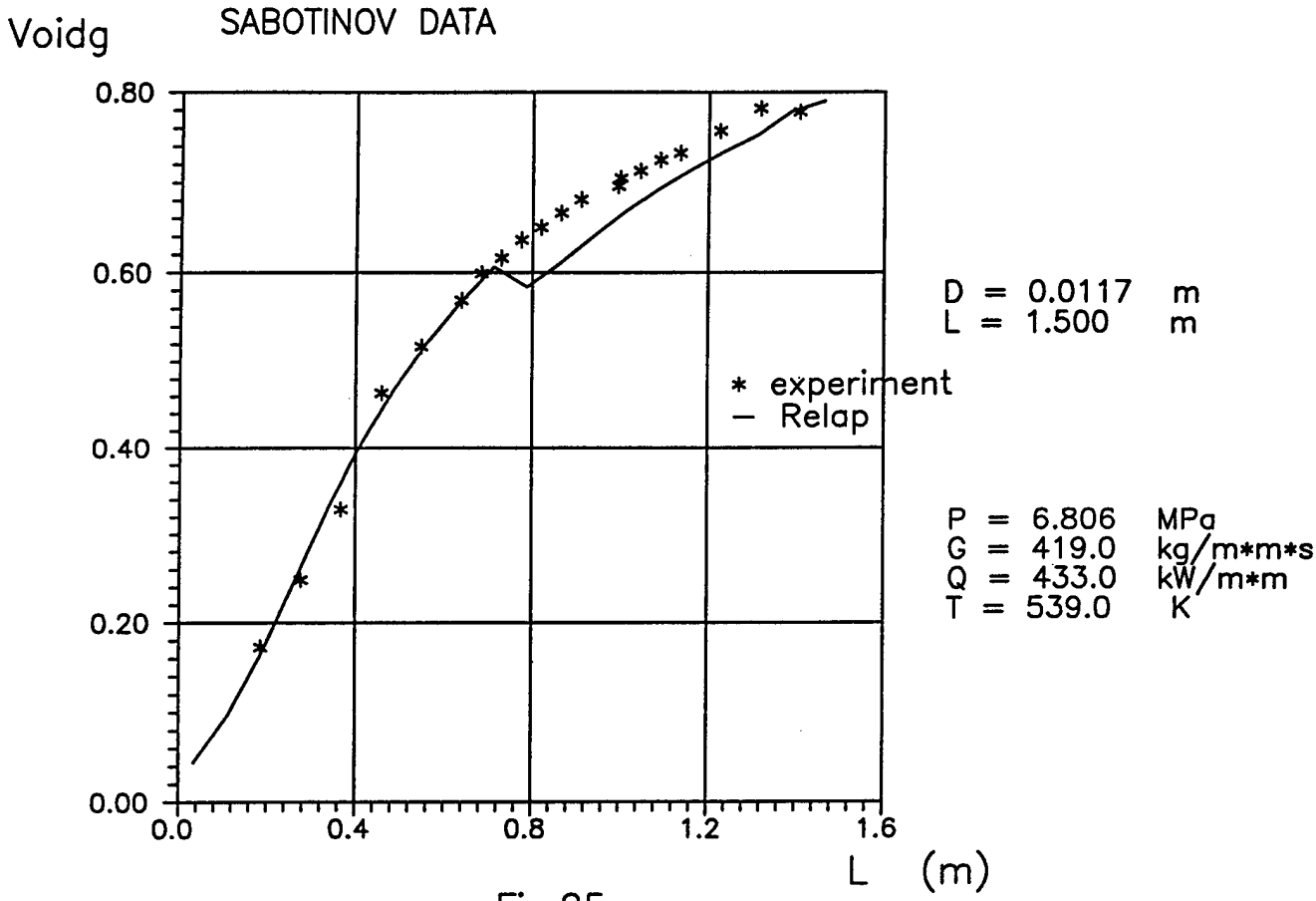
Voidg
SABOTINOV DATA
0.80
0.60
0.40
0.20
0.00
0.0
0.4
0.8
1.2
1.6
L (m)
* experiment
— Relap
D = 0.0117 m
L = 1.500 m
P = 6.806 MPa
G = 419.0 kg/m*m*s
Q = 433.0 kW/m*m
T = 539.0 K

Fig.25

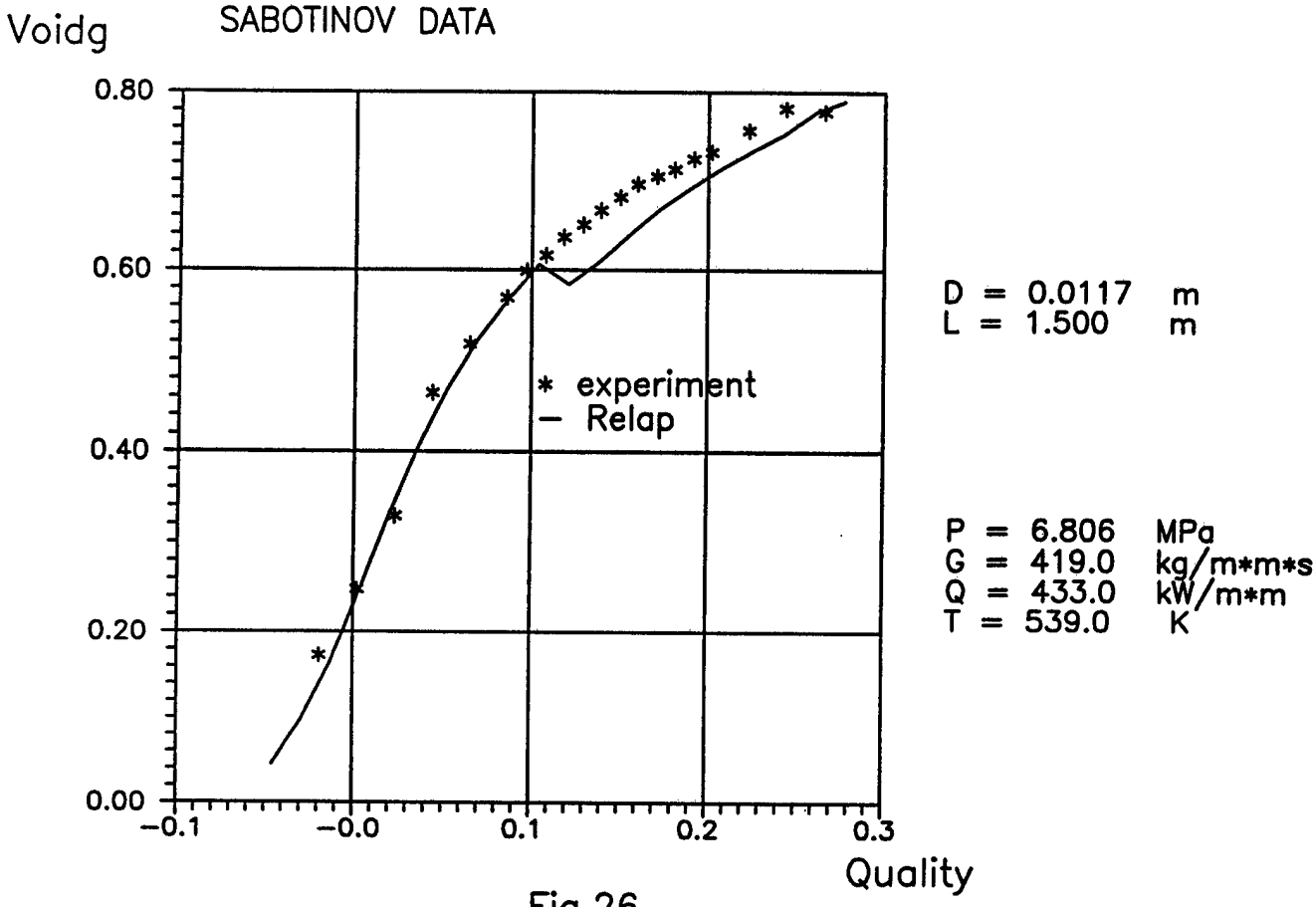
Voidg
SABOTINOV DATA
0.80
0.60
0.40
0.20
0.00
−0.1
−0.0
0.1
0.2
0.3
Quality
* experiment
— Relap
D = 0.0117 m
L = 1.500 m
P = 6.806 MPa
G = 419.0 kg/m*m*s
Q = 433.0 kW/m*m
T = 539.0 K

Fig.26

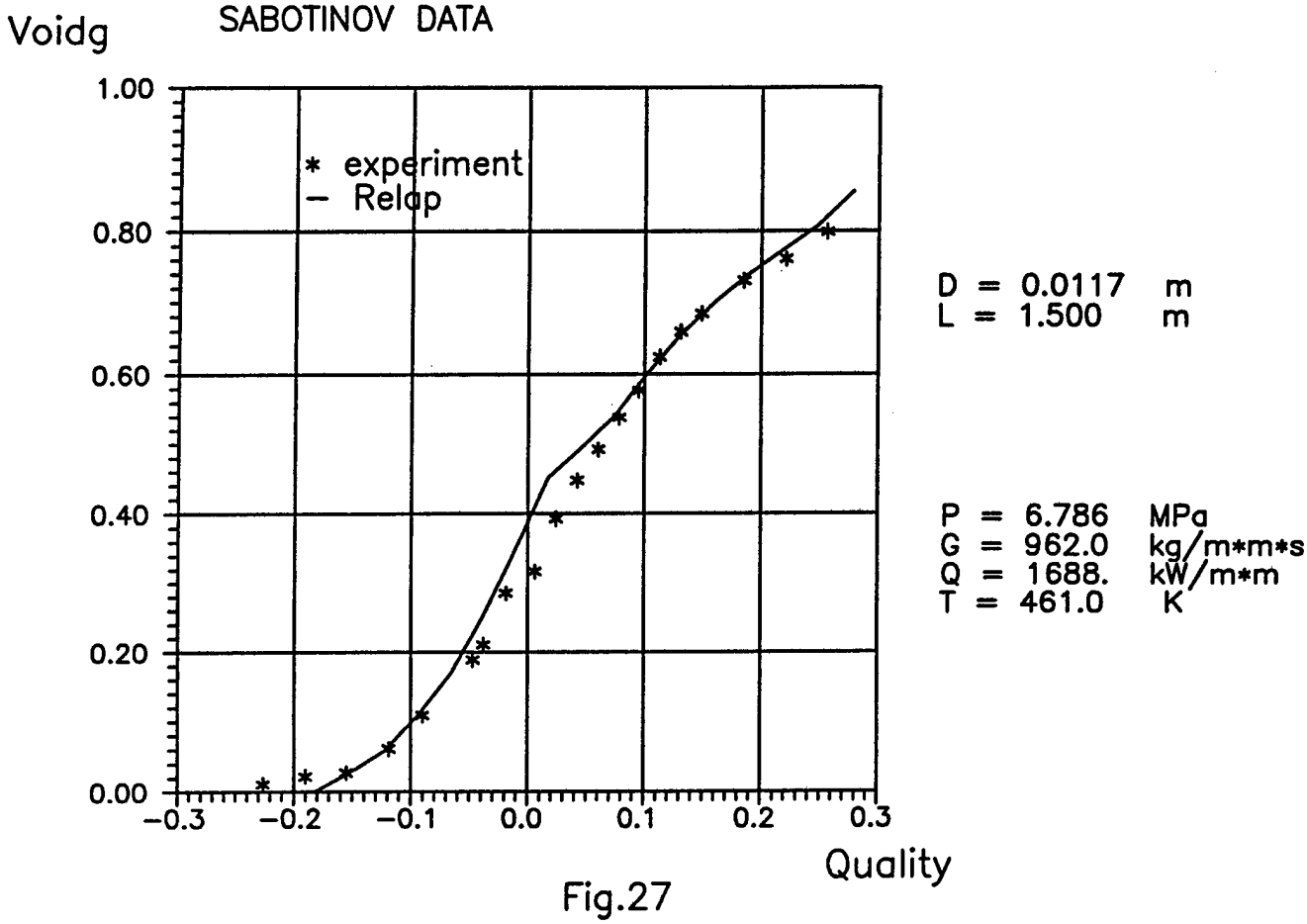
Voidg
SABOTINOV DATA
1.00
0.80
0.60
0.40
0.20
0.00
−0.3
−0.2
−0.1
0.0
0.1
0.2
0.3
Quality
* experiment
— Relap
D = 0.0117 m
L = 1.500 m
P = 6.786 MPa
G = 962.0 kg/m*m*s
Q = 1688. kW/m*m
T = 461.0 K

Fig.27

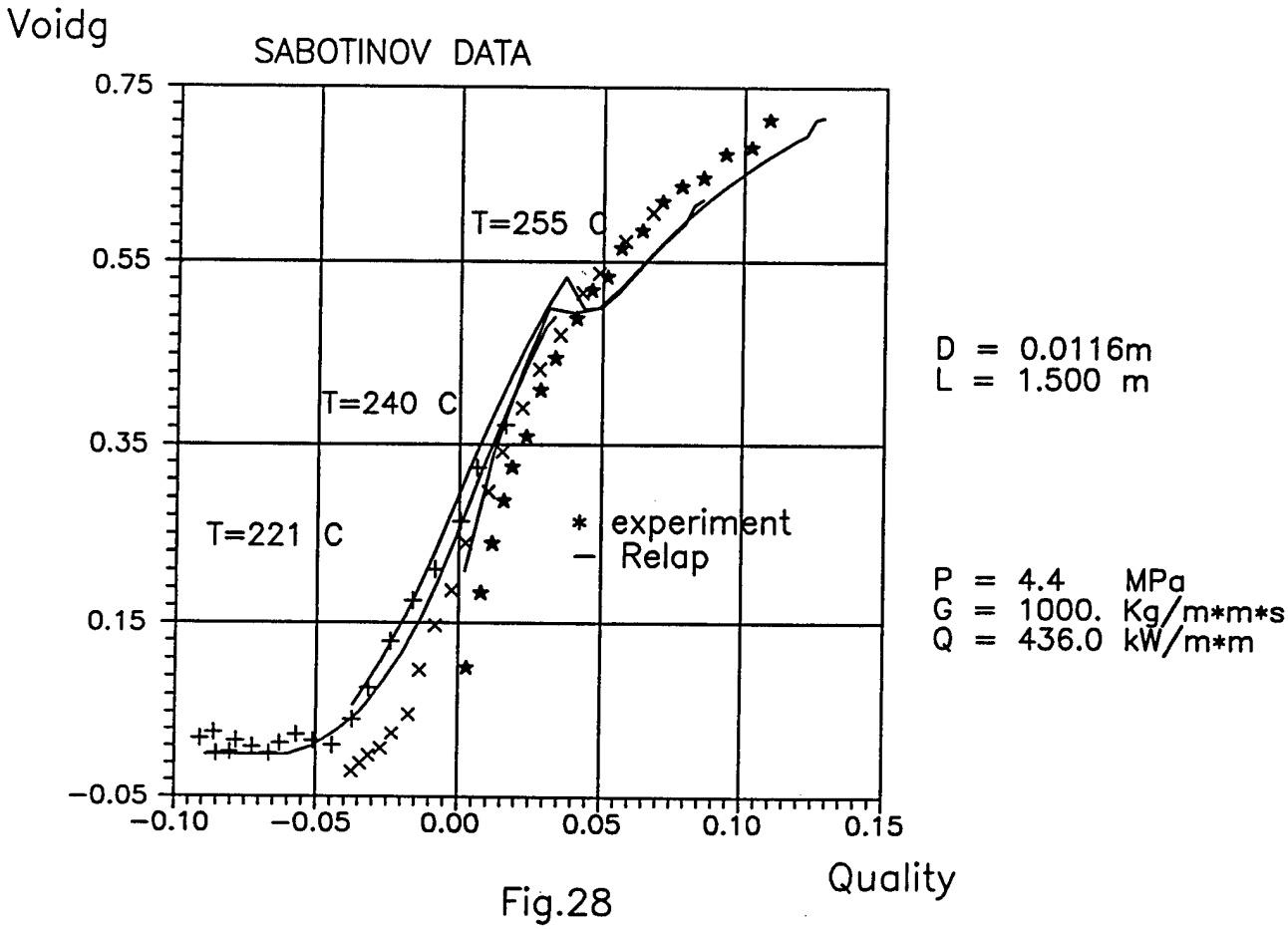
Voidg
SABOTINOV DATA
0.75
0.55
0.35
0.15
−0.05
−0.10
−0.05
0.00
0.05
0.10
0.15
T=255 C
T=240 C
T=221 C
* experiment
— Relap
D = 0.0116m
L = 1.500 m
P = 4.4 MPa
G = 1000. Kg/m*m*s
Q = 436.0 kW/m*m
Quality

Fig.28

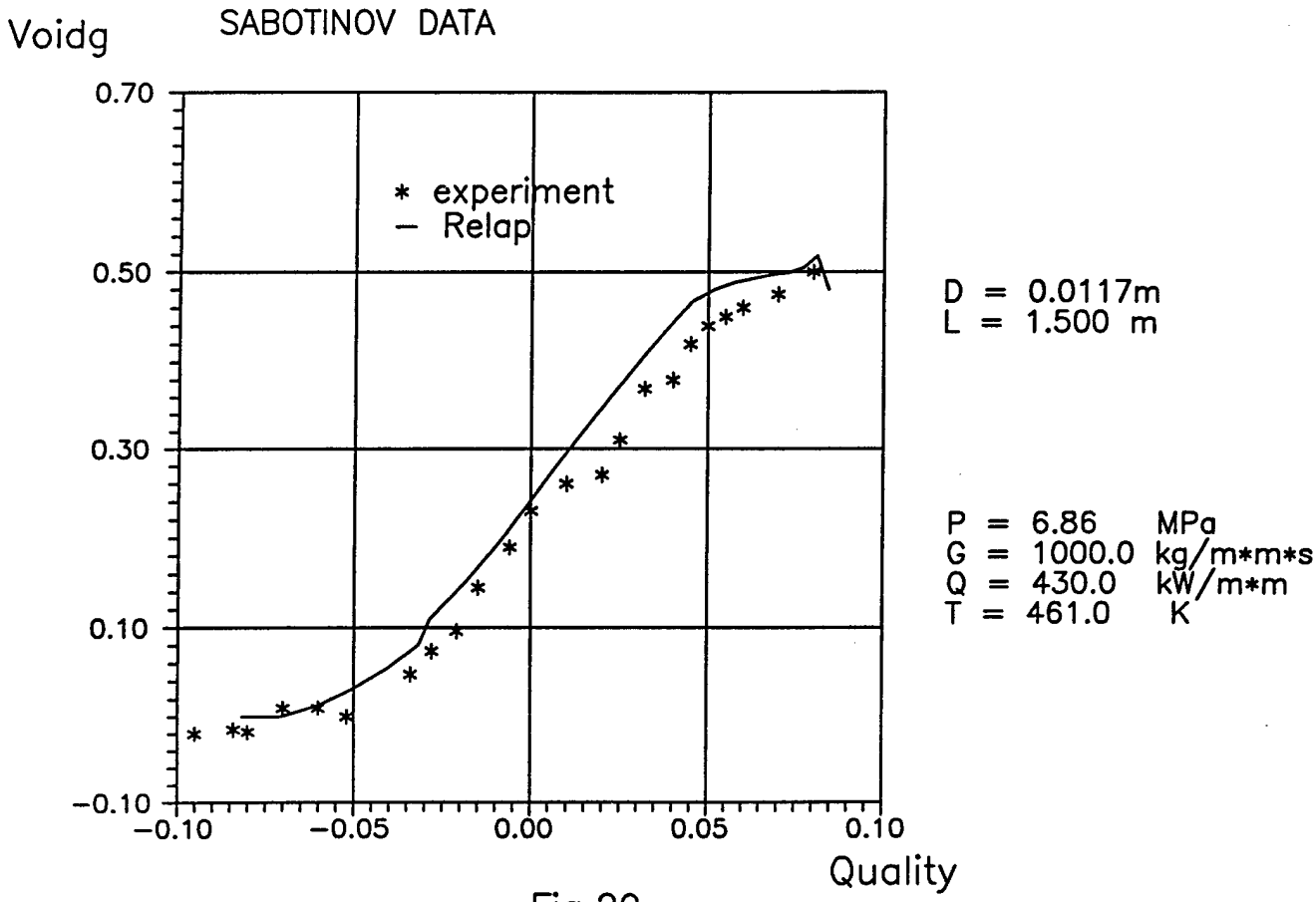
Voidg
SABOTINOV DATA
0.70
0.50
0.30
0.10
−0.10
−0.10
−0.05
0.00
0.05
0.10
Quality
* experiment
— Relap
D = 0.0117m
L = 1.500 m
P = 6.86 MPa
G = 1000.0 kg/m*m*s
Q = 430.0 kW/m*m
T = 461.0 K

Fig.29

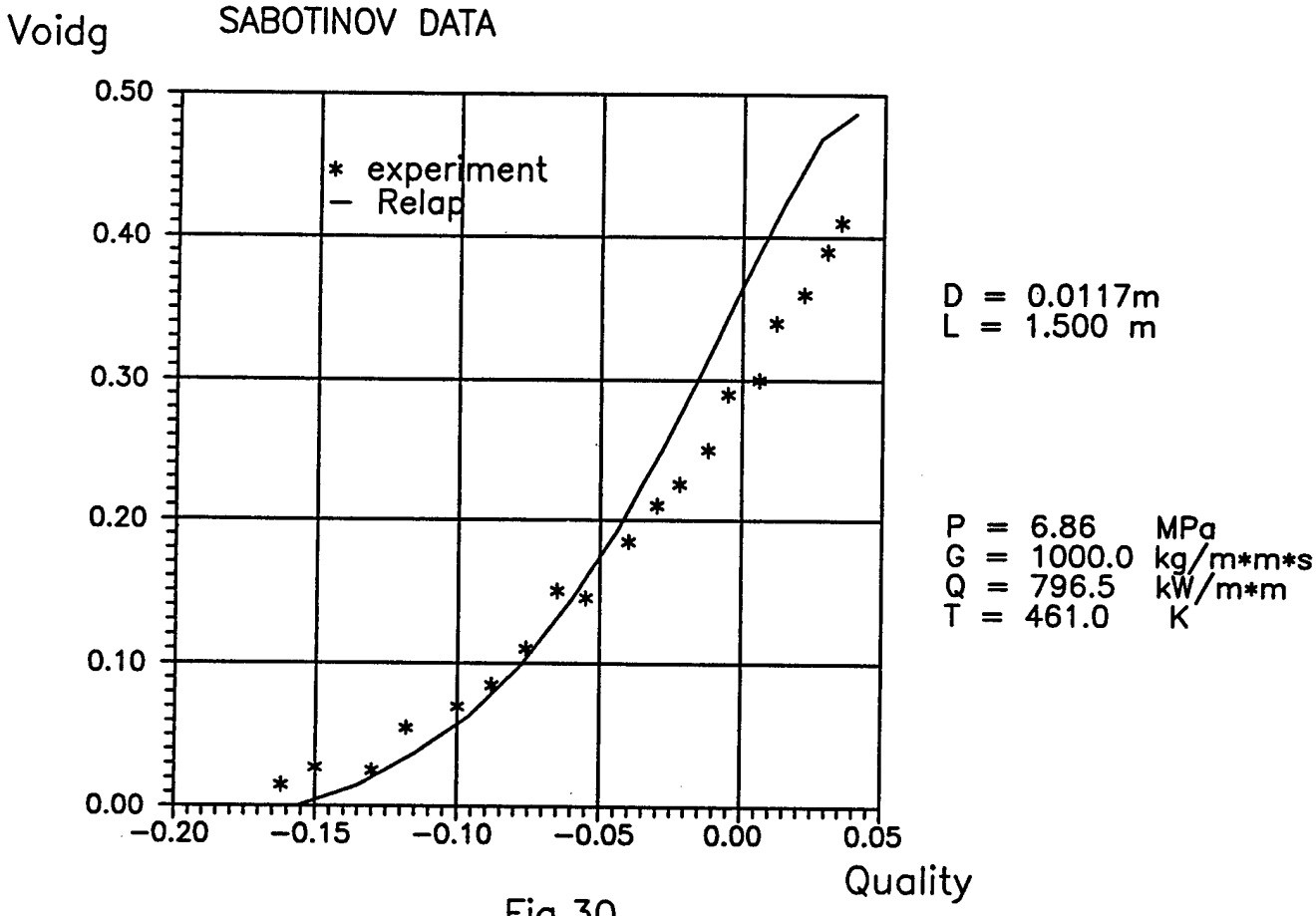
Voidg
SABOTINOV DATA
0.50
0.40
0.30
0.20
0.10
0.00
* experiment
— Relap
−0.20
−0.15
−0.10
−0.05
0.00
0.05
Quality
D = 0.0117m
L = 1.500 m
P = 6.86 MPa
G = 1000.0 kg/m*m*s
Q = 796.5 kW/m*m
T = 461.0 K

Fig.30

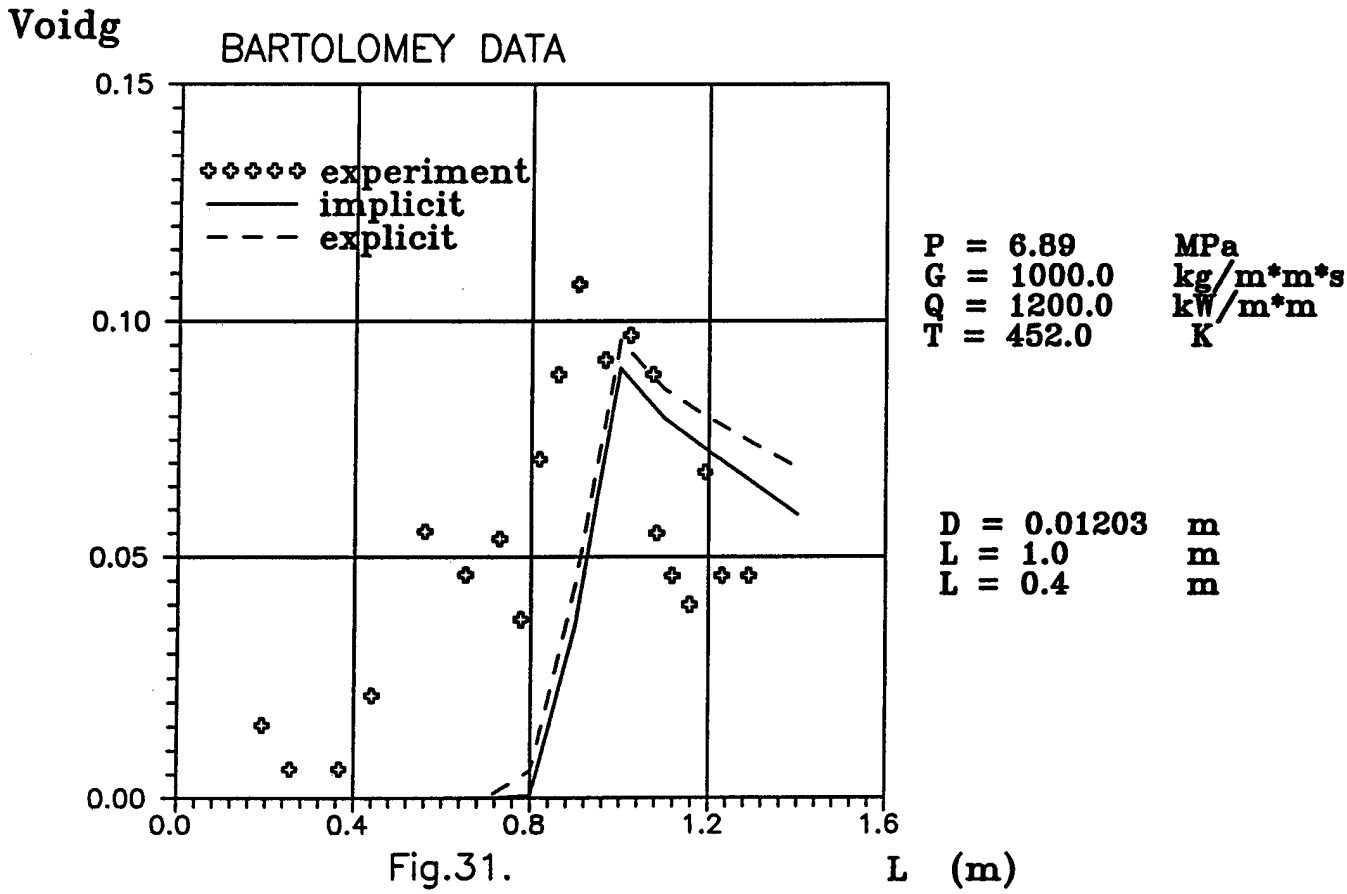
Voidg
BARTOLOMEY DATA
0.15
0.10
0.05
0.00
0.0
0.4
0.8
1.2
1.6
experiment
implicit
explicit
P = 6.89 MPa
G = 1000.0 kg/m*m*s
Q = 1200.0 kW/m*m
T = 452.0 K
D = 0.01203 m
L = 1.0 m
L = 0.4 m
L (m)

Fig.31.

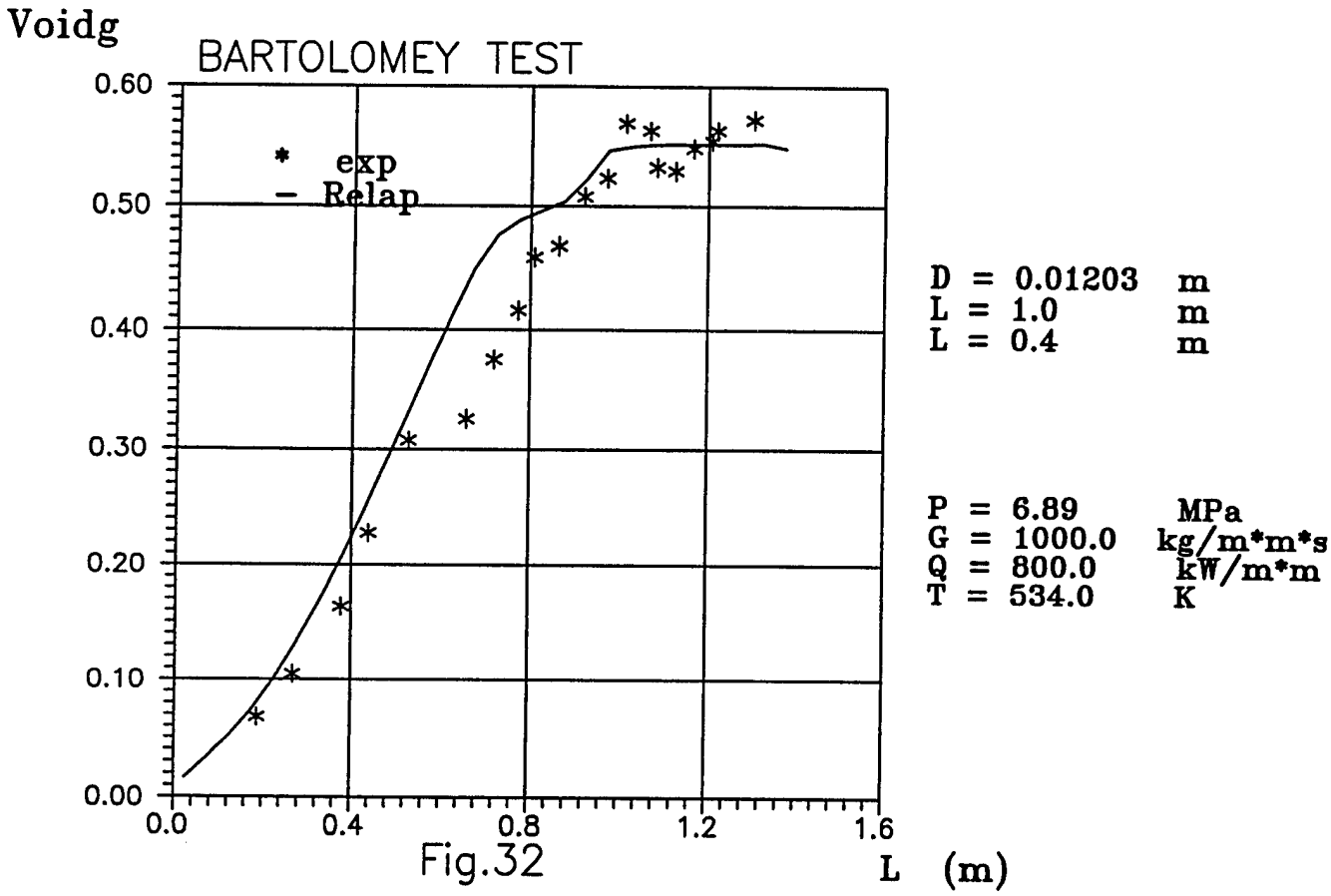
Voidg
BARTOLOMEY TEST
* exp
– Relap
0.60
0.50
0.40
0.30
0.20
0.10
0.00
0.0
0.4
0.8
1.2
1.6
L (m)
D = 0.01203 m
L = 1.0 m
L = 0.4 m
P = 6.89 MPa
G = 1000.0 kg/m*m*s
Q = 800.0 kW/m*m
T = 534.0 K

Fig.32

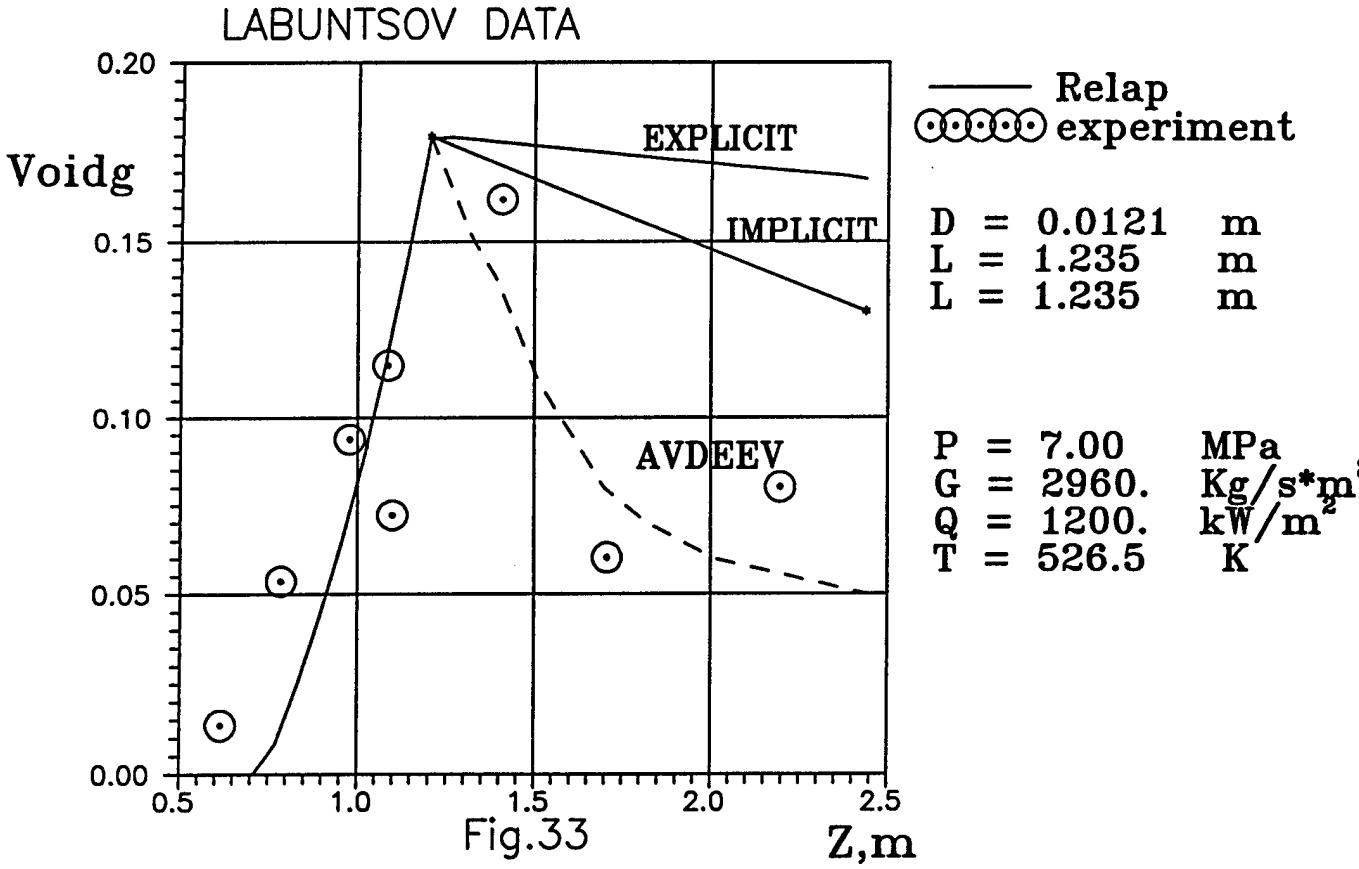
LABUNTSOV DATA
Voidg
0.20
0.15
0.10
0.05
0.00
0.5
1.0
1.5
2.0
2.5
Z,m
EXPLICIT
IMPLICIT
AVDEEV
Relap
experiment
D = 0.0121 m
L = 1.235 m
L = 1.235 m
P = 7.00 MPa
G = 2960. Kg/s*m²
Q = 1200. kW/m²
T = 526.5 K

Fig.33

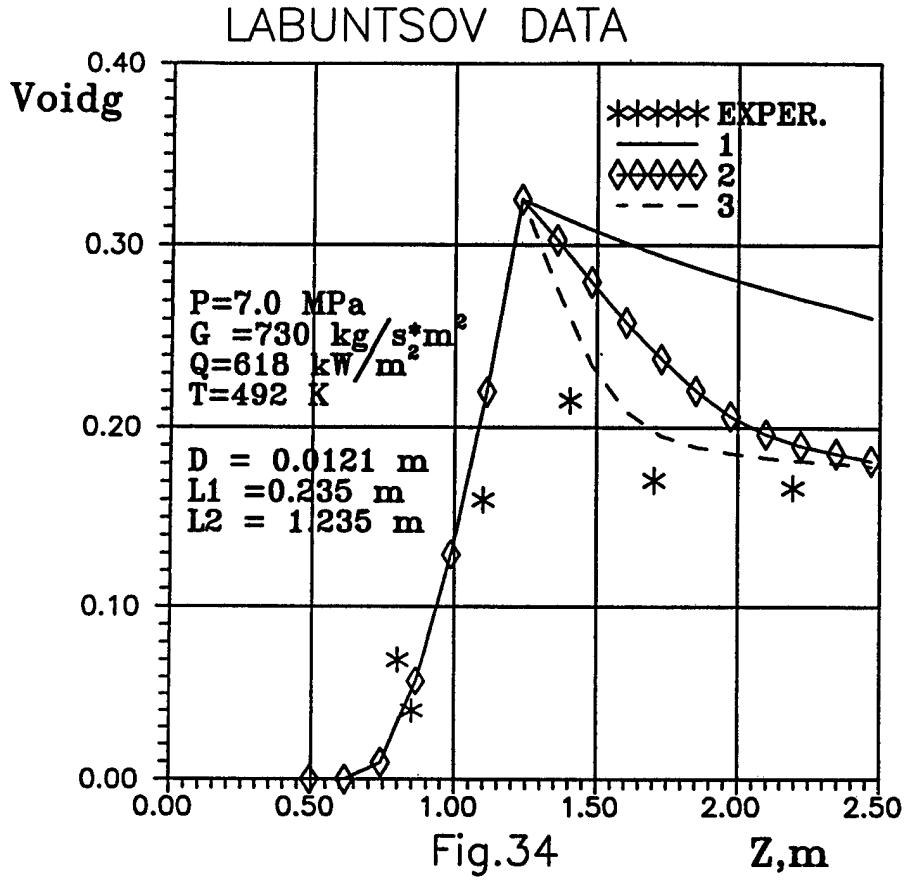
LABUNTSOV DATA
Voidg
0.40
0.30
0.20
0.10
0.00
0.00
0.50
1.00
1.50
2.00
2.50
Z,m
EXPER.
1
2
3
P=7.0 MPa
G =730 kg/s*m2
Q=618 kW/m2
T=492 K
D = 0.0121 m
L1 =0.235 m
L2 = 1.235 m

Fig.34

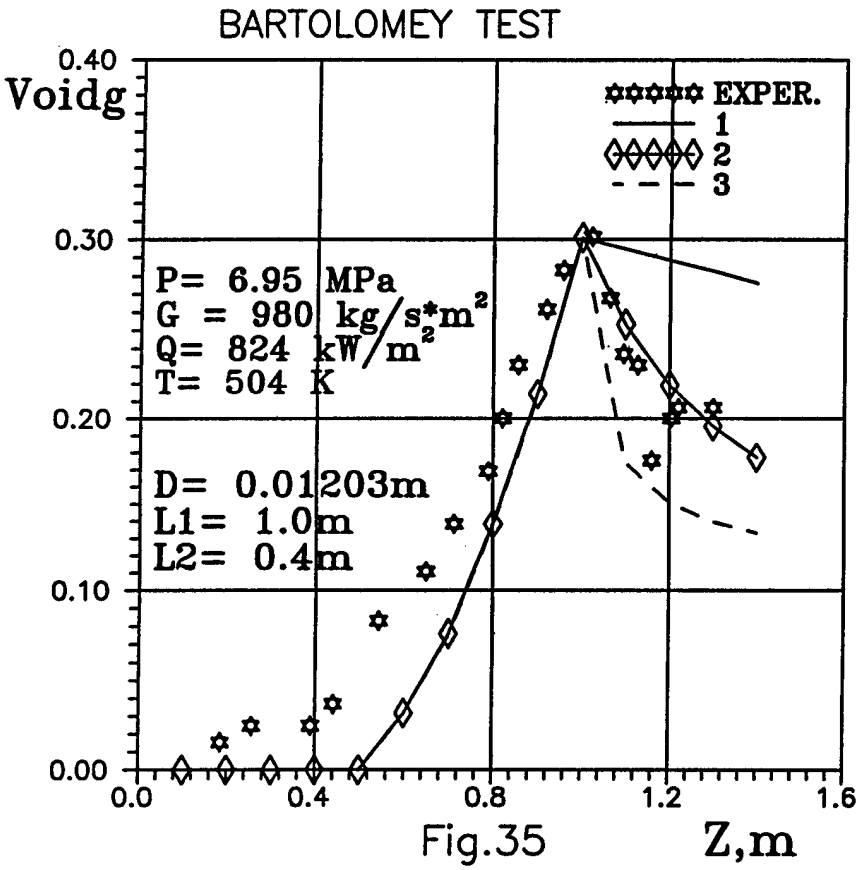
BARTOLOMEY TEST
Voidg
0.40
0.30
0.20
0.10
0.00
EXPER.
1
2
3
P= 6.95 MPa
G = 980 kg/s*m²
Q= 824 kW/m²
T= 504 K
D= 0.01203m
L1= 1.0m
L2= 0.4m
0.0
0.4
0.8
1.2
1.6
Z,m

Fig.35

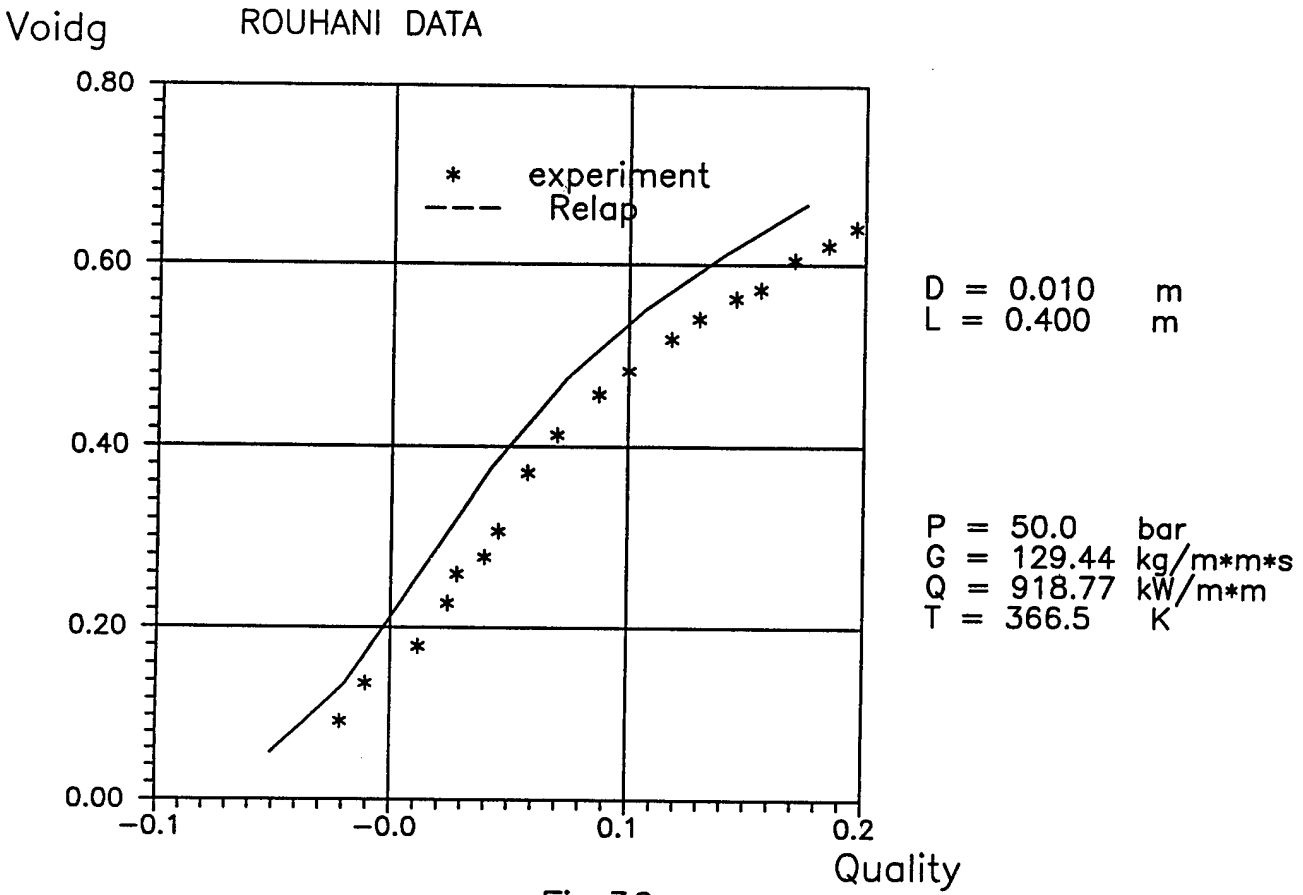
Voidg
ROUHANI DATA
0.80
0.60
0.40
0.20
0.00
−0.1
−0.0
0.1
0.2
Quality
* experiment
Relap
D = 0.010 m
L = 0.400 m
P = 50.0 bar
G = 129.44 kg/m*m*s
Q = 918.77 kW/m*m
T = 366.5 K

Fig.36

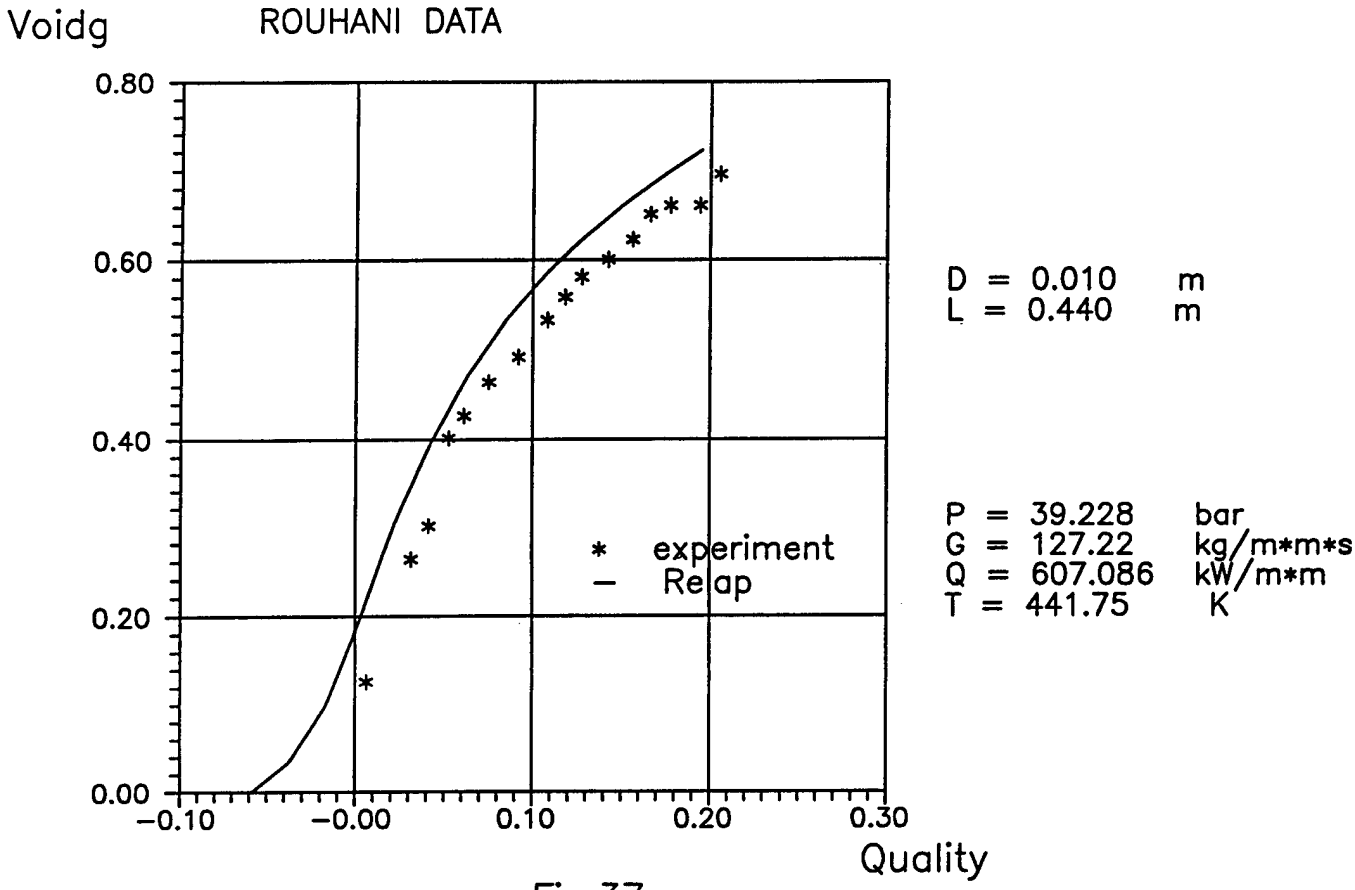
Voidg
ROUHANI DATA
0.80
0.60
0.40
0.20
0.00
−0.10
−0.00
0.10
0.20
0.30
Quality
* experiment
— Reap
D = 0.010 m
L = 0.440 m
P = 39.228 bar
G = 127.22 kg/m*m*s
Q = 607.086 kW/m*m
T = 441.75 K

Fig.37

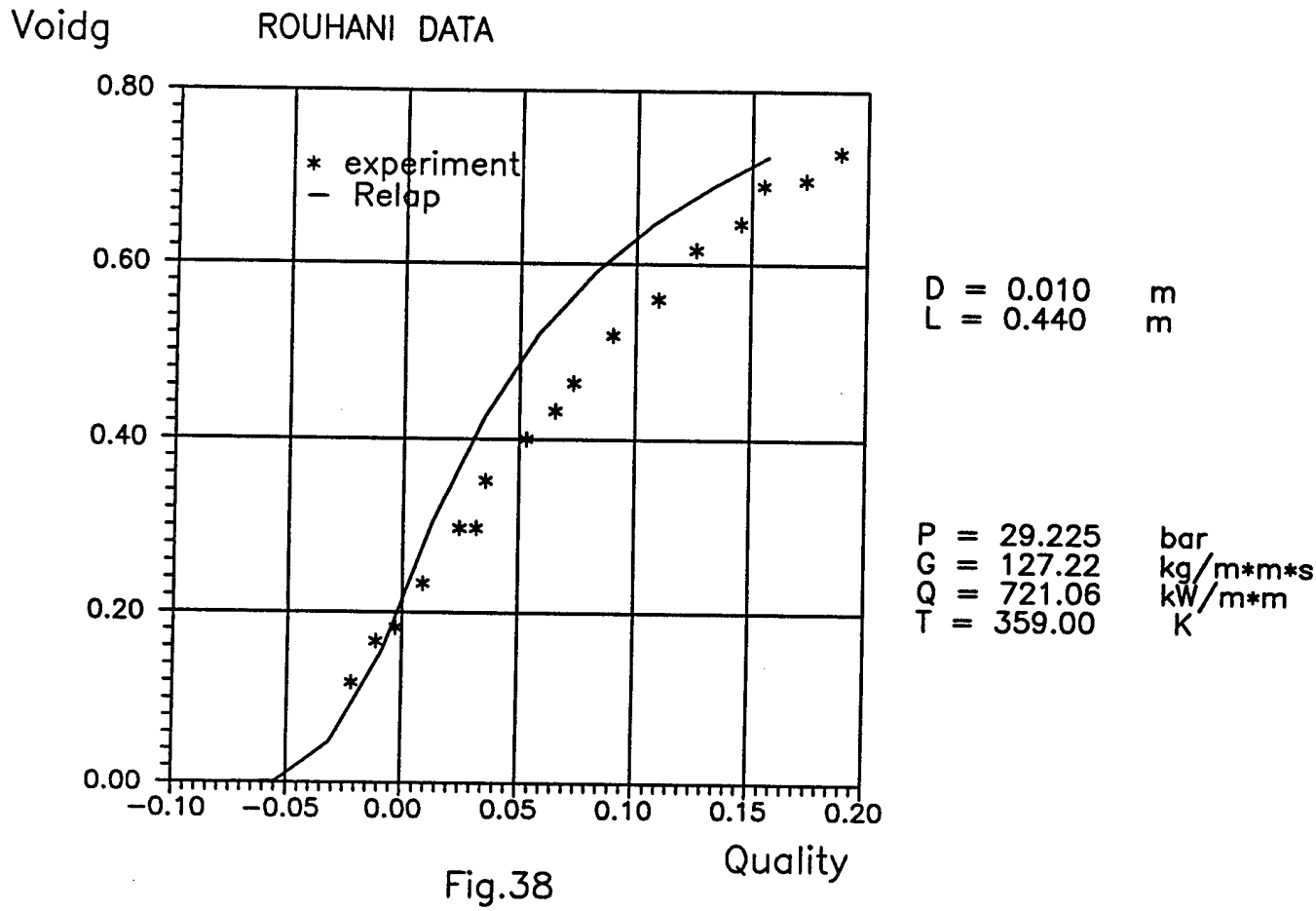
Voidg
ROUHANI DATA
0.80
0.60
0.40
0.20
0.00
* experiment
— Relap
−0.10
−0.05
0.00
0.05
0.10
0.15
0.20
Quality
D = 0.010 m
L = 0.440 m
P = 29.225 bar
G = 127.22 kg/m*m*s
Q = 721.06 kW/m*m
T = 359.00 K

Fig.38

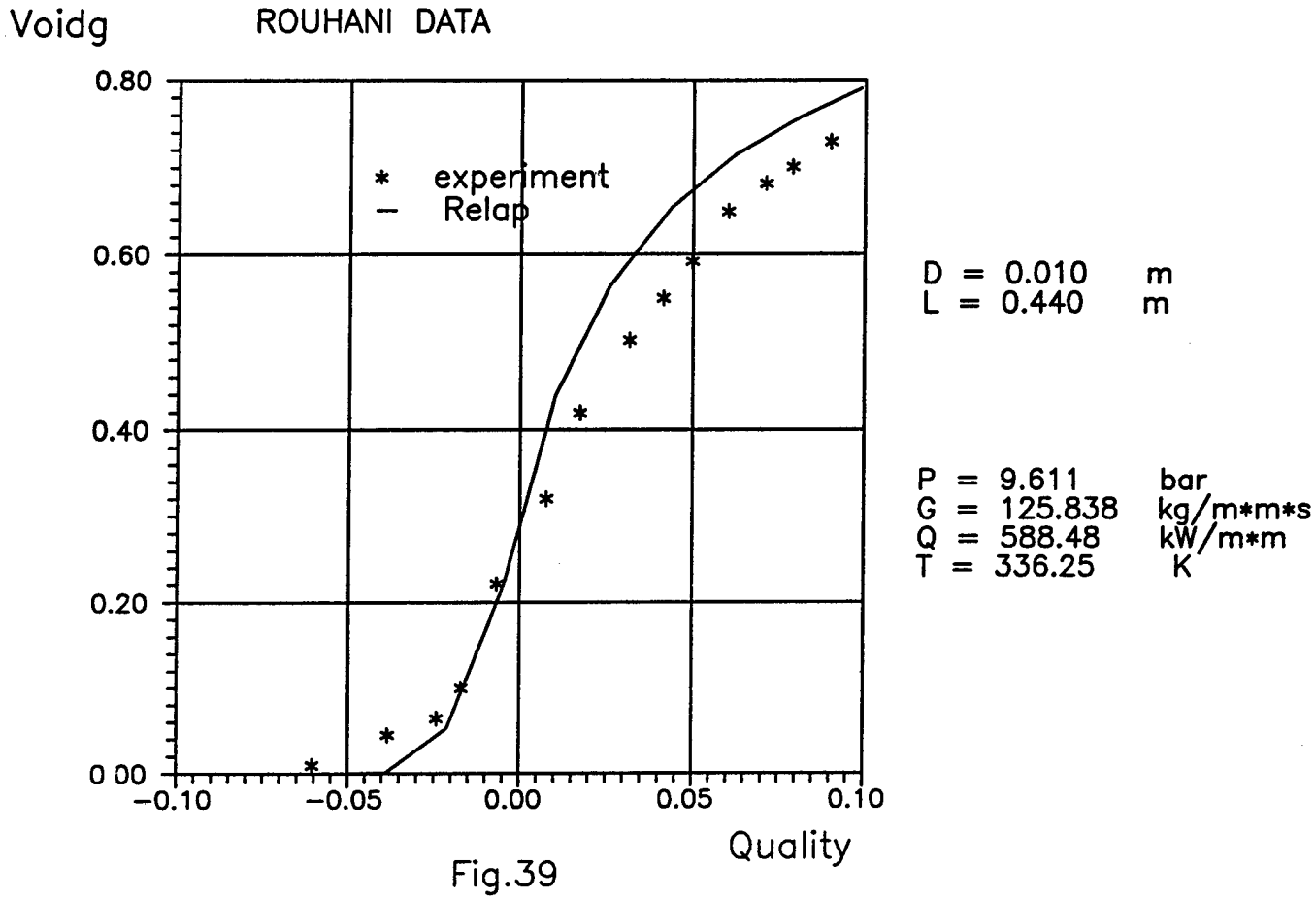
Voidg
ROUHANI DATA
0.80
0.60
0.40
0.20
0 00
* experiment
— Relap
−0.10
−0.05
0.00
0.05
0.10
Quality
D = 0.010 m
L = 0.440 m
P = 9.611 bar
G = 125.838 kg/m*m*s
Q = 588.48 kW/m*m
T = 336.25 K

Fig.39

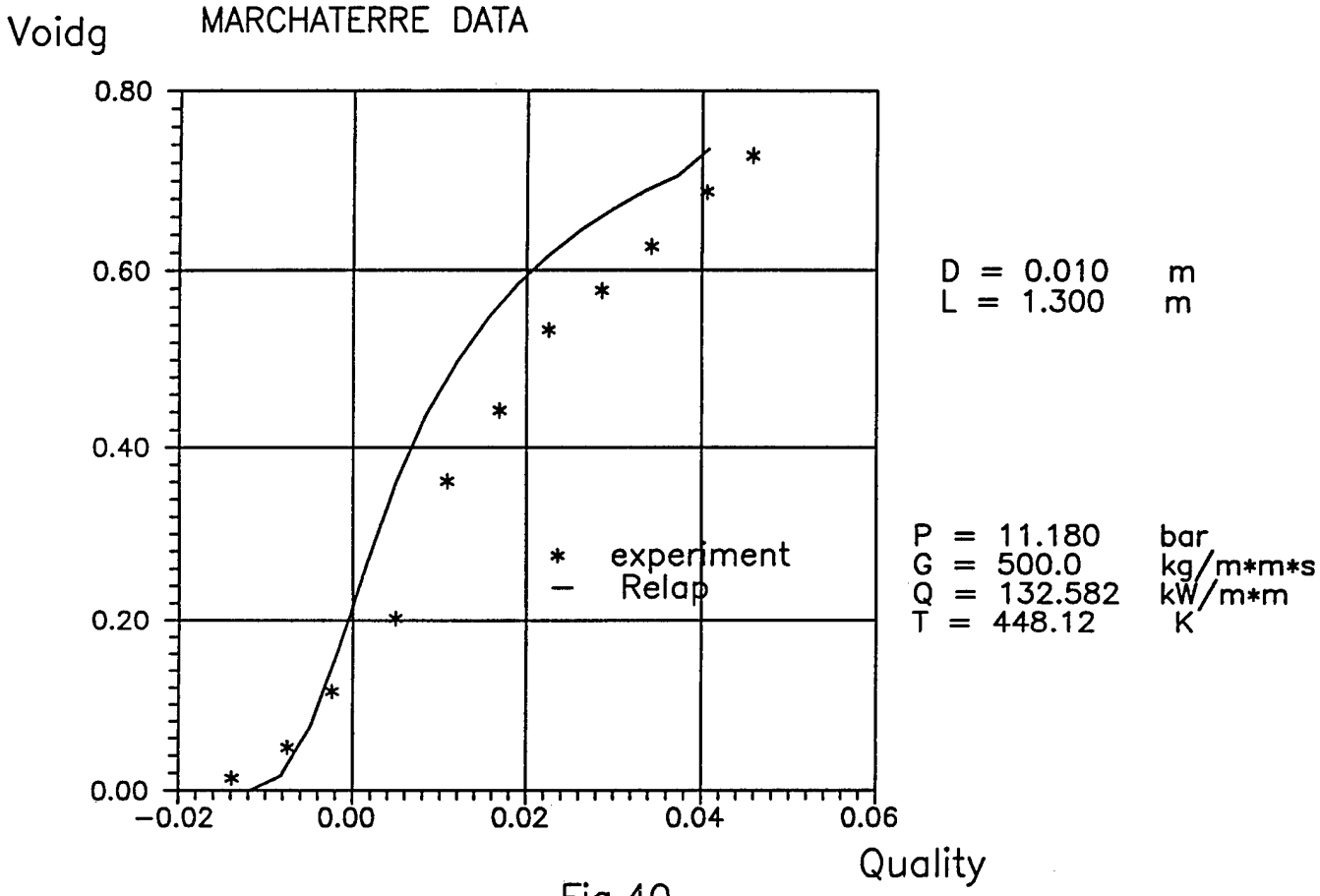
Voidg
MARCHATERRE DATA
0.80
0.60
0.40
0.20
0.00
−0.02
0.00
0.02
0.04
0.06
Quality
* experiment
— Relap
D = 0.010 m
L = 1.300 m
P = 11.180 bar
G = 500.0 kg/m*m*s
Q = 132.582 kW/m*m
T = 448.12 K

Fig.40

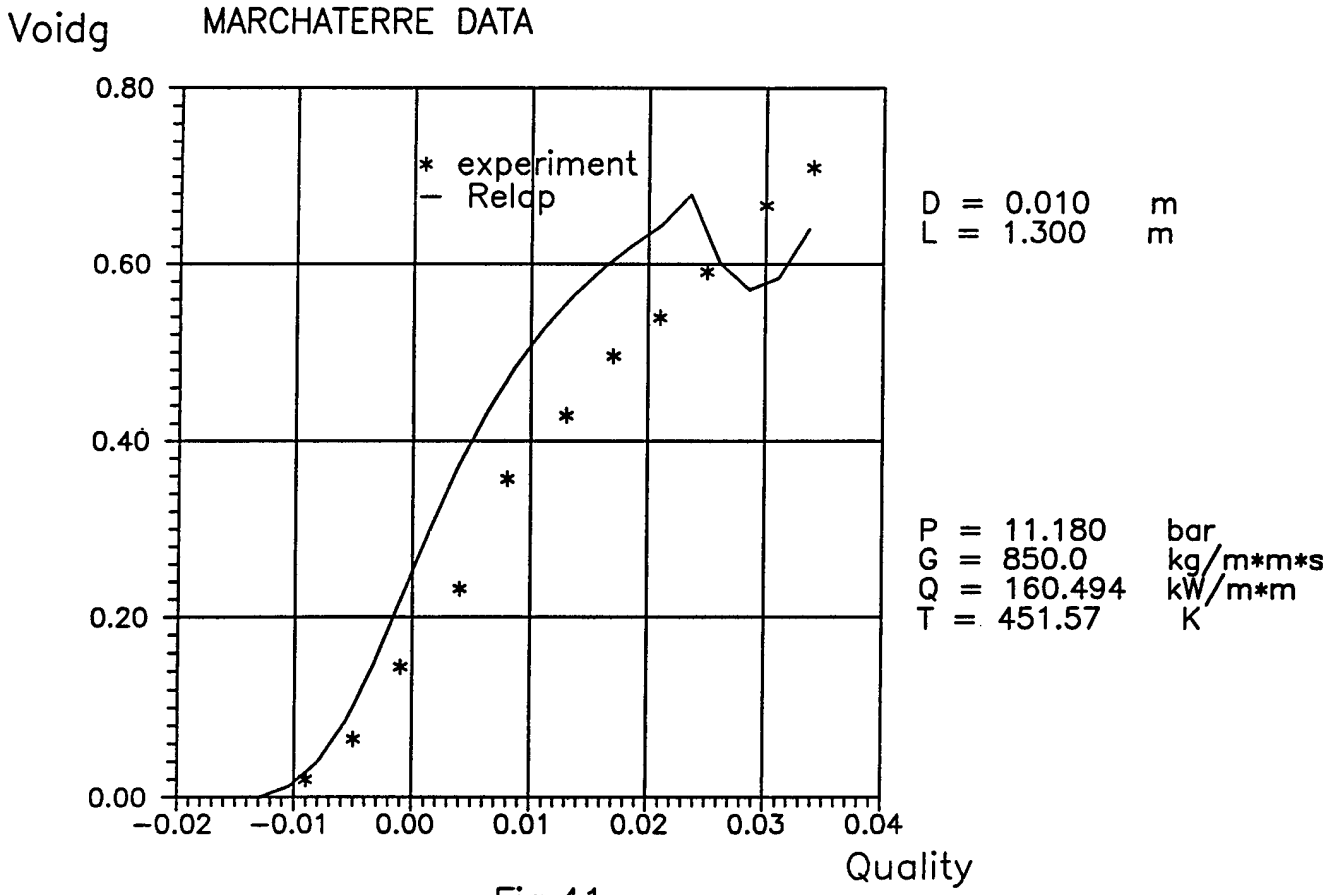
Voidg
MARCHATERRE DATA
0.80
0.60
0.40
0.20
0.00
−0.02
−0.01
0.00
0.01
0.02
0.03
0.04
Quality
* experiment
— Relap
D = 0.010 m
L = 1.300 m
P = 11.180 bar
G = 850.0 kg/m*m*s
Q = 160.494 kW/m*m
T = 451.57 K

Fig.41

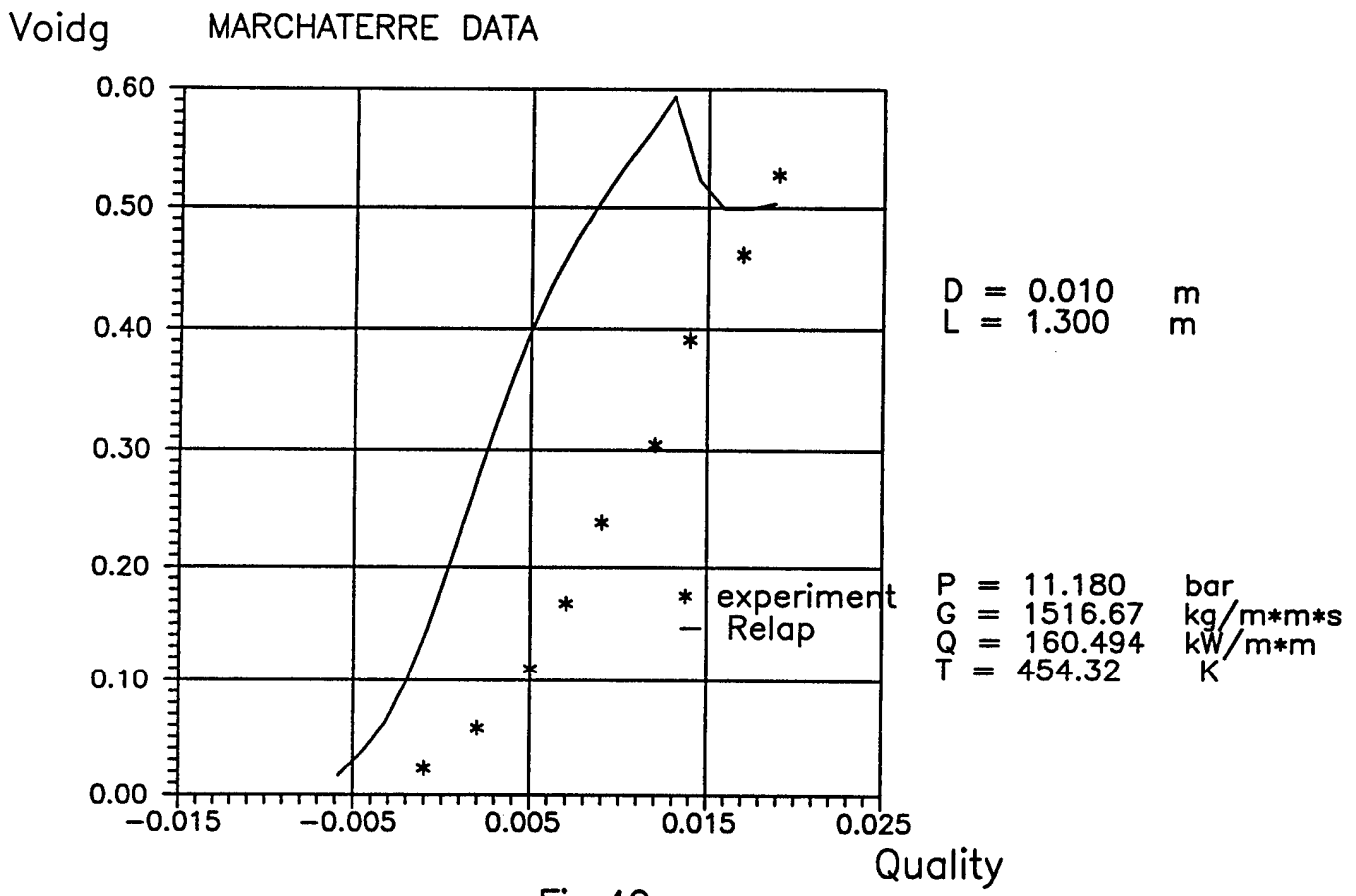
Voidg
MARCHATERRE DATA
0.60
0.50
0.40
0.30
0.20
0.10
0.00
−0.015
−0.005
0.005
0.015
0.025
Quality
experiment
Relap
D = 0.010 m
L = 1.300 m
P = 11.180 bar
G = 1516.67 kg/m*m*s
Q = 160.494 kW/m*m
T = 454.32 K

Fig.42

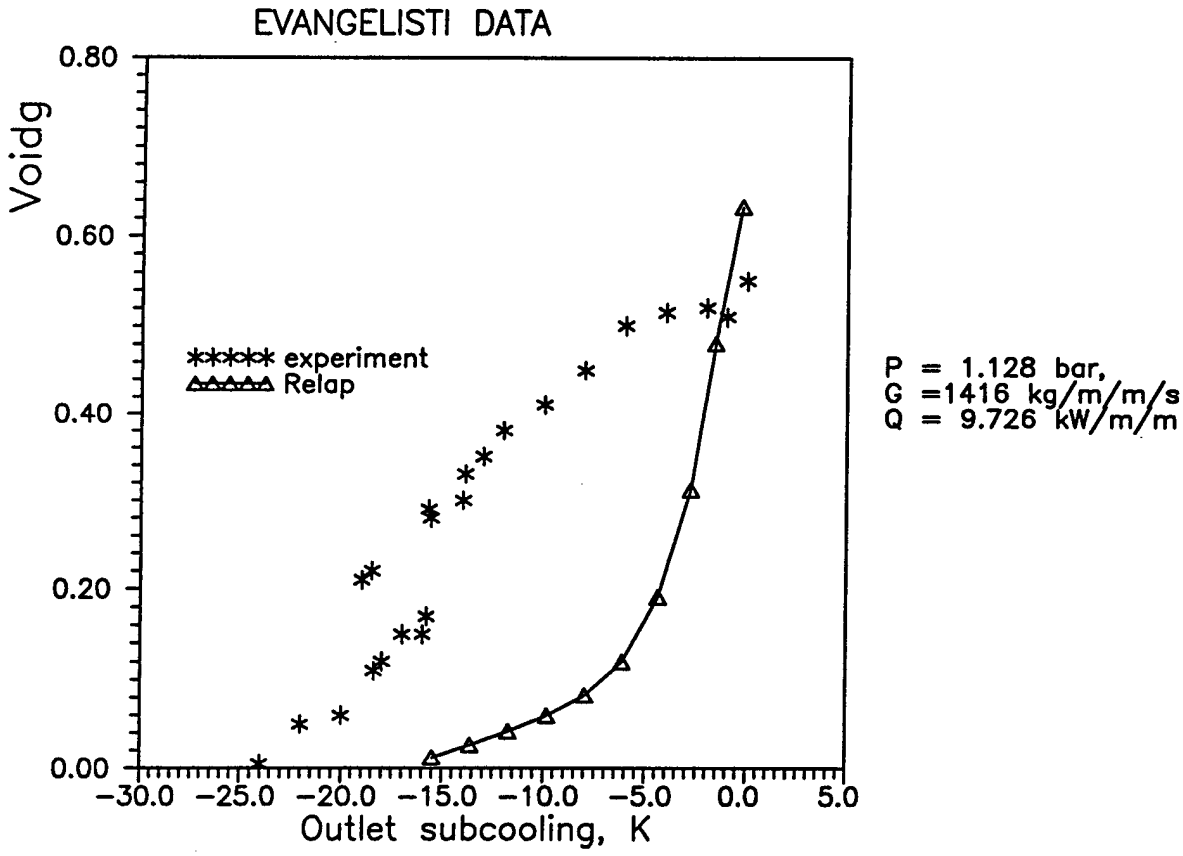
EVANGELISTI DATA
Voidg
0.80
0.60
0.40
0.20
0.00
−30.0 −25.0 −20.0 −15.0 −10.0 −5.0 0.0 5.0
Outlet subcooling, K
***** experiment
Relap
P = 1.128 bar,
G =1416 kg/m/m/s
Q = 9.726 kW/m/m

Fig.43

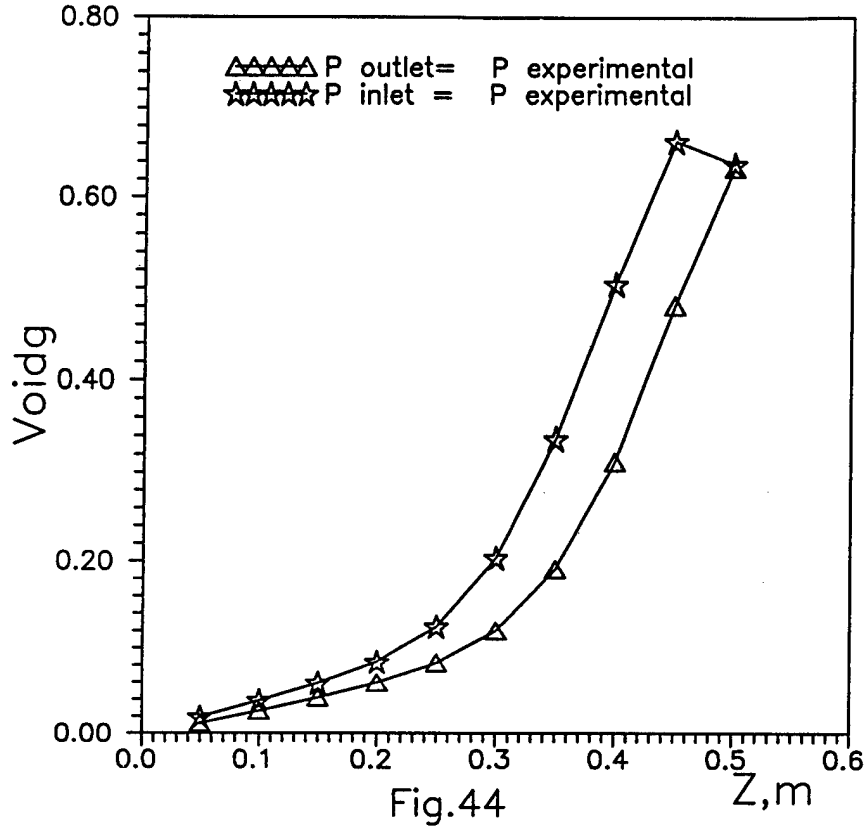

Fig.44

Evangelisti data with different pressure boundary conditions

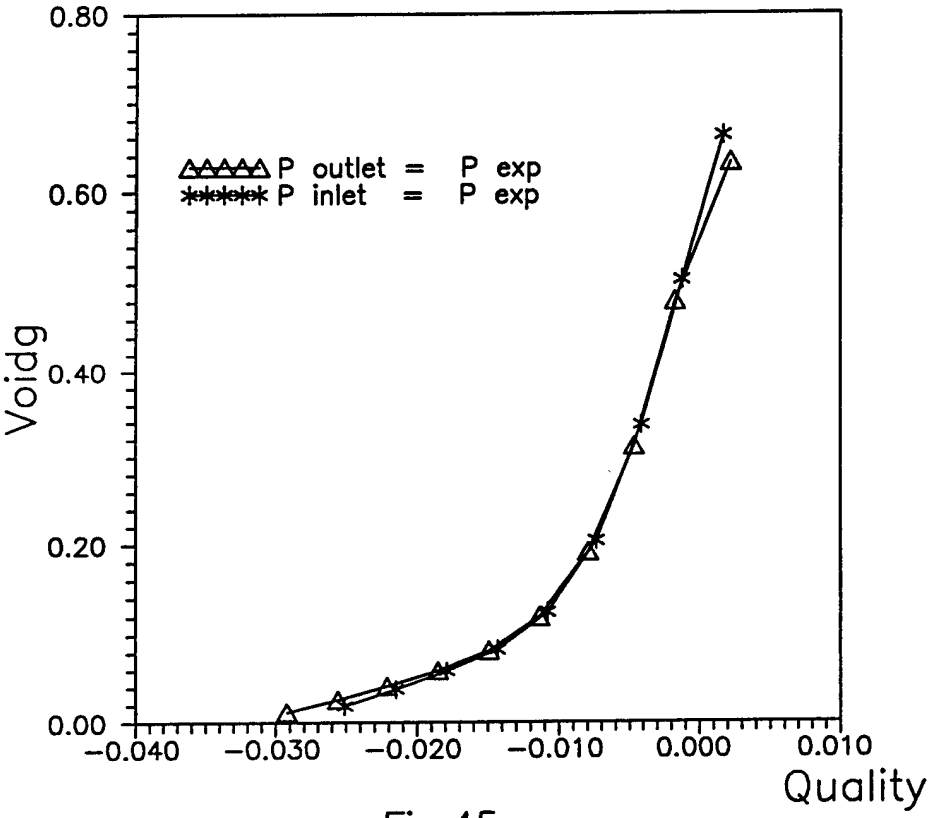
0.80
0.60
0.40
0.20
0.00
Voidg
P outlet = P exp
P inlet = P exp
−0.040
−0.030
−0.020
−0.010
0.000
0.010
Quality

Fig.45

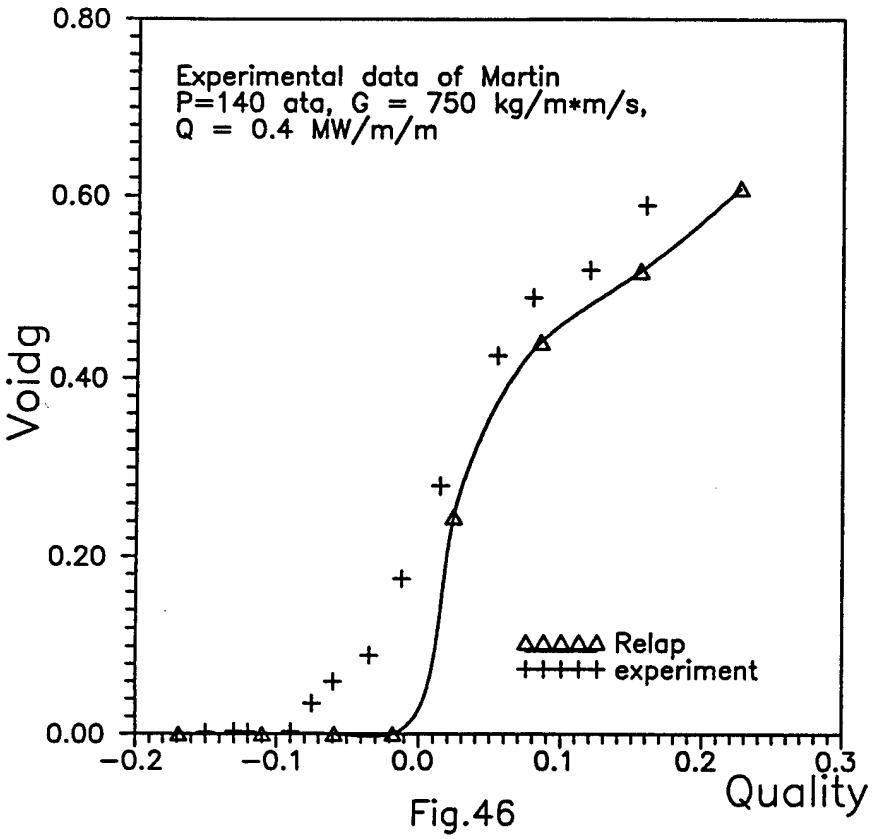
Experimental data of Martin
P=140 ata, G = 750 kg/m*m/s,
Q = 0.4 MW/m/m
Relap
experiment
Voidg
Quality
0.80
0.60
0.40
0.20
0.00
−0.2
−0.1
0.0
0.1
0.2
0.3

Fig.46

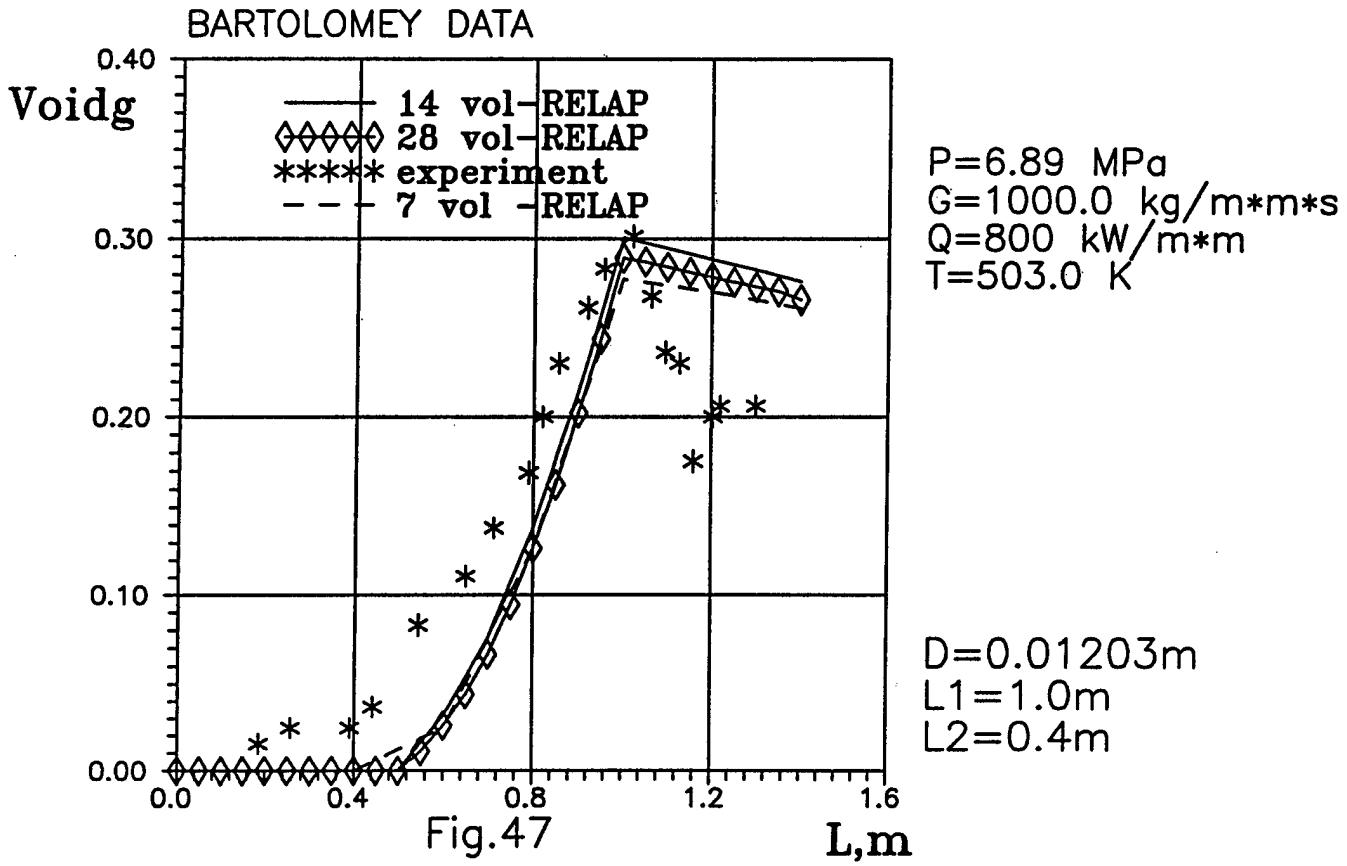
BARTOLOMEY DATA
Voidg
14 vol-RELAP
28 vol-RELAP
experiment
7 vol -RELAP
0.40
0.30
0.20
0.10
0.00
0.0
0.4
0.8
1.2
1.6
L,m
P=6.89 MPa
G=1000.0 kg/m*m*s
Q=800 kW/m*m
T=503.0 K
D=0.01203m
L1=1.0m
L2=0.4m

Fig.47

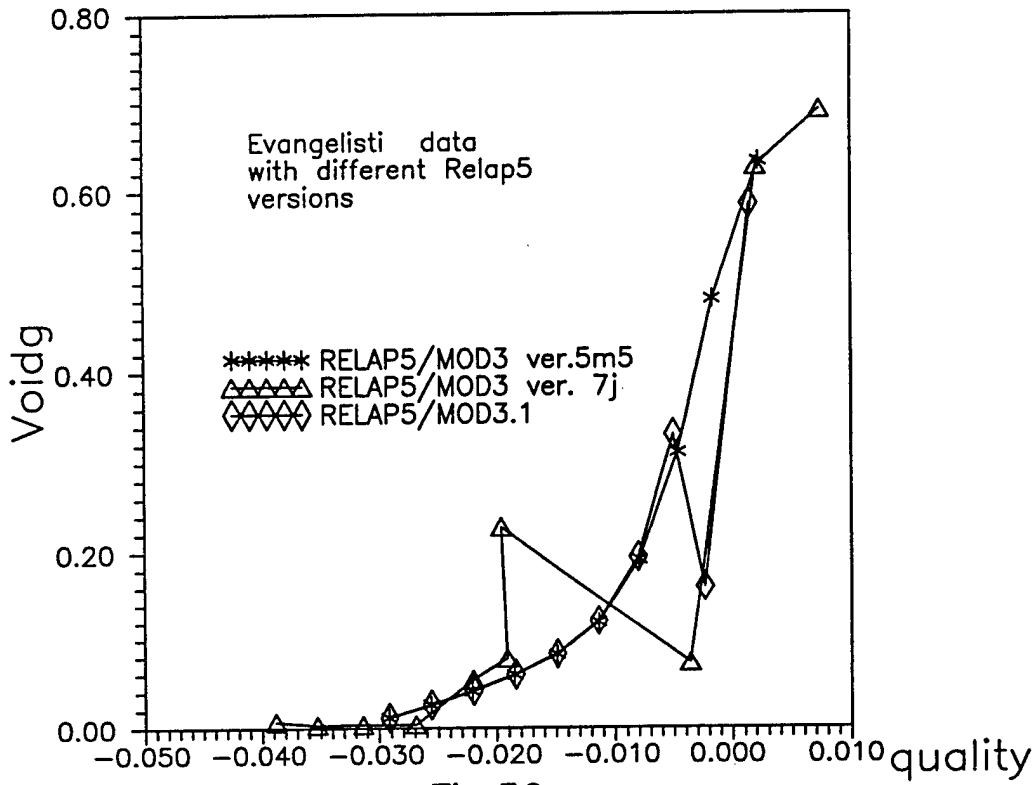
Evangelisti data
with different Relap5
versions
***** RELAP5/MOD3 ver.5m5
RELAP5/MOD3 ver. 7j
RELAP5/MOD3.1
Voidg
0.80
0.60
0.40
0.20
0.00
−0.050
−0.040
−0.030
−0.020
−0.010
0.000
0.010
quality

Fig.50

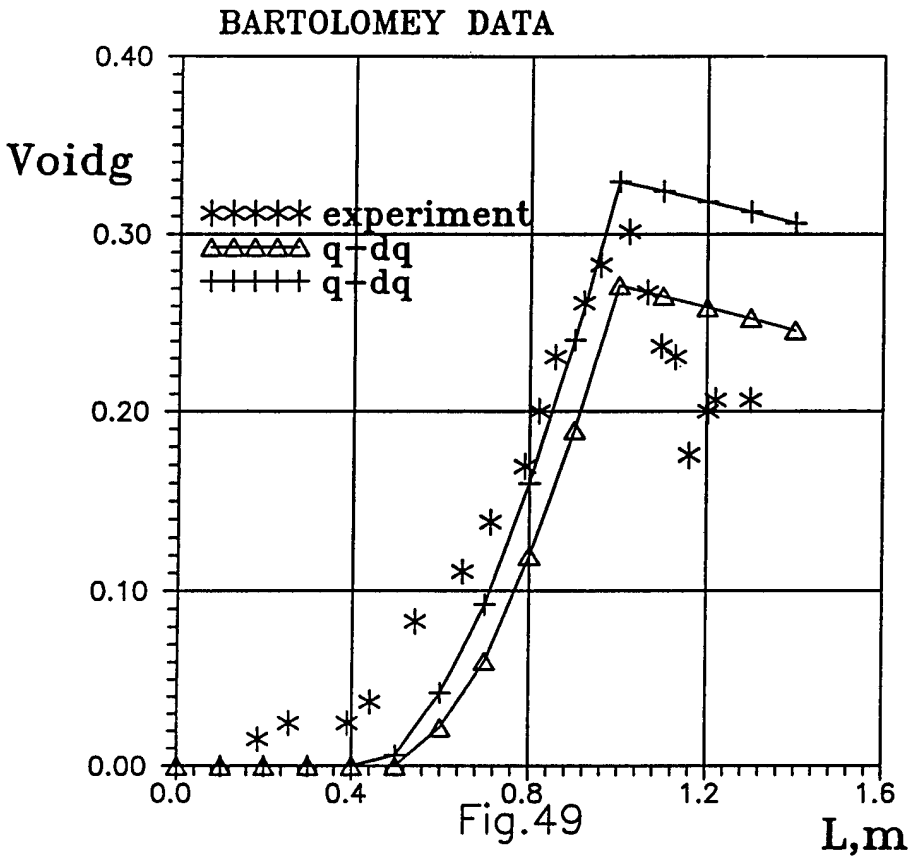
BARTOLOMEY DATA
Voidg
0.40
0.30
0.20
0.10
0.00
experiment
q-dq
q-dq
0.0
0.4
0.8
1.2
1.6
L,m

Fig.49

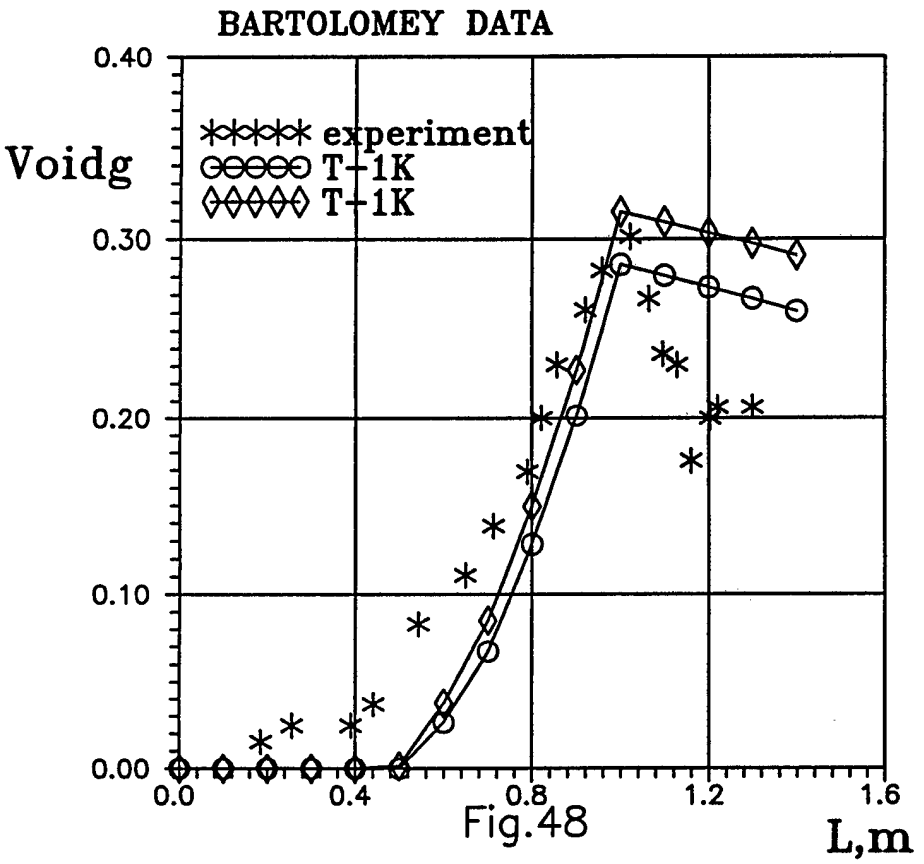
BARTOLOMEY DATA
0.40
0.30
0.20
0.10
0.00
Voidg
experiment
T-1K
T-1K
0.0
0.4
0.8
1.2
1.6
L,m

Fig.48

NRC FORM 335 (2-89) NRCM 1102, 3201, 3202

U.S. NUCLEAR REGULATORY COMMISSION

BIBLIOGRAPHIC DATA SHEET

(See instructions on the reverse)

1. REPORT NUMBER (Assigned by NRC, Add Vol., Supp., Rev., and Addendum Numbers, if any.)

NUREG/IA-0025

2. TITLE AND SUBTITLE

RELAP5/MOD3 Subcooled Boiling Model Assessment

3. DATE REPORT PUBLISHED

MONTH	YEAR
May	1998

4. FIN OR GRANT NUMBER

5. AUTHOR(S)

A. S. Devkin and A. S. Podosenov

6. TYPE OF REPORT

Technical

7. PERIOD COVERED *(Inclusive Dates)*

8. PERFORMING ORGANIZATION - NAME AND ADDRESS *(If NRC, provide Division, Office or Region, U.S. Nuclear Regulatory Commission, and mailing address; if contractor, provide name and mailing address.)*

Nuclear Safety Institute, Russian Research Center, "Kurchatov Institute"
Kurchatov Square 1,
123182, Moscow,
Russia

9. SPONSORING ORGANIZATION - NAME AND ADDRESS *(If NRC, type "Same as above"; if contractor, provide NRC Division, Office or Region, U.S. Nuclear Regulatory Commission, and mailing address.)*

Division of Systems Technology
Office of Nuclear Regulatory Research
U.S. Nuclear Regulatory Commission
Washington, D.C. 20005-0001

10. SUPPLEMENTARY NOTES

S. Smith, NRC Project Manager

11. ABSTRACT *(200 words or less)*

This report presents the assessment of the RELAP5/Mod3 (5m5 version) code subcooled boiling process model, which is based on a variety of experiments. The accuracy of the model is confirmed for a wide range of regime parameters for the case of uniform heating along the channel. The condensation rate is rather underpredicted, which may lead to considerable errors in void fraction behavior prediction in subcooled boiling regimes for nonuniformly or unheated channels.

12. KEY WORDS/DESCRIPTORS *(List words or phrases that will assist researchers in locating the report.)*

RELAP5/Mod3 (5m5 version) code
subcooled boiling regimes
void fraction behavior prediction

13. AVAILABILITY STATEMENT

unlimited

14. SECURITY CLASSIFICATION

(This Page)

unclassified

(This Report)

unclassified

15. NUMBER OF PAGES

16. PRICE

Report Number (14) NUREG/IA--0025

Publ. Date (11) 199805

Sponsor Code (18) NRC, XF

UC Category (19) UC-000, DOE/ER

no 1332.15 in folder